Hydrologic contributions of subsurface flow during snowmelt and rainfall in a forest catchment, coastal British Columbia.

by

Hyeon Jeong Kim

B.Sc. (Forest Management), Kangwon National University, 1996

A THESIS SUBMITTED IN PARTIAL FULFILLMENT OF

THE REQUIREMENTS FOR THE DEGREE OF

Master of Science

in

THE FACULTYOF GRADUATE STUDIES

The Faculty of Forestry

Department of Forest Science

We accept this thesis as conforming
to the required standard

The University of British Columbia

October 2001

Department of Forestry

The University of British Columbia
Vancouver, Canada

Date October 9, 2001

ABSTRACT

This research investigated hillslope subsurface flow processes and the mechanisms of runoff generation in a forested catchment in British Columbia in response to rainfall and snowmelt events. Observations at a hillslope segment included subsurface outflow from a soil pit, ground water levels, hydraulic conductivities, and snow water equivalent. Stream discharge and meteorological data were monitored in the catchment.

Subsurface flow at the hillslope segment responded rapidly enough to inputs of rain and snowmelt to contribute to stormflow at the catchment scale. On a contributing area basis, outflow from the pit at the hillslope segment exceeded peak stream discharge and total runoff, indicating that subsurface flow is able to contribute significantly to peak stormflow and event runoff at the catchment scale.

Estimates of catchment-wide subsurface flow cannot be reliably estimated by scaling up pit outflow using the ratio of pit length to the length of stream bank seepage faces in the watershed. Estimates of effective contributing area to pit drainage at the hillslope segment that were derived from runoff ratios, surface topography, and water-balances varied. Contributing area estimates based on runoff ratio were much higher than estimates based on topographic survey and water balance method. This lack of agreement indicates that it is problematic measured pit outflow to extrapolate to the catchment scale using contributing area ratios.

Peak rainfall intensity explained 79% of the variation in total subsurface flow volume from mineral section 2 of the pit for 7 rainfall events in 1998-99 and total

precipitation and 7-day precipitation prior to storm were not significant. However, drier antecedent soil moisture conditions have a major role in generating subsurface flow.

During the snowmelt season, outflow from the organic horizon was generated as saturated throughflow and overland flow as a result of the rising water table. However, during the autumn storms, outflow from the organic horizon occurred as a lateral subsurface flow despite the fact that the mineral soil was unsaturated, possibly due to the existence of hydrophobicity at the boundary between the organic horizon and mineral soil.

The results of this study contradict assumptions of quasi-steady state, topographically driven flow in models such as TOPMODEL and TOPOG. For the wet soil moisture conditions, the fraction of outflow from the individual mineral sections varied with time and with changes in total mineral horizon outflow throughout the melt season. For dry soil moisture conditions, the fraction of outflow from the organic horizon and individual mineral sections varied with changes in pit outflow. In addition, relations between hillslope discharge and water table elevation measured from the well throughout the melt season and during autumn storms showed marked hysteresis.

Saturated hydraulic conductivity back-calculated from Darcy's law was more than an order of magnitude higher than the saturated hydraulic conductivity values derived from slug tests. However, both methods generated values within the range of results of other studies in forested areas. The larger estimated hydraulic conductivities are likely due to existence of root channels as preferred pathways in forested hillslope.

TABLE OF CONTENTS

LIST OF TABLES

LIST OF FIGURES

ACKNOWLEDGEMENTS

First of all, I would like to express my deepest appreciation to my supervisors Dr. R. D. Moore and Dr. Roy C. Sidle for their guidance, patience, and encouragement throughout the course of study. Appreciation is also extended to the committee member, Dr. David Tait for his valuable inputs and suggestions. I would like to thank the people who provided support for this project. Dr. Rob Hudson provided some research instruments and data. Russell, Matt, Dino, John, and Micah provided assistance and cooperation in setting the field instrumentation. A very heartfelt thanks goes to my parents and brother in South Korea for their support and encouragement during my college career. Finally, thanks go to graduate students in the University of British Columbia Forest Hydrology group, including Paula, Gomi, Adam, Ahmed, Clay, Dave, and Julie. Gratitude is also extended to my friends; Nazip, Liew, Rumi, Atsuko, and Doug for their support and friendship.

CHAPTER 1

INTRODUCTION

The study of runoff processes has been a continuing subject in hydrology since 1930 (Anderson and Burt, 1990). Traditionally, runoff processes were studied as a basis for understanding stream flow variability, particularly flood estimation, and water yield; lately, more research has focused on runoff processes as a basis for understanding a broader range of phenomena, including water quality, hillslope stability, and surface erosion.

Headwater catchments play a fundamental role as source areas and transient sinks for water, nutrients, sediments, and biota (Sidle et al., 1995, 2000) so that understanding hillslope stormflow processes and their flow paths of storm runoff generation are important for streamflow forecasting and prediction, understanding surface water acidification, modelling slope stability and secondary salinization (O'Loughlin, 1986; McDonnell, 1990; Mulholland et al., 1990; Wilson et al., 1990; Hendershot et al., 1992; Peters et al., 1995; Wu and Sidle, 1995;). This thesis examines hillslope runoff processes based on hydrometric studies, to contribute to the development of a comprehensive understanding of runoff processes in the forested area during rainfall and snowmelt events.

1.1 RUNOFF PROCESSES IN TEMPERATE FORESTED CATCHMENTS

1.1.1 Is subsurface flow an important mechanism for stormflow generation?

In the past 40 years, many studies have examined the mechanisms of storm runoff generation in forested drainage basins. As a consequence, considerable advances have been made in our understanding of these processes (e.g., Kirkby 1978). Most storm runoff studies in temperate forested catchments found that generation of Hortonian overland flow, where rainfall intensity and/or snowmelt rates exceed the soil infiltration capacity, did not occur because source areas having bare or little vegetation, impermeable soils, and low hydraulic conductivity are rare in forested watersheds (Tsukamoto, 1961; Whipkey, 1965; and Troendle, 1970). Instead of this mechanism, three other types of flow have been recognized as sources of storm runoff generation: saturation overland flow (e.g., Dunne and Black, 1970a,b), groundwater ridging (e.g., Sklash and Farvolden, 1979), and subsurface stormflow (e.g., Whipkey, 1965; Tsukamoto and Ohta, 1988).

Saturation overland flow is generated where soil is partly saturated by lateral flow due to a rising water table. Dunne and Black (1970a, b) found that saturated overland flow was the main mechanism of stormflow generation on a pastured site in northeastern Vermont, produced by a combination of return flow from the upper soil horizon and direct precipitation onto the saturated area. However, this process has some limitations related to stormflow generation in temperate forests. Saturation source areas typically form in low-gradient foot slope areas near stream channels. While such areas were extensive in Dunne and Black's (1970a, b) gently sloping agricultural catchment, many forested headwaters have restricted riparian corridors due to steep and incised topography (e.g., Sidle et al., 2000).

Groundwater ridging has been suggested as an alternative mechanism of streamflow generation (Sklash and Farvolden, 1979; Abdul and Gillham, 1984). Abdul and Gillham (1984) demonstrated that if the capillary fringe, the zone of tension saturation, extends to ground surface, then the application of a relatively small amount of water can cause a rapid rise in the water table. However, such findings were based on laboratory experiments rather than field studies. Field studies conducted by McDonnell (1990) in the steep, humid Maimai catchment showed valley bottom groundwater responded rapidly to rainfall inputs. However, this study also indicated that sufficient volumes of old water did not discharge through the near-stream area to explain total catchment runoff volumes. In addition, Buttle and Sami (1992) tested the groundwater ridging hypothesis during snowmelt in a forested catchment on the Canadian Shield and found that the response of water-table levels in near-stream areas to initial melt did not support a rapid flux of ground water to the wetland and stream. McDonnell and Buttle (1998) mentioned that the associated increase in pre-event contributions to stormflow is not necessarily attributable only to groundwater, thus other hydrological processes should be considered as well.

Subsurface flow is generally believed to be the dominant mechanism of generating storm flow in forest watersheds in humid temperate regions (Whipkey 1965, 1969; Weyman, 1970; Mosley, 1979; Tanaka et al., 1988; Tsukamoto and Ohta, 1988;

Pearce, 1990; Wilson et al., 1990). Subsurface stormflow is infiltrated water that moves laterally through the soil mantle toward the stream channel. This mechanism has been documented in catchments with steep slopes and highly permeable surface soils underlain by an impermeable or semi permeable layer. In these areas, subsurface flow occurs within a perched saturated zone above the basal confining layer, which can be bedrock (e.g. Burt and Butcher, 1985) or compacted glacial till (e.g. Hutchinson and Moore, 2000). Forested soils are known to have extensive macropore systems, which are capable of delivering subsurface flow to stream channels at velocities much greater than the surrounding soil matrix (Pilgrim and Huff, 1978; Mosley, 1982; Beven and Germann, 1982; Wilson and Luxmoore, 1988; Jardine et al., 1989; Kitahara, 1993; Tsuboyama et al., 1994). Tsukamoto and Ohta (1988) mentioned that some macropores may become invisible after storms, but may still function as preferential flow pathways during storms. Other studies have shown that the interaction of macropores with surrounding mesopores during wet conditions may facilitate preferential flow (Tsuboyama et al., 1994; Noguchi et al., 1999, 2001). Such field evidence lends support to the concept of the expansion and lateral extension of macropore networks during wet conditions (Luxmoore and Ferrand, 1993; Tsuboyama et al., 1994; Sidle et al., 2000, 2001).

1.1.2 Are simple approaches to scaling up subsurface flow using hillslope: catchment contributing areas or flow widths valid?

A common problem in hydrologic research is "scaling up" measurements made at plot or hillslope scales to the catchment scale. To estimate catchment-wide subsurface flow, some researchers simply multiplied plot outflow measurements by simple ratios such as the length of streambank to pit width (Weyman, 1970; McDonnell, 1990; Turton et al., 1992), or catchment area to pit contributing area (Sidle et al., 1995). Although these approaches have usually been justified due to absence of other information, whether small-scale measurements of subsurface flow can be extrapolated to larger catchment (Woods and Rowe, 1996) is not clear.

1.1.3 Can lateral flow occur in zones above the perched water table?

Perched saturated zone in shallow hillslope soils is believed to be an important subsurface flowpath that contributes to rapid stormflow (Chappell et al., 1990; Jenkins et al., 1994; Brown et al., 1999). Lateral subsurface stormflow occurred via a perched saturated zone above the Bt2/Bt3 soil horizon interface in a forested hillslope (e.g., Wilson et al., 1989; 1990; Mulholland et al., 1990). Based on the simple conceptualization of hydrological processes, many operational models (e.g. TOPMODEL [Beven and Kirkby, 1979; Beven, 1986], DHSVM [Wigmosta et al., 1994; Storck et al., 1998]; TOPOG [O'Loughlin, 1986; Vertessy et al., 1993] and conceptual models [McDonnell, 1990; Tani, 1997]) assume that downslope flow occurs mainly in a perched saturated zone. However, McDonnell et al. (1991) defined a pseudo-Hortonian overland flow process, where large differences in saturated hydraulic conductivity at the organic-mineral soil boundary create lateral flow in the shallow soil horizon. The hydrophobic nature of organic matter in the soil O-horizon might contribute to increased lateral flow (Brown et al., 1999). Sevink et al. (1989) mentioned that hydrophobicity could induce preferential flow by concentrating water in the organic soil above the hydrophobic layer.

1.1.4 How does subsurface flow respond during the snowmelt periods?

In mountainous regions of western North American and other similar areas of the world, spring snowmelt generally represents the major hydrologic event (Roberge and Plamondon, 1987; Kane and Stein, 1984; Marks et al., 1999). However, snowmelt runoff processes have been studied less than rainfall runoff processes due to the complexity of the soil system. For example, unfrozen water exists as films on the surface of the soil particles, both ice and air occupy pore space, and there is a strong interaction between the snowpack and the underlying seasonally frozen ground (Kane and Stein, 1984). The timing, magnitude, contributing area, and runoff pathways of snowmelt during changing climatic conditions might differ due to episodic water inputs and widespread presence of seasonal ground frost (Roberge and Plamondon, 1987). Relative importance of snowmelt runoff pathways among groundwater flow, subsurface flow and overland flow were highly variable among sites. Eschner et al. (1969) found little change in soil moisture values during most of the winter and the snowmelt season; additionally, the seasonal peak of streamflow occurred before the peak of soil moisture. Price and Hendrie (1983) studied vertical runoff processes in a relatively low-gradient forested area in the Perch

Lake drainage basin, Ontario, with relatively deep surficial aeolian and glaciofluvial outwash sands. Although Horton overland flow occurred in the basin, this contribution to streamflow was not important. Unsaturated recharge to the water table was a major factor contributing to streamflow generation (Price and Hendrie, 1983). Roberge and Plamondon (1987) studied snowmelt runoff pathways in a boreal forest hillslope with an orthic humoferric podzol ('ferrod'; USDA classification) (Jurdant and Bernier, 1965). Based on hydrometric observations, they found that unsaturated flow was an insignificant element of the downslope flow and the groundwater flow from an aquifer within a till was the major pathway for hillslope snowmelt flow; however, when groundwater rose to near the surface, turbulent pipeflow occurred. Kane and Stein (1983) found that for dry conditions and permafrost soils in interior Alaska, neither overland flow nor subsurface flow occurred. Slaughter and Kane (1979) found that a shallow surface layer of slightly decomposed organic material in permafrost buffered heat loss and facilitated rapid downslope flow, thus generating streamflow. Tracer studies in the discharge area of a forested glacial till revealed that macropore channels of old root remains conduct water rapidly through the unsaturated and frozen matrix without displacing the soil-bound water (Espeby, 1990). Troendle and Reuss (1997) estimated snowpack accumulation and water outflow from clearcut and forested plots within a mixed conifer forest in Colorado using direct hydrometric measurements (i.e., trench measurements). They demonstrated that both snowpack accumulation and stream discharge were higher on clearcut plots than on forested plots. The correspondence of hydrological parameters derived from direct measurements compared to those determined by indirect methods (e.g., isotope or geochemical hydrograph separation) should be carefully considered when the hydrological parameters and plot area are estimated (Troendle and Reuss, 1997).

1.1.5 Does the distribution of subsurface flow across a hillslope confirm to commonly used modelling assumptions?

Topographically based hydrological models, e.g. TOPMODEL (Beven and Kirkby, 1979; Beven, 1986) and TOPOG (O'Loughlin, 1986; Vertessy et. al., 1993) have been widely utilized in catchment modeling and hydrological modeling problems in the last two decades. To simplify modelling hillslope flow, topographic-driven hydrological models make several important assumptions.

1. The hydraulic gradient is equal to the local surface slope.
2. The local vertical recharge rate to the water table is spatially constant.
3. The subsurface flow system is in a quasi-steady state.

Much research related to TOPMODEL has focused on the distribution of the topographic index, $C = a / \tan \beta$, where a is the area of the hillslope unit contour length; $\tan \beta$ is the hydraulic gradient of the saturated zone (e.g. Quinn et al., 1991; Wolock and Price, 1994; Quinn et al., 1995; Wolock and McCabe, 1995). However, very few studies have tried to validate the assumptions underling topographically driven hydrological models (e.g. Lamb et al., 1997; Freer et al. 1997; Hutchinson and Moore, 2000). In a wide range of recent modelling studies, it has been assumed that for a specified time interval the subsurface flow through a given length of contour segment will be proportional to the upslope contributing area. Woods and Rowe (1996) studied changes in spatial variability of subsurface flow along the base of a hillslope at Maimai, New Zealand, using 30 troughs during a 110-day period. They found that subsurface flow varied with surface topography, particularly convergent and divergent hillslopes. Based on Woods and Rowe's (1996) findings, McDonnell (1997) tried to further elucidate the factors controlling spatial variability of subsurface flow by introducing the influence of bedrock (subsurface) topography. Freer et al. (1997) examined both surface and subsurface topographic controls on hillslope flow paths for two different catchments: the Maimai catchment in New Zealand and the Panola Mountain Research Watershed in USA. In the case of the Maimai catchment, surface and subsurface topography was highly correlated, thus suggesting that surface topography could be used to estimate hydraulic gradients along subsurface flow paths. However, in Panola, discharge and peak flow patterns were strongly related to bedrock topography rather than surface topography and the spatial correlation between surface and subsurface topographies on the hillslope was not significant. Field studies at Hitachi Ohta, Japan, acknowledged the importance of substrate topography on subsurface runoff paths, but found that the spatial resolution used to determine bedrock topography in other studies was inadequate to assess the actual pathways that occurred in hillslopes (Noguchi et al., 1999; Sidle et al., 2000); thus, variability in subsurface flow may be attributed to other factors such as self-organization of preferential flow paths during periods of increasing moisture (Sidle et al., 2001). Woods et al. (1997) proposed a new topographic index based on spatial variability of subsurface flow as influenced by both topography and wetness. Field studies conducted by Hutchinson and Moore (2000) reported that mean trough throughflow proportions varied systematically with total plot discharge.

1.1.6 Can lateral saturated hydraulic conductivity be determined by conventional field techniques?

Reliable and representative soil hydraulic characteristics have become increasingly important for prediction of soil water flow. One of the most important hydraulic characteristics is saturated hydraulic conductivity (K). Slug tests have been widely used to provide simple and quick estimates of the hydraulic conductivity (Hovorslev, 1951). The small volume of soil that contributes to such K estimates limits the extrapolation of these values because such estimates of K are known to vary by orders of magnitude from location to location (Stagnitti et al., 1992). Also, slug tests are only able to predict flow in the bulk soil and do not predict flow in the macropores. Many field studies performed in forested mountain watersheds found root channels in the upper soil profile (deVries and Chow, 1978; Peters et al., 1995; Noguchi et al, 1997, 1999; Hutchinson and Moore, 2000).

One way to circumvent the problem of spatial variability of K is to use "effective" K values, representing the entire hillslope segment. These can be estimated via subsurface discharge measurements from soil pits at the base of the hillslope (e.g., Talsma and Hallan, 1980). Such values can be back-calculated from Darcy's law for laminar flow conditions. However, if turbulent flow occurs in pipes or macropores (Whipkey, 1967), Darcy's law may not apply. Thus, Darcy's law and particularly slug tests may not be appropriate to characterize distributed K over hillslopes or watersheds (deVries and Chow, 1978). However, values of K from slug tests have not previously been compared to "effective" values back-calculated from Darcy's law for forest soils.

1.2 OBJECTIVES

This study employs an integrated set of hydrometric field measurements to investigate hillslope subsurface flow processes and the mechanisms of runoff generation in a headwater catchment in Gray Creek, British Columbia, Canada, in response to rainfall and snowmelt events. Within this framework there are 4 specific objectives:

1. extend site measurements to the catchment scale to determine the importance of subsurface flow as a stormflow generating process;
2. evaluate the variability of subsurface flow in a forest hillslope during both rainfall and snowmelt events, in relation to the subsurface flow pathways;
3. evaluate the validity of assumptions used to model subsurface flow in a forest hillslope and catchments during both rainfall and snowmelt events, in relation to the subsurface flow pathways; and
4. compare the effective K derived from pit discharge (and back calculated by Darcy's law) with K determined from slug tests.

1.3 OUTLINE OF THESIS

The remainder of the thesis is comprised of four chapters. Chapter 2 provides a description of the study area, instruments, and measurements employed. Chapter 3 presents data analysis and results. Chapter 4 discusses the results based on research objectives. Chapter 5 addresses overall conclusions and recommendations for further research.

CHAPTER 2

METHODS

In this chapter, physical characteristics of the Gray Creek watershed and the experimental hillslope segment are described. Details on instrumentation and measurements are presented.

2.1 STUDY AREA

2.1.1 Location

Gray Creek is the community water supply for the District of Sechelt and surrounding areas located in southwestern British Columbia about 45 km northwest of Vancouver. Gray Creek is about 18 km long and has a drainage area of 4030 ha (40 km^2) above the intake. Elevations within the Gray Creek watershed vary from 1645 m at the summit of Mount Steele to 300 m at the intake of the municipal water supply. The entire Gray Creek watershed is within the Sechelt Indian Band traditional territory, which the Sechelt people utilize for a variety of social, economic and cultural resources, including fresh water, fish, game, timber, roots, berries and herbs.

Located on a small second-order tributary of Gray Creek at 49.6° N 123.6° W, the upper Gray Creek catchment was established as a hydrological research site in 1995. The study catchment has an area of 149.5 ha and ranges in elevation from 950 to 1200 m (Figure 2.1). There are small ponds / lakes located in the central and upper portions of the catchment. Within this catchment, a north-facing hillslope segment was chosen for

Figure 2.1 The Gray Creek research catchment in southwestern British Columbia with locations of soil pit in hillslope segment (contour interval is 100 m).

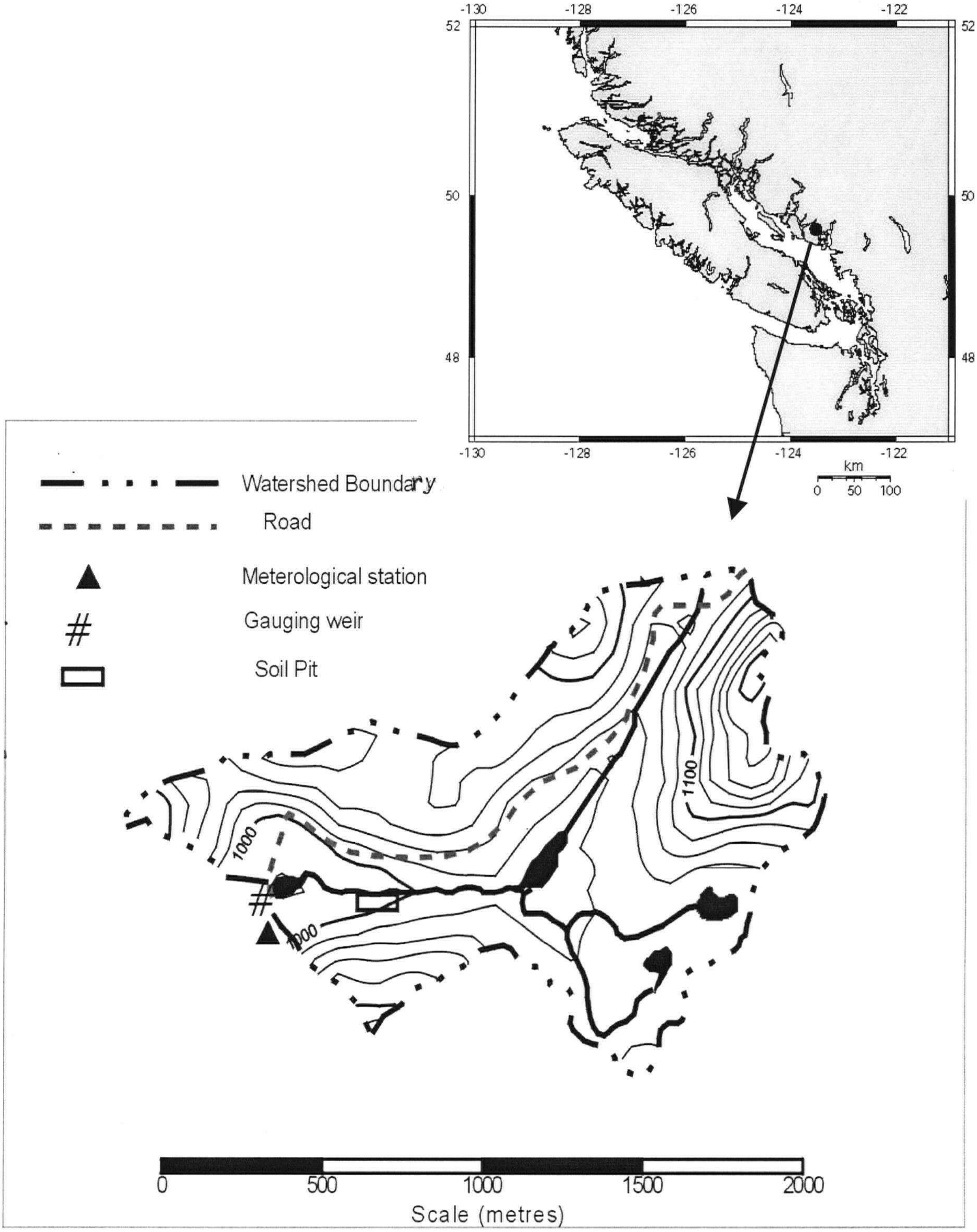

intensive subsurface hydrologic investigations. Topography is moderate to relatively steep, with slopes ranging 20 to 50%, dominantly in the range of 30-45%. The monitored hillslope segment has an average slope of 33.2%. Lakes and ponds in the upper portion of the catchment may attenuate peak flows, especially during dry antecedent moisture events.

2.1.2 Climate

The Gray Creek watershed is located in the mild marine climate zone of coastal BC. Precipitation comes mainly from frontal storm systems originating in the Pacific Ocean. Most precipitation falls during the winter months, with highest precipitation occurring in November and December and lowest in July, August and September. A high proportion of annual precipitation occurs as snow. The runoff from melting snow in spring is a main water supply for the District of Sechelt. Large snow accumulation can also cause flooding during the spring snowmelt period.

2.1.3 Soils, geology and geomorphology

Quartz diorite and granodiorite appear to dominate the surface bedrock throughout the entire Gray Creek catchment, although some volcanic and sedimentary rocks exist (Ministry of Forests, 1998). Gray Creek occupies an extended valley with steep sides that were carved by glaciers. Meltwater released during interglacial periods and during glacial retreat resulted in widespread sand and gravel deposits into which the streams incised. The effect on groundwater has not been established. In general, the terrain within the study watershed has relatively low to landslide potential and stream impact following clearcutting. The most common soils at lower elevations are humo-ferric podsols that are gradually replaced with ferro humic podsols and humic podsols at higher elevations. The humic fraction increases with poorer drainage conditions. Basal till forms a virtually impermeable boundary at the base of the soil. However, this does not exist continuously based on observations in the pit.

2.1.4 Forest cover

The Gray Creek Watershed is within the Sechelt Provincial Forest and comprises part of the Sunshine Coast Timber Supply Area. The productive land base within the watershed supports coastal western hemlock, mountain hemlock, amabalis fir, yellow cedar, and western red cedar (Hudson, 2000). At elevations lower then 750 meters above sea level, planting is generally carried out for reforestation. At the upper elevation areas above 750 meters, reforestation normally occurs by natural regeneration. Higher elevation areas are also plotted if there is inadequate natural regeneration.

Much of the study area was gradually logged over a period of time from the early 1950s to the late 1970s. Individual blocks were logged in 1951, 1966, 1973 and 1979, although differences in growth rates of tree species and fires from site to site have resulted in an irregular second-growth forest (Hudson, 2000). The second-growth stands are naturally regenerated in the study area and reforestation consists of a combination of subalpine fir (*Abies lasiocarpa* (Hook.) Nutt.), western hemlock (*Tsuga heterophylla* (Raf.) Sarg.), mountain hemlock (*Tsuga mertensiana* (Bong.) Carr.), western red-cedar (*Thuja plicata Donn*) and yellow-cedar (*Chamaecyparis nootkatensis* (D. Don) Spach).

2.1.5 Hillslope and soil pit

Instrumentation upslope of the soil pit in the hillslope segment is shown in Figure 2. 2. Three piezometers and one well were installed upslope of the soil pit in the hillslope segment. Hillslope above the soil pit was surveyed using an engineers level and metric tapes. A topographic map was then constructed to define contributing area.

2.2 DATA COLLECTION

The study was conducted from October 16, 1998, to November 21, 1999. Subsurface outflow and ground water levels in a hillslope segment, stream discharge, meteorological data (total precipitation, rainfall and average temperature), and snow water equivalent were recorded.

2.2.1 Pit outflow

2.2.1.1 Description of pit

A soil pit was excavated at the base of a hillslope (3.5 m upslope of the stream bank) and instrumented to measure subsurface flow (Figure 2.1). By locating the pit just upslope of the stream bank, the effects of excavation on the subsurface flow hydrograph and contributing drainage area were minimized (Atkinson, 1978).

The description of the soil profile is shown in Figure 2.3. Depths from the soil surface above compact till and bedrock in the soil pit ranged from 56.5 to 79 cm. The soil

Figure 2.2 Locations of piezometers and a well in the hillslope segment

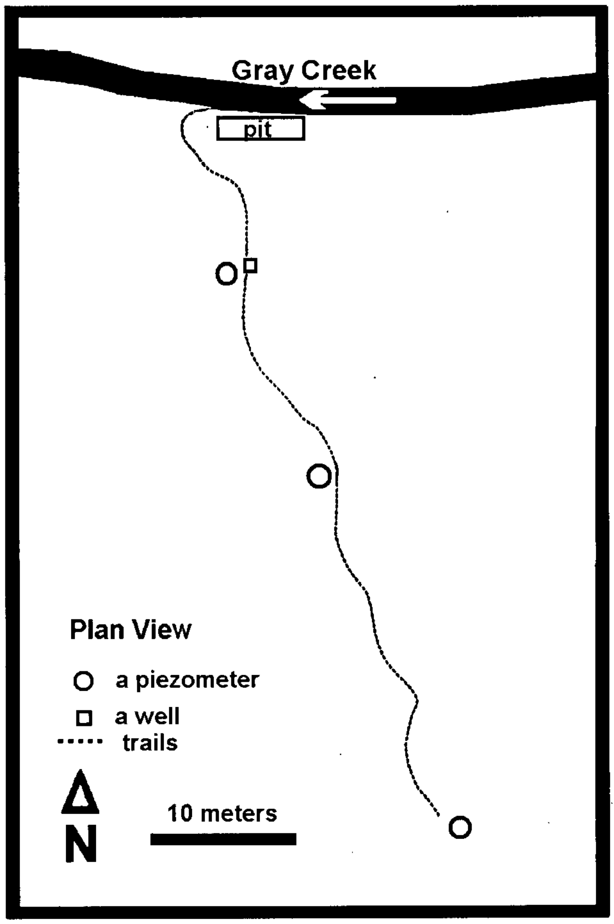

Figure 2.3 Description of soil profile at the pit face with respect to arbitrary datum point

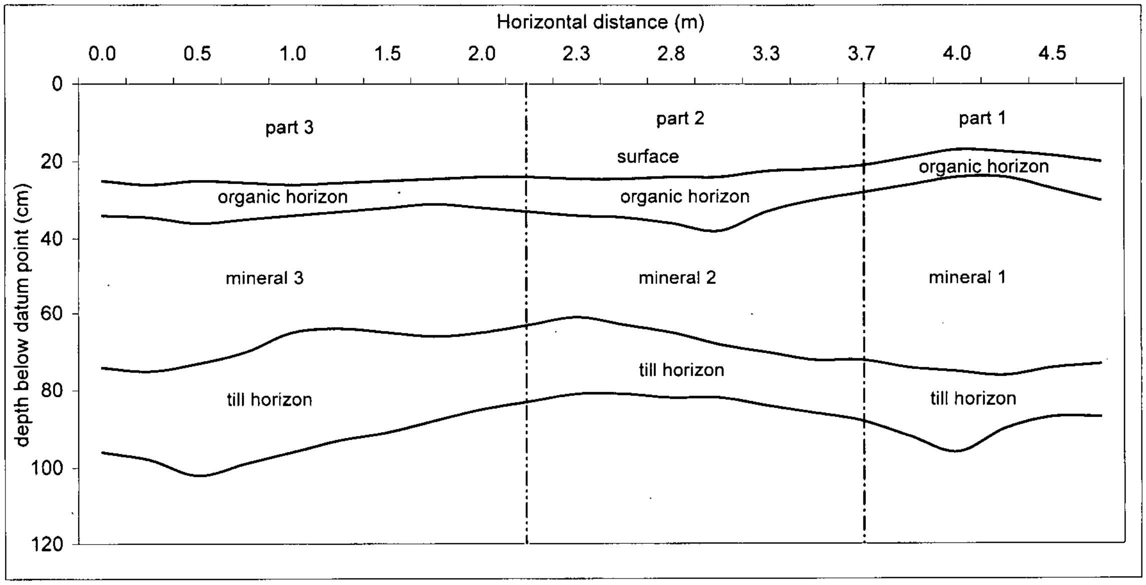

Table 2.1 Observations of preferential flow and their locations at the soil pit

Horizontal distance (m)	Depth below datum point (cm)	Comment
0.8	40	diffuse seepage zone
1.4	15	small macropores but difficult to say with diffuse seepage zone below it
1.45	25	diffuse seepage zone throughout entire soil face
1.7	18	diffuse seegage zone and flow around roots
2.73	17	concentrated seepage area
3.08	24	concentrated flow, possibly macropore

profile consists of three major layers. One is an organic-rich horizon comprising O and A horizons, another is mineral subsoil consisting of B and possibly C horizons, and the third is weathered till and possibly the less developed portion of the C horizon above compact till and bedrock. Observations of preferential flow and their locations at the soil pit are described in Table 2.1. The soil characteristics of hillslope pit sections are summarized in Table 2.2. A plastic roof was constructed over the soil pit, extending about 1 m from the pit. The roof protected the pit face and instrumentation. The roof could be tilted downward to protect the pit face during periods when the site was not visited and during the snow season (Figure 2.7).

2.2.1.2 Measurement of outflow

The system for measuring outflow from the pit is shown in Figure 2.8. Discharge is measured separately for the two horizons of the soil profile in the hillslope segment: outflow from the organic-rich horizon (including A horizon; 0-10 cm of soil depth) and outflow from the mineral horizon (including B, B/C, and C horizon; 10-45 cm of soil depth). The entire organic-rich horizon above the three subsoil sections was isolated by inserting a flexible metal sheet about 7 cm into the soil at the organic-mineral boundary. While inserting the metal sheets into the soil, we tried not to disrupt the profile. Short pieces of plastic gutter were attached to the metal sheeting and routed into funnels to collect runoff from the organic-rich layer (Figure 2.9). A concrete trough was built into the till below the mineral horizon to collect the outflow from the mineral soil profile. The concrete trough was divided into three sections to collect subsurface flow from the three subsoil profiles. Outflow from the concrete troughs was directed through pipes that in

Table 2.2 Summaries of soil characteristics at the pit

					pit				
length (m)					4.75				
depth (cm)		average			minimum		maximum		
organic layer (including A horizon)		8.8			6.5		14		
mineral layer (B or BC horizon)		37.5			27		52		
till layer (C horizon)		20.2			13		31		
	part 1 (figure 2.4) *			***part 2 (figure 2.5)***			***part 3 (figure 2.6)***		
characteristics	very permeable coarse soil, with a high content of gravel and rock			a fine textured mineral soil layer			middle size of soil material between part 1 and 2		
length (m)	1.1			1.5			2.15		
depth (cm)	average	minimum	maximum	average	minimum	maximum	average	minimum	maximum
organic layer (including A horizon)	7.7	6.5	10	10	7	14	8.4	6.5	11
mineral layer (B or BC horizon)	47.5	43	52	33.4	27	44	34.6	30	40.5
till layer (C horizon)	16	13	21	16.6	14	20	25.1	20	31

* an abrupt boundary between the organic layer and the relatively mineral horizon.

Figure 2.4 Right side of soil pit - 1.1 m in length (part 1).

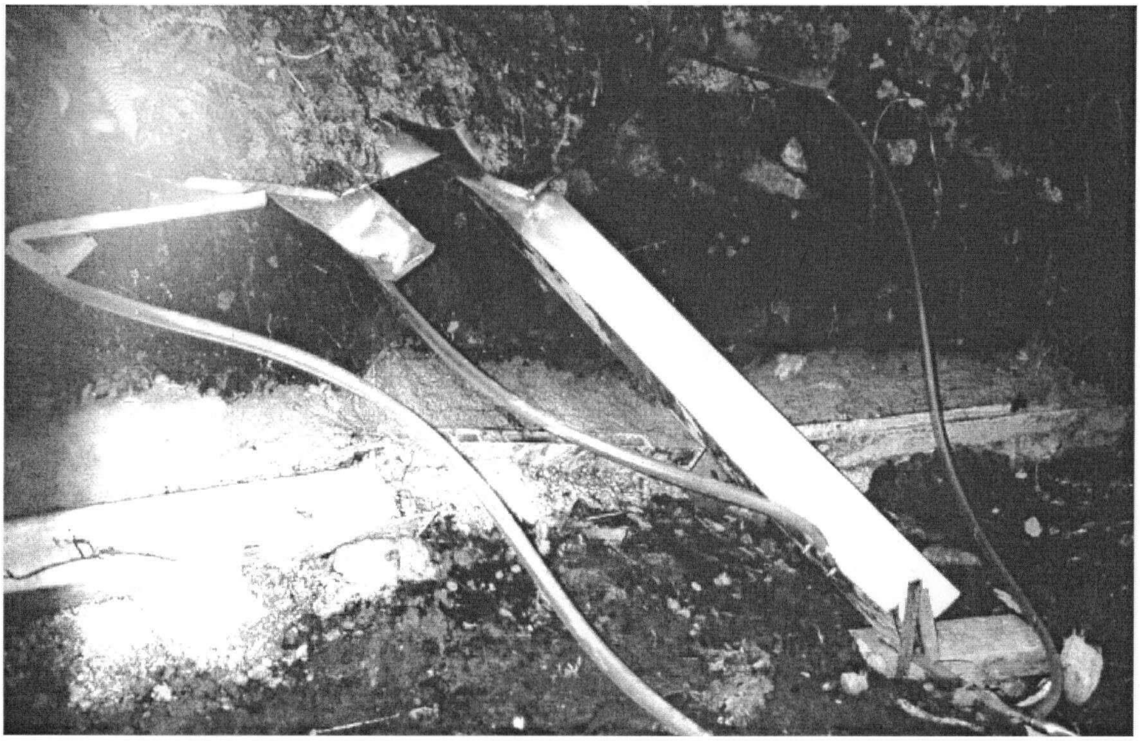

Figure 2.5 Middle part of soil pit - 1.5 m in length (part 2).

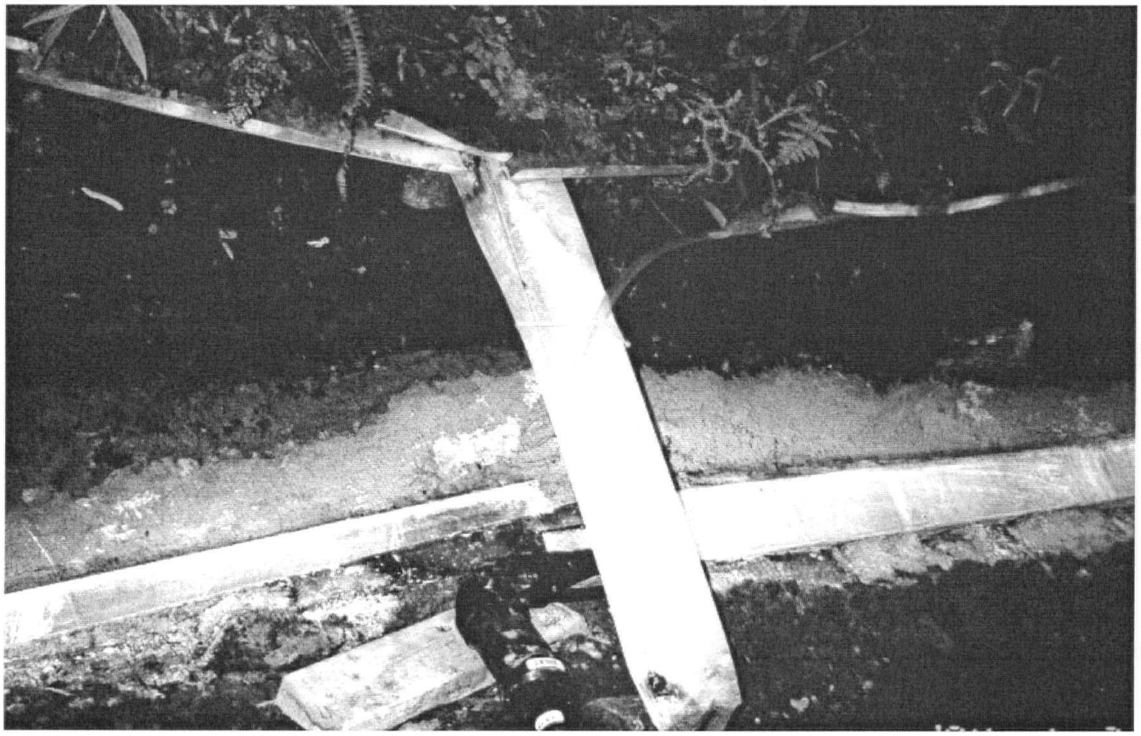

Figure 2.6 Left side of soil pit - 2.15 m in length (part 3).

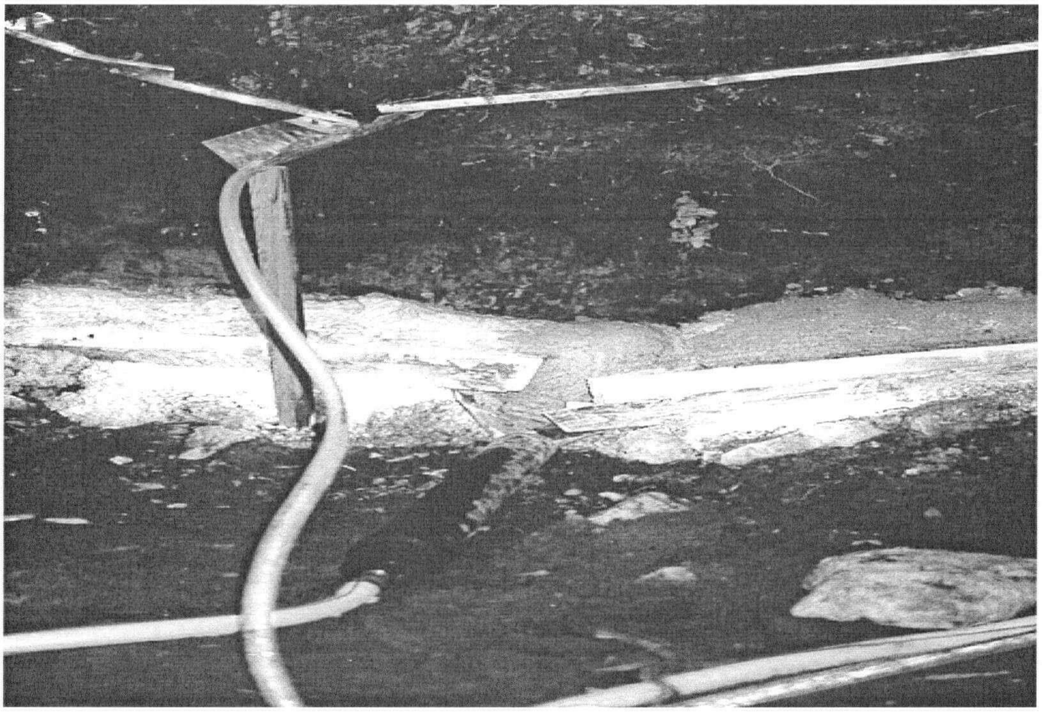

Figure 2.7 Plastic sheeting roof and covers.

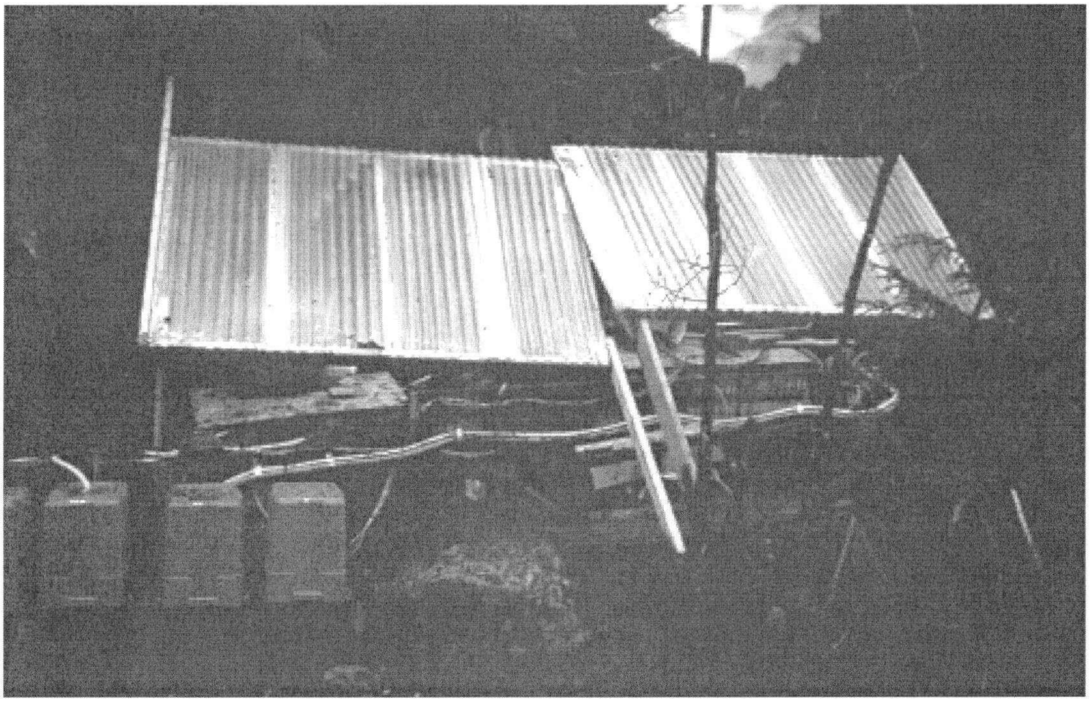

Figure 2.8 Instruments in soil pit at the hillslope segment.

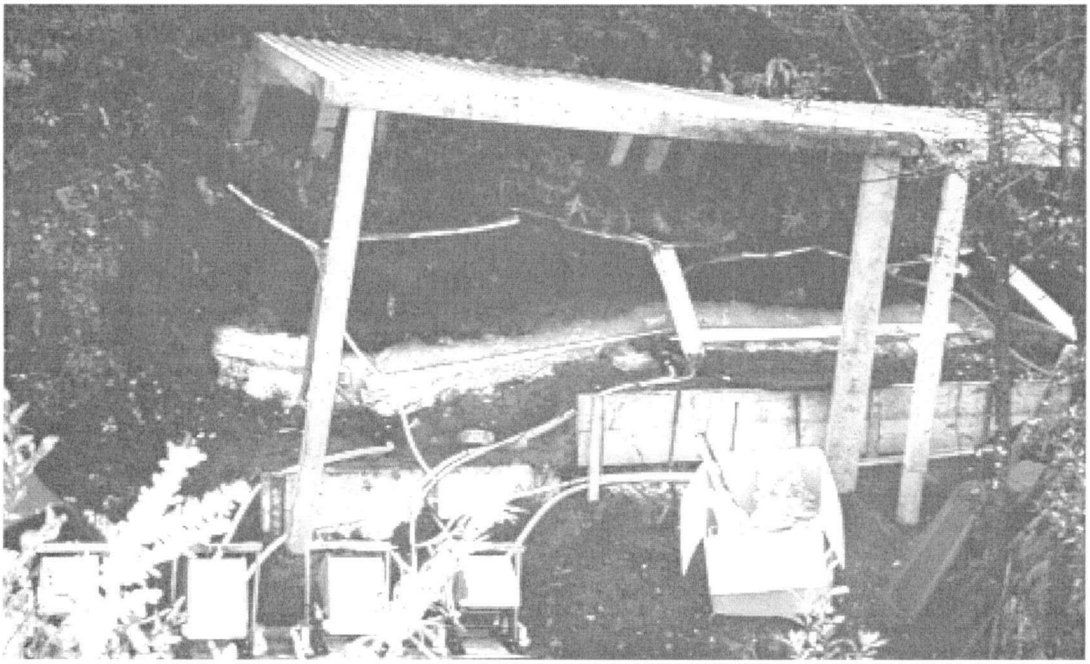

Figure 2.9 Collection of organic (funnels) and mineral (trough) outflows.

turn were connected to flexible garden hose. The end of the hose was linked to a tipping bucket through a hole on top of a protective plastic container (Figure 2.10). Outflow from a gutter at the base of the organic layer was directly connected to plastic hoses and then directed in the same manner to the tipping bucket. Each tip of the bucket activates a reed switch that alternately causes a record to be transmitted to a multi-channel event logger. The bucket volume was adjusted according to outflow and varied from 0.25 L to 1.0 L. Using this system of four tipping buckets allowed for real-time monitoring of subsurface flow. The volume of runoff was recorded at 5-minute intervals to develop a relation with either rainfall or snowmelt.

2.2.2 Streamflow

Stream discharge from the upper Gray Creek catchment was measured at a 140° broad crested V-notch weir with side contractions (Figure 2.11). Stage was measured by a Unidata capacitive water depth probe and continuously recorded on a Unidata Starlogger (high-resolution data logger; ±1 mm) every 15 minutes.

2.2.3 Wells and Piezometers

2.2.3.1 Measurement of water level

Water table elevation on the hillslope segment was measured by a pressure transducer in a well located 11 m upslope from the soil pit. Water table elevation was continuously recorded on a Unidata Starlogger every 5 minutes with a 5 second scan rate. The depth of the 0.137 m diameter well was 0.755 m below the soil surface.

Figure 2.10 Tipping bucket systems.

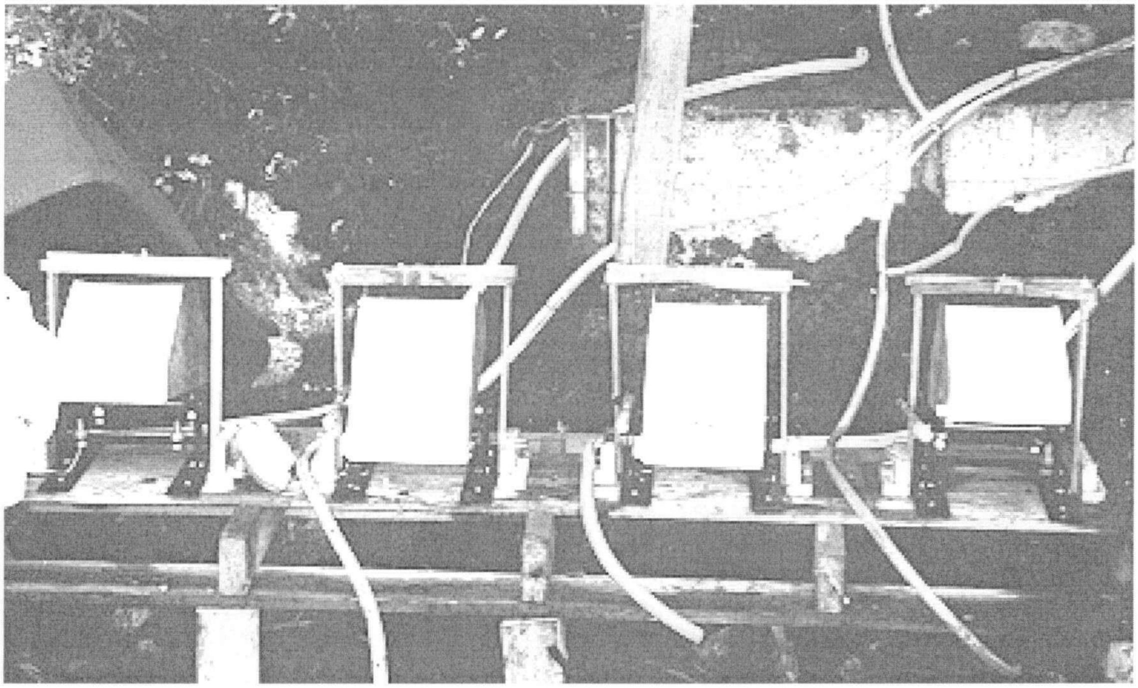

Figure 2.11 A weir at the outlet of Gray Creek study catchment.

2.2.3.2 Measurement of hydraulic conductivities

To estimate hydraulic conductivities of the hillslope soils, 3 piezometers (diameter 0.0127 m) were inserted to the impermeable till layer just above bedrock. One was inserted 11 m upslope of the pit near the groundwater well. The depth of piezometer opening below the soil surface is 1.05 m. Another piezometer was placed 26 m upslope of the pit; depth of opening below soil surface is 0.92 m. The third is located 51 m upslope of pit and depth of piezometer opening below soil surface is 0.73 m. Slug tests were conducted in piezometers by the following procedure:

1) A funnel was placed in the piezometer and water was poured into the funnel until it flowed over the top of the piezometer
2) An electronic water level probe (standard device; ± 0.5 cm of accuracy) was placed in the piezometer. The probe has an open contact that is closed by contact with the water; a light indicates water depth when the contact is closed.
3) Water depths were read every 30 seconds until water level returned to the static/initial level

Hydraulic conductivity is calculated from piezometric data using (Amoozeger and Warrick, 1986):

$$K = \{\pi r^2 / [C(t_{i+1} - t_i)]\} \ln(y_i / y_{i+1}) \qquad (3\text{-}14)$$

where, K is saturated hydraulic conductivity (m/s); r is the radius of the cavity (m); y_i is the difference between the depth of groundwater and the depth of water in the piezometer (m) at time t_i (s); and C is a shape factor (m).

2.2.4 Meteorological data

Measurements of total precipitation, rainfall and temperature were made near the V-notch weir at an elevation of 955 meters. Total precipitation, rainfall, and temperature were measured at 3 m above the ground surface and recorded every 15 minutes with a Unidata Macro high-resolution data logger. Total precipitation was measured by a 41 cm inside diameter PVC standpipe gauge that contained antifreeze for melting snow. The wide diameter of the standpipe gauge prevents bridging or capping of the gauge. A pump mixed the solution to keep the water and antifreeze from separating during periods of low temperature. A pressure transducer that has an accuracy of 0.1% was used to measure fluid level in the gauge. Rainfall was measured by means of a tipping-bucket rain gauge with a 1 mm tip, which gave readings of rainfall intensity and total rainfall volume. Air temperature was measured with ± 0.5 °C of accuracy (Unidata Macro high-resolution data logger).

2.2.5 Snowpack water equivalent

Snow surveys were conducted near the soil pit with a Mount Rose snow sampler. Snow courses were surveyed regularly before and during melt periods to measure snow water equivalent (SWE) between March 24 and July 10, 1999. Eight measurements were taken along the snow course. The distance between measurement points was about 10-12

m. In some cases, the space between snow measurement points was increased to avoid tops of fallen logs, standing trees, groundwater seeps, and over-steepened slopes (Hudson, 2000).

CHAPTER 3

RESULTS

In this chapter the results of the field study are presented. The chapter begins with an evaluation of climatic conditions during the study period compared to longer-term climate patterns. Next, precipitation, pit outflow, water table elevations, and stream discharge data are presented for the snowmelt season of 1999, followed by the rain events (summer-autumn) of 1998-99. Estimates of the hydraulic conductivity of the hillslope segment are then presented. The chapter ends with summaries of the key findings.

3.1 CLIMATIC PERSPECTIVE

The study included the period from October 1998 to November 1999. Daily mean temperature and precipitation during the study period was compared to long-term climate averages (Table 3.1). Average total annual precipitation, based on 1961-1990 climate records from the Atmospheric Environment Service (AES) climate station at Powell River A (elevation 121 m, 49°50-N 124°30), was 1233 mm. Daily mean temperatures ranged from –0.4 °C in January to 11.4 °C in July and August, with an annual average of 4.9 °C. Daily mean temperature difference and the percent departure of precipitation during the study period from the long-term averages are also shown in Table 3.1. Weather in winter 1998-99 was much warmer and wetter than the long-term average. Weather in spring during the study period was cooler than the long-term average. The weather in the summer of 1999 was cooler and drier than the long-term average.

Table 3.1 Comparisons of daily mean temperature and total monthly precipitation between the study period and climate normals (1961-1990) at the Powell River A (elevation 121 m, 49°50-N 124°30).

	Daily mean temperature (°C)			Precipitation (mm)		
	study period	**Climate Normal**	**Difference**	**study period**	**Climate Normal**	**% Departure**
Oct, 98	9.8	9.2	0.6	151.2	151.3	-0.1
Nov	6.7	5.0	1.7	272.2	179.0	52.1
Dec	3.3	2.7	0.6	176.6	171.7	2.9
Jan, 99	4.0	2.3	1.7	202.4	159.4	27.0
Feb	4.2	3.5	0.7	234.6	105.2	123.0
Mar	4.8	5.2	-0.4	142.6	110.9	28.6
Apr	7.5	7.8	-0.3	56.4	72.0	-21.7
May	10.0	11.3	-1.3	101.4	68.2	48.7
Jun	13.5	14.7	-1.2	91.4	61.5	48.6
Jul	16.5	16.9	-0.4	36.0	45.6	-21.1
Aug	17.9	16.9	1.0	55.0	46.8	17.5
Sep	13.6	13.7	-0.1	44.6	61.2	-27.1
Oct	8.8	9.2	-0.4	79.4	151.3	-47.5
Nov	6.6	5.0	1.6	262.8	179.0	46.8

Monthly average, minimum, and maximum temperature and total monthly precipitation during the study period are shown in Figure 3.1. Monthly average air temperature ranged from –2.4 °C to 13.6 °C, with an annual average of 4.6 °C. Total annual precipitation was about 1951 mm, about 65% of which occurred between November and March (41% of this winter precipitation was snow). Snow cover was continuous from winter through spring. Snow course water equivalents in the south coastal drainage area of British Columbia during the past 26 years are shown in Figure 3.2. Their locations are shown in Figure 3.3. Snow course water equivalents in Chapman Creek have been measured since 1993. During 1999, the snow water equivalent was very high compared to past years in this region.

In 1999, snowmelt occurred from April 1 to July 10. This period was much longer than in the previous 5 years (Figure 3.4). The weather during this melt period was generally sunny and clear. Approximately 330 mm of rain fell during the snowmelt season. Daily mean temperature from April 1 to July 10, 1999, ranged from 4.0 °C to 27.7 °C, with an average of 5.8 °C. Comparisons of melt rates and peak snow accumulations at the Gray Creek study site during the past several years are given in Table 3.2. Melt rates were calculated according to

$$M = \frac{\Delta SWE}{\Delta t} \qquad (3.1)$$

Figure 3.1 Monthly average, minimum, and maximum temperature and total monthly precipitation during the study period (98-99) measured at the Gray Creek study site.

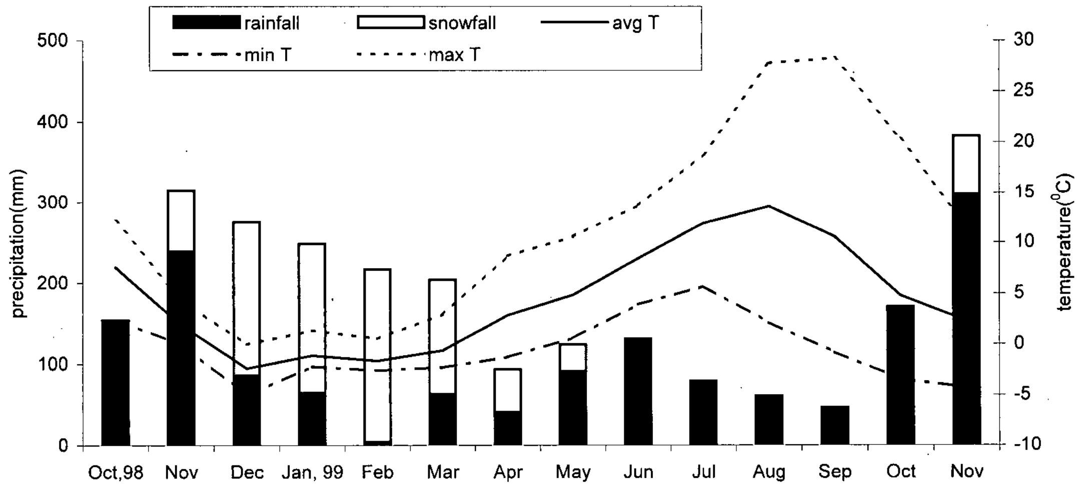

Figure 3.2 Snow course water equivalents measured about April 1 in South Coastal drainage area of British Columbia during 1984-2001

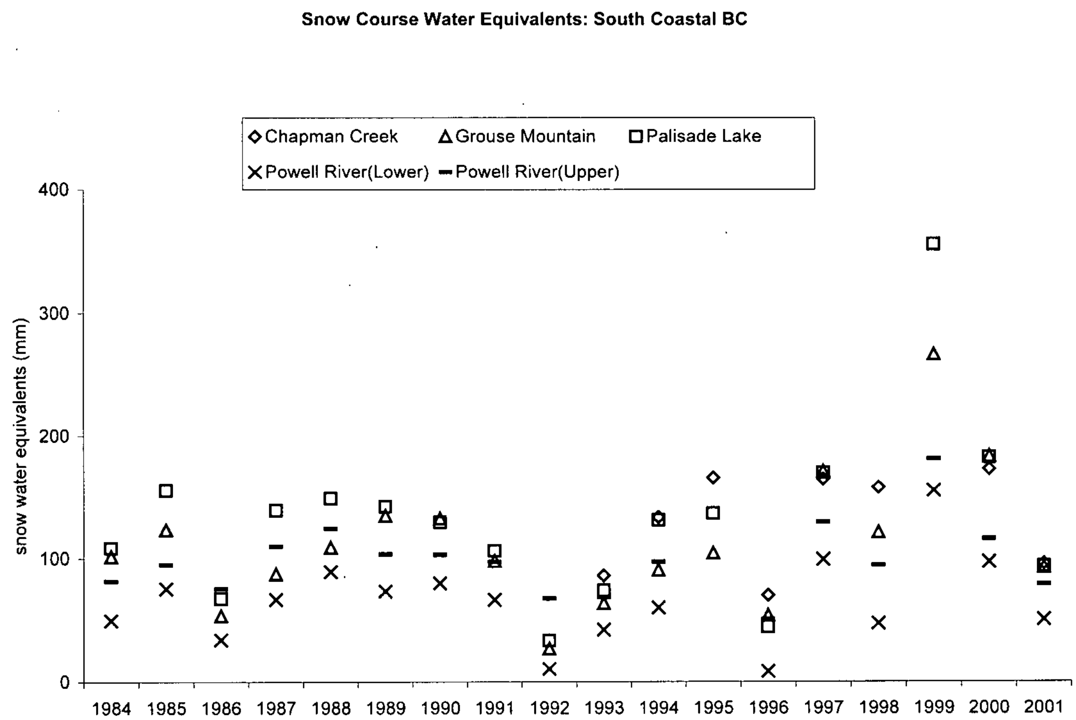

Figure 3.3 Location of snow courses in South Coastal drainage area of British Columbia

	Location	Elevation(m)	Latitude	Longitude
A	Grouse Mountain	1100	49-23	123-05
B	Powell River(Upper)	1040	50-16	124-18
C	Powell River(Lower)	910	50-16	124-19
D	Palisade Lake	880	49-27	123-02
E	Chapman Creek	1020	49-35	123-35

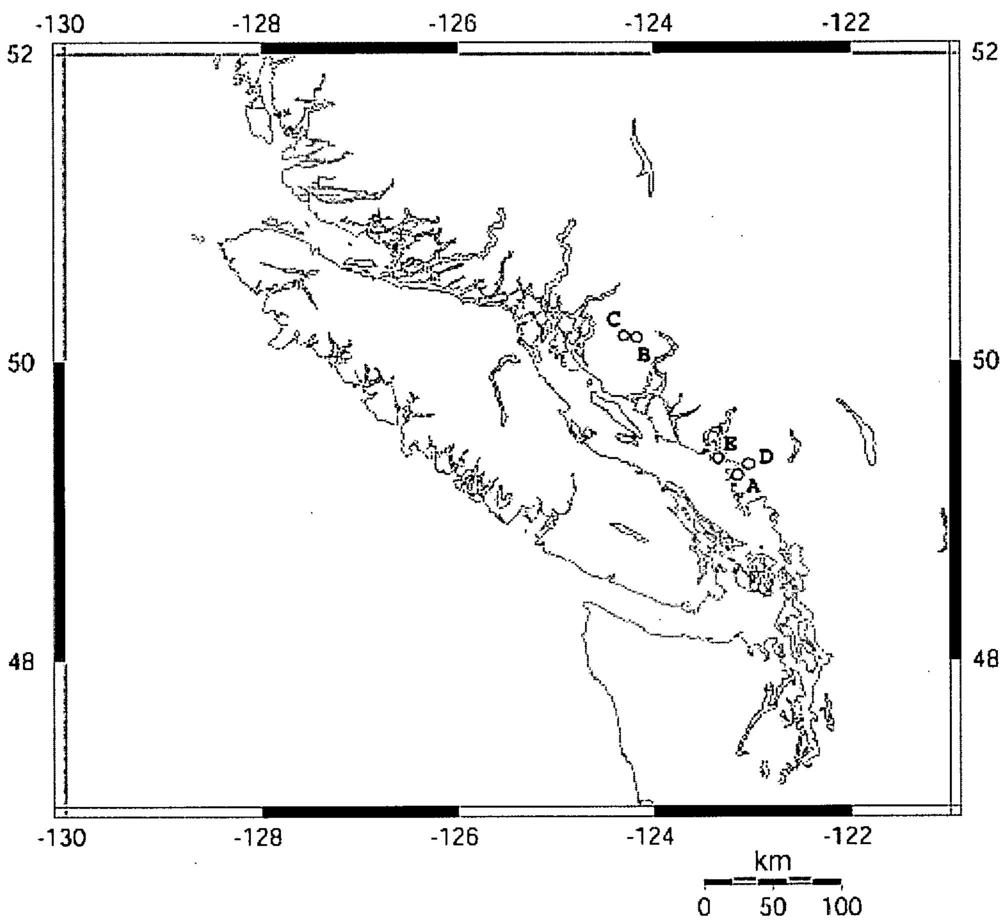

Figure 3.4 Snow water equivalents for 6 years at the Gray Creek study site.

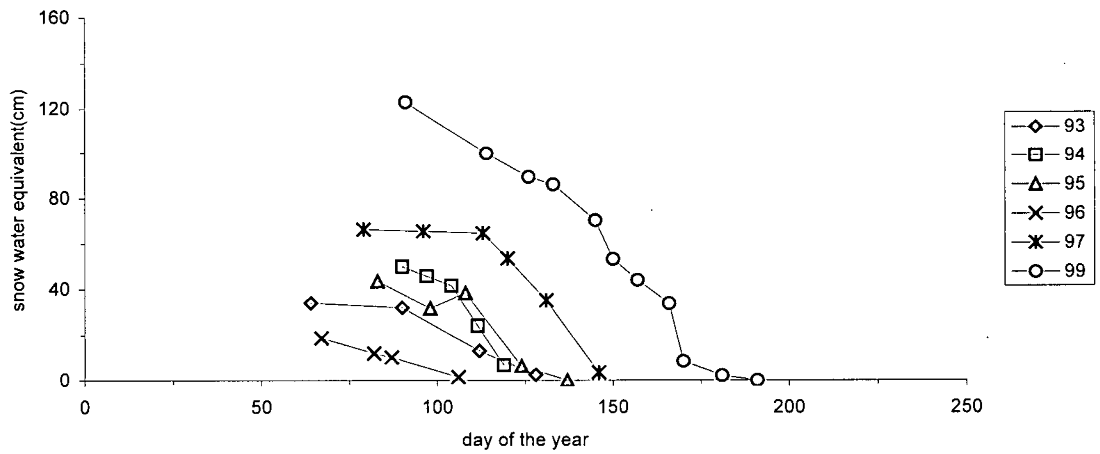

Table 3.2 Snow melt rates and peak snow accumulation at the Gray Creek study site during the past several years.

	1993	1994	1995	1996	1997	1999
melt rates (cm/day)	0.49	1.49	0.81	0.44	1.86	1.23
peak accumulation (cm)	34.4	50	43.6	17.4	66.5	123.1

where M is mean melt rate (cm/day), SWE is snow water equivalent (cm), and t is the calendar day of the year. Two calendar days for t were selected -- initial and final water equivalents of the snow pack.

Peak snow accumulation in 1999 was 1.23 m on April 1, which was much higher than for the past 5 years (Figure3.4). Analyses of snow melt rates and peak snow accumulation data revealed no relation between the two sets of data; no distinguishable trends were observed during the six year period (Table 3.2).

3.2 SNOWMELT SEASON OF 1999

3.2.1 Overview

About 152 mm of rain fell during the spring snowmelt season from June 16 to July 21st, 1999. Daily mean temperature ranged from 2.6°C to 24°C, with an average of 10°C during the monitored portion of the melt season (June 16 to July 21, 1999). Figure 3.5 shows patterns of hourly precipitation (mm), hourly mean temperature (°C) with snow water equivalent (cm), and hydrological responses of streamflow, pit outflow, and water table elevation through the melt season. Notations for hydrographs are summarized in Table 3.3. From July 2, the diurnal fluctuation of hourly mean temperature greatly increased. Pit outflow at the hillslope segment, streamflow for the entire watershed and water table elevation responded similarly to snowmelt and rainfall during the snowmelt season of 1999. Hydrographs for the hillslope segment and the entire watershed had long recession limbs after the last peak flow event. However, there were some different responses between the hillslope segment and the entire watershed.

Figure 3.5 Patterns of hourly precipitation, hourly mean temperature, and snow water equivalent and hydrological responses of stream discharge, pit outflow, and water table elevation through the melt season.

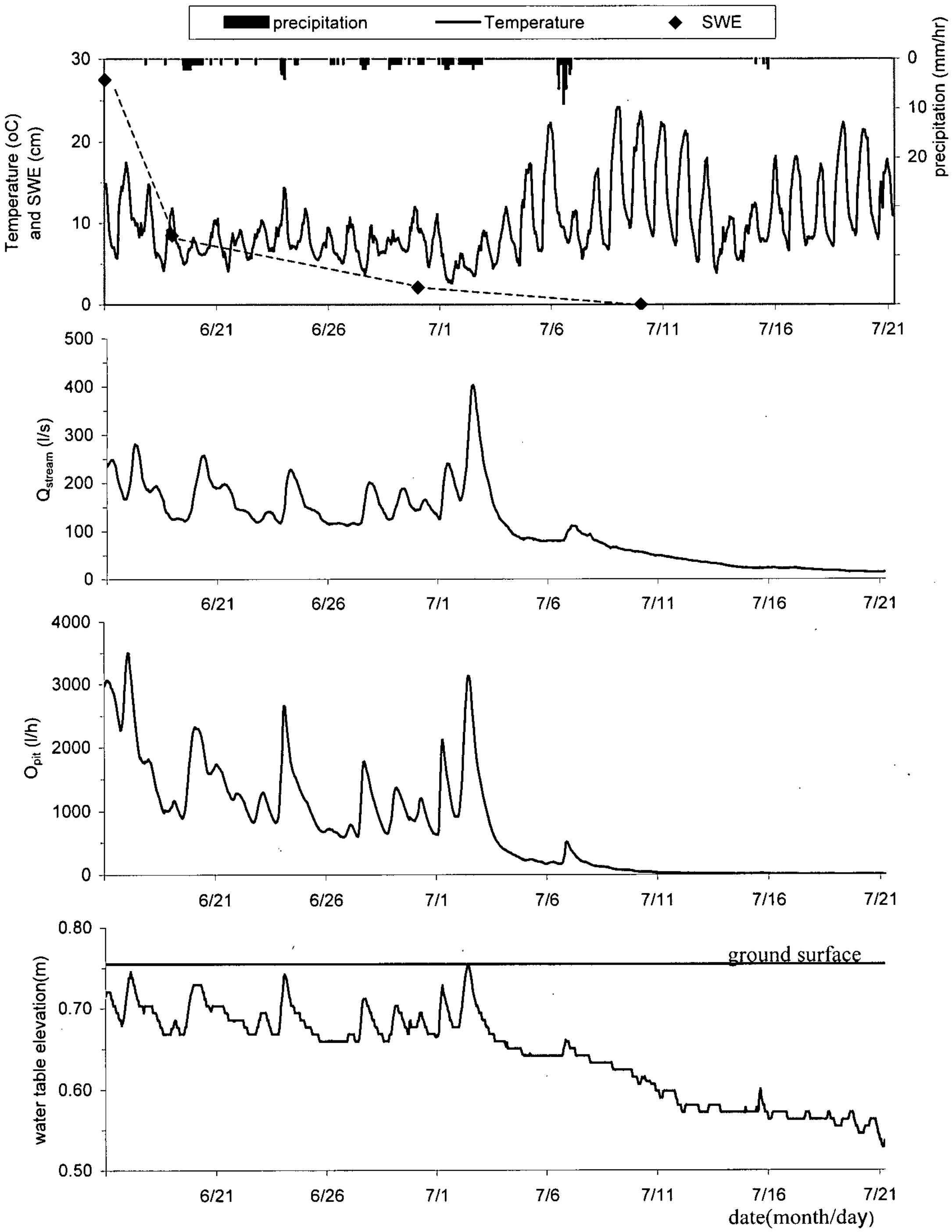

Table 3.3 Notations for hydrographs

O_{pit}= outflow from the pit $= O_{org}+O_{m1}+O_{m2}+O_{m3}$
O_{org}= outflow from the organic layer
O_{mt}= total outflow from the mineral horizon
O_{m1}= outflow from the mineral section 1
O_{m2}= outflow from the mineral section 2
O_{m3}= outflow from the mineral section 3

Both rising limbs and recession limbs of the pit outflow hydrograph were relatively steeper than those of the stream hydrograph. This might indicate the presence of rapid flowpaths to the pit in the hillslope segment or the effects of greater storage opportunity at the catchment scale.

3.2.2 Comparison of pit outflow and stream discharge

3.2.2.1 Comparison of total volumes during melt season

About 152 mm of precipitation, a mixture of rain, fell during the melt period from June 16 (15:00) to July 21 (20:00) 1999 and produced considerable runoff at all scales within the catchment. Total pit outflow from the hillslope segment during the period was 625 m^3 with an average outflow of 738 l/h and a range from 1.20 l/h to 3503 l/h. Total outflow from the mineral horizons in the hillslope segment produced 499 m^3 with an average flow of 590 l/h and a range from 1.20 l/h to 2431 l/h. Total stream discharge during the period was $3.38 \cdot 10^5$ m^3 with an average stream discharge of 0.111 m^3/s, and a range from 0.014 m^3/s to 0.403 m^3/s.

3.2.2.2 Hydrologic and morphologic ratio comparisons

The ratio of total pit outflow (O_{pit}) to total stream discharge (Q_{stream}) from June 16 to July 21, 1999 is

$$R_{qpit} = \frac{O_{pit}}{Q_{stream}} \qquad (3\text{-}2)$$

A similar ratio for total outflow from the mineral horizon (O_{mt}) of the pit is

$$R_{qmt}=\frac{O_{mt}}{Q_{stream}} \tag{3-3}$$

The ratio of pit length (L_{pit}) to the length of streambank seepage faces (L_w) in the entire watershed is

$$R_L=\frac{L_{pit}}{L_w} \tag{3-4}$$

The ratio of the topographically defined contributing area of the pit (A_{pit}) to watershed area (A_w) is

$$R_A=\frac{A_{pit}}{A_w} \tag{3-5}$$

The ratios calculated from equations 3-2, 3-3, 3-4, and 3-5 are summarized in Table 3.4. Ratios of the total observed pit outflow to total stream discharge (R_{qpit}) were about 2 to 4 times higher than either R_L or R_A.

Table 3.4 Comparison ratio of total pit outflow/streamflow to other ratios: during monitored melt period from June 16 to July 21, 1999.

	R_{qpit}	R_{qmt}	R_L	R_A
	Q_{pit} / Q_{stream}	Q_{mt} / Q_{stream}	L_{pit} / L_w	A_{pit} / A_w
Ratio	$1.80 \cdot 10^{-03}$	$1.50 \cdot 10^{-03}$	$0.70 \cdot 10^{-03}$	$0.4 \cdot 10^{-03}$

3.2.2.3 Calculation of effective contributing area for snowmelt period

The effective area contributing to pit drainage was estimated by three different methods. The first method was based on hillslope topography. The contributing area of the pit was computed from an actual topographic survey using the program SURFER (Golden Software, 1994), which determined effective contributing area up to 51 m above the soil pit.

The second method to estimate contributing area was based on runoff volume. Contributing area of the soil pit was computed based on the ratio of total snowmelt pit runoff versus total snowmelt stream discharge, as follows:

$$A_{pit} = \frac{Q_{pit} \bullet A_w}{Q_{stream}} \qquad (3\text{-}6)$$

The third method to estimate effective contributing area to pit drainage was based on water balance calculations. A simple water balance can be expressed as follows:

$$Q_{pit} = (P - (W_2 - W_1) - E - \Delta S) A_{pit} \quad (3\text{-}7)$$

$$A_{pit} = \frac{Q_{pit}}{(P - (W_2 - W_1) - E - \Delta S)} \quad (3\text{-}8)$$

where P is precipitation (mm); W_1 and W_2 are initial and final water equivalents of the snow pack (mm) respectively; E is evaporation losses; and ΔS is change in soil moisture storage. Measurements of evaporation malfunctioned due to heavy snowpack. E was assumed to be 0 during the relatively short periods used. Although ΔS can be assumed to be 0 for long periods (e.g., at least 1 year), ΔS might be negligible during the snowmelt season because the water table was high (i.e., soils are likely near saturation during the period from June 16 to 19, 1999; Figure 3.5). This assumption may slightly underestimate the effective contributing area of soil pit drainage calculated using the outflow method (equation 3.8). During the period from June 16 to 19, 1999, total pit outflow was 154 m^3, 2 mm of rain fell, and snow water equivalent decreased by 192 mm.

Table 3.5 Comparisons of three different methods to estimate effective contributing area to pit drainage during the snowmelt season of 1999.

Topographic survey (m^2)	Runoff volume ratio (m^2)	Water balance calculations (m^2)
635	2759	801

The effective areas that contribute to pit drainage as calculated by the three different methods are summarized in Table 3.5. The effective contributing area calculated by the runoff volume ratio was much higher than estimates by the topographic survey or water balance calculation.

3.2.2.4 Timing of peak flows

To understand whether subsurface flow can respond quickly enough to inputs of rain that occurs during the snowmelt season and snowmelt to be considered a significant source of stormflow (as opposed to contributing only to baseflow), the timing of peak outflows from the pit (including organic horizon) and the mineral horizon were compared to the timing of peak stream discharge at the weir. During the melt period, pit outflow (including outflow from the organic horizon) might not be truly generated as subsurface flow because the water table rose to near the ground surface. Outflow from the organic horizon might include some saturation overland flow via return flow from the mineral soil into the organic horizon and deflection of rainfall and snowmelt infiltrating to the saturated area in the organic horizon. However, outflow from the mineral horizon can be considered as a true subsurface flow. These peak discharge comparisons were made for both daily and aggregated values for the monitored portion of the melt season.

The simultaneous discharges from the entire pit and mineral horizon draining the hillslope segment and for the entire catchment are plotted in Figure 3.6. Outflow from the pit, the mineral horizon, and streamflow responded similarly to inputs of rain and snowmelt. Hydrographs of both the pit and the mineral horizon consistently had relatively steeper rising and falling limbs compared to the streamflow hydrograph.

Table 3.6 compares the timing and magnitudes of daily peak outflows from the pit and the mineral horizon to those of daily peak stream discharge. For 16 consecutive days during the melt season, lag times ranged from 1 to 7 h between peak flows from the pit and the stream discharge and also between outflow from the mineral horizon and the stream discharge. The timing of daily peak outflows from the pit and the mineral horizon generally occurred in the late afternoon; however, comparison of daily events revealed no distinct trends in relative timing of daily peak outflows. Daily peak stream discharge usually occurred late in the evening; however, no relation was observed between daily peak discharge and time throughout the melt season. Ratios between peak outflow from the pit and stream discharge and also between peak outflow from the mineral horizon and stream discharge varied from day to day (Figure 3.7). The ratios of peak pit outflow and peak mineral horizon outflow to peak stream discharge averaged 0.0024 and 0.0019, respectively, over the 16-day period. Accumulated pit outflow and mineral horizon outflow contributed 0.0018 and 0.0015 of total stream discharge. Thus, pit outflow and

Figure 3.6 Simultaneous plots of pit outflow, outflow from mineral horizon, and stream discharge, in accordance with rainfall.

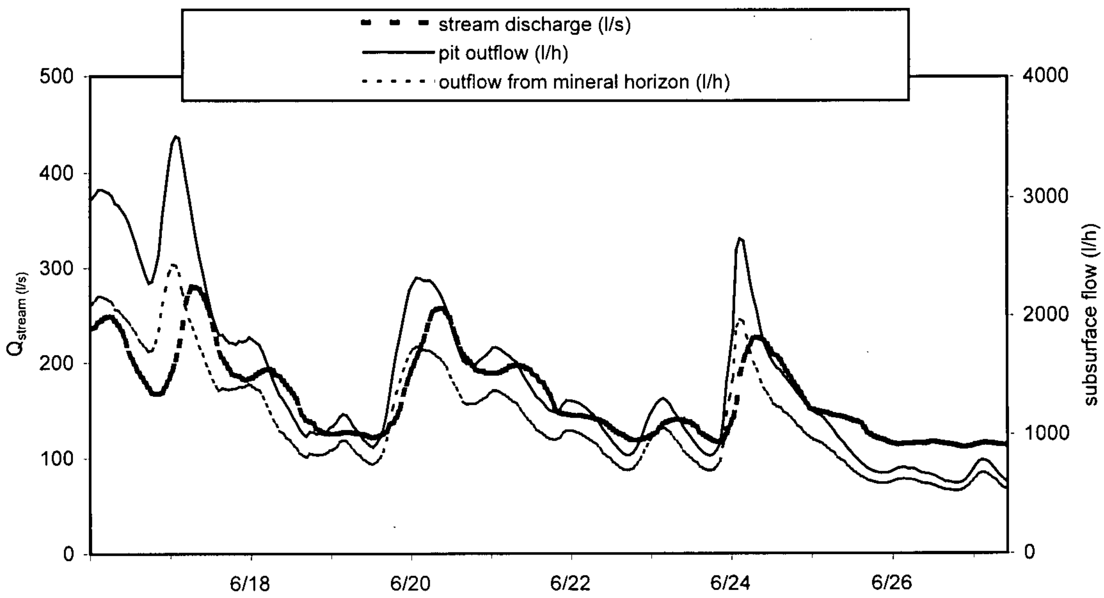

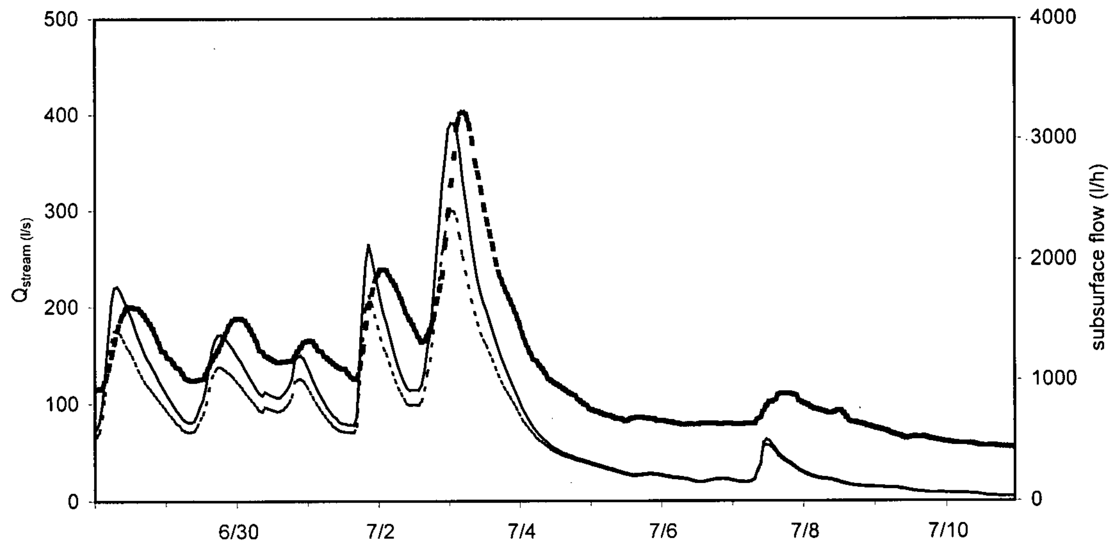

Table 3.6 Comparison of the timing and magnitudes of daily peaks among outflow from pit, outflow from the mineral horizon, and stream discharge for 16 daily events during the 1999 melt season.

	The timing of daily peaks			Magnitudes of daily peaks			Ratio of magnitudes of daily peaks	
	pit	mineral horizon	stream discharge	O_{pit}(l/h)	O_{mt}(l/h)	Q_{stream}(l/h)	O_{pit}/Q_{stream}	O_{mt}/Q_{stream}
6/16/99	18:00	18:00	20:00	3062	2156	895644	0.0034	0.0024
6/17/99	16:00	15:00	21:00	3503	2431	1011096	0.0035	0.0024
6/18/99	14:00	14:00	20:00	1818	1425	697887	0.0026	0.002
6/19/99	18:00	18:00	20:00	1169	953	457812	0.0026	0.0021
6/20/99	16:00	16:00	23:00	2315	1739	925731	0.0025	0.0019
6/21/99	16:00	16:00	22:00	1733	1370	713394	0.0024	0.0019
6/23/99	18:00	18:00	0:00	1301	1058	506376	0.0026	0.0021
6/24/99	17:00	17:00	22:00	2654	1968	818244	0.0032	0.0024
6/26/99	18:00	18:00	22:00	723	625	419580	0.0017	0.0015
6/27/99	17:00	17:00	18:00	785	682	419580	0.0019	0.0016
6/28/99	8:00	7:00	12:00	1774	1401	723852	0.0025	0.0019
6/29/99	19:00	19:00	0:00	1370	1108	675864	0.0020	0.0016
6/30/99	22:00	22:00	1:00	1202	1011	595044	0.0020	0.0017
7/01/99	21:00	21:00	1:00	2116	1696	862236	0.0025	0.0020
7/03/99	1:00	1:00	5:00	3129	2404	1451412	0.0022	0.0017
7/07/99	12:00	12:00	17:00	509	465	398763	0.0013	0.0012

Figure 3.7 Comparison between ratio of peak outflow from pit / peak stream discharge and ratio of peak outflow from mineral horizon / stream discharge among 16 daily events throughout the melt season.

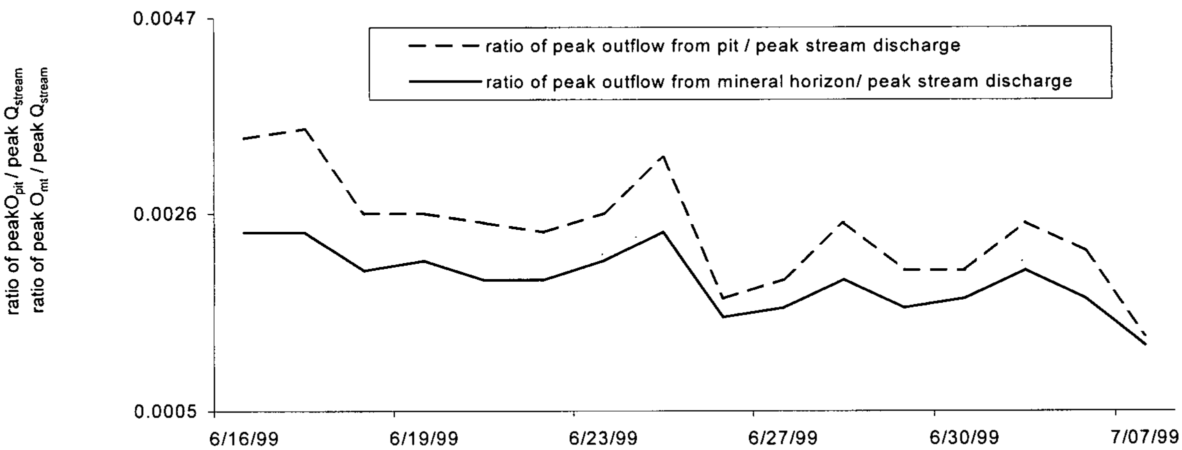

mineral horizon outflow from the hillslope segment appear to be the "flashier" than stream discharge during the snowmelt study period.

To investigate whether routing could explain the lag time between peak outflow from the hillslope segment and peak stream discharge, lag times were plotted against peak stream discharge (Table 3.7, Figure 3.8). The relation between lag times and peak stream discharge was weak, even though we would expect lag times during higher peak discharges to be lower if channel routing caused lags.

Cross-correlation analysis was used to estimate an aggregated lag time between pit outflow and stream discharge (as opposed to the lags) based on peak flows for the monitored portion of the melt season. This procedure compares two time series at successive lags, and is applied to snowmelt data from June 16 to July 21, 1999. The cross-correlation function, cc(τ), is computed as

$$cc(\tau) = \frac{\sum (X(t)-\overline{X})(Y(t+\tau)-\overline{Y})}{\left[\sum \left(X(t)-\overline{X}\right)^2 \sum \left(Y(t+\tau)-\overline{Y}\right)^2\right]^{1/2}} \qquad (3\text{-}9)$$

where X(t) is the hourly hillslope outflow series from the pit (including mineral horizon outflow); Y is the hourly stream discharge series at time t; τ is a lag; and $\overline{X}$ and $\overline{Y}$ are average hillslope outflow and stream discharge, respectively. Negative time lags indicate lagged stream discharge. For example, cc(-1) represents the correlation between the current hillslope outflow and the stream outflow in the preceding hour. Positive time lags

Table 3.7 The summary of lag time between peak outflow from the pit and peak stream discharge among 16 daily events

Date	lag time (h)	peak stream discharge(l/s)
6/16	2	248.8
6/17	5	280.9
6/18	6	193.9
6/19	2	127.2
6/20	7	257.1
6/21	6	198.2
6/23	6	140.7
6/24	5	227.3
6/26	4	116.6
6/27	1	116.6
6/28	4	201.1
6/29	5	187.7
6/30	3	165.3
7/1	4	239.5
7/3	4	403.2
7/7	5	110.8

Figure 3.8 Relations between lag time and peak stream discharge of 16 daily events during the 1999 snowmelt season.

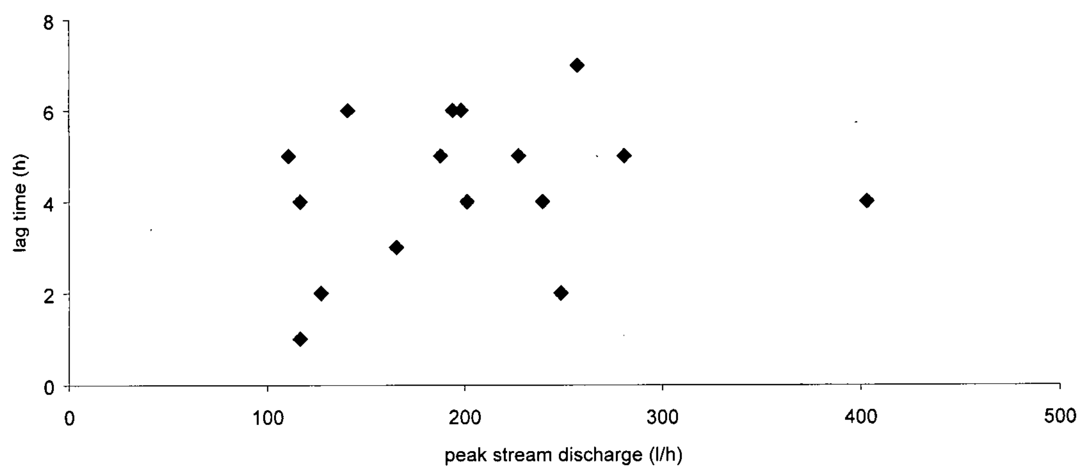

where lag time is time difference between peak outflow from the pit and peak stream discharge in daily event basis.

are correlations between the current hillslope outflow and the stream discharge at earlier times.

During the snowmelt season, the maximum cross-correlation between outflow from the pit and stream discharge was 0.93 for a lag of 4 hr (Figure 3.9). For the same time period, the maximum cross-correlation between outflow from the mineral horizon and stream discharge was 0.95 for a lag of 4 hr (Figure 3.10). The cross-correlations between outflow from the pit and stream discharge and between outflow from the mineral horizon and stream discharge display flattened responses for lags between 20 and 28 hours and between –20 and –28 hr as a result of diurnal fluctuation.

3.2.3 Variability of outflow within the pit

3.2.3.1 Time series graphs

Outflows from the organic horizon and individual sections of the mineral horizon were plotted during the snowmelt season in order to understand temporal patterns (Figure 3.11). Outflows from the organic horizon, mineral section 1, and mineral section 2 had similar response to precipitation. However, hydrographs from section 3 were different. Peak outflows from the organic horizon, mineral section 1, and mineral section 2 were 1132 l/h, 2016 l/h, and 365 l/h, respectively during the maximum melt period. During the maximum melt period, outflow from the mineral section 3 was only 120 l/h, but by the last rainfall event of the melt season (July 5), peak outflow from mineral section 3 increased to 535 l/h.

Figure 3.9 Cross-correlation between outflow from the pit and stream discharge during the monitored portion of the melt season of 1999.

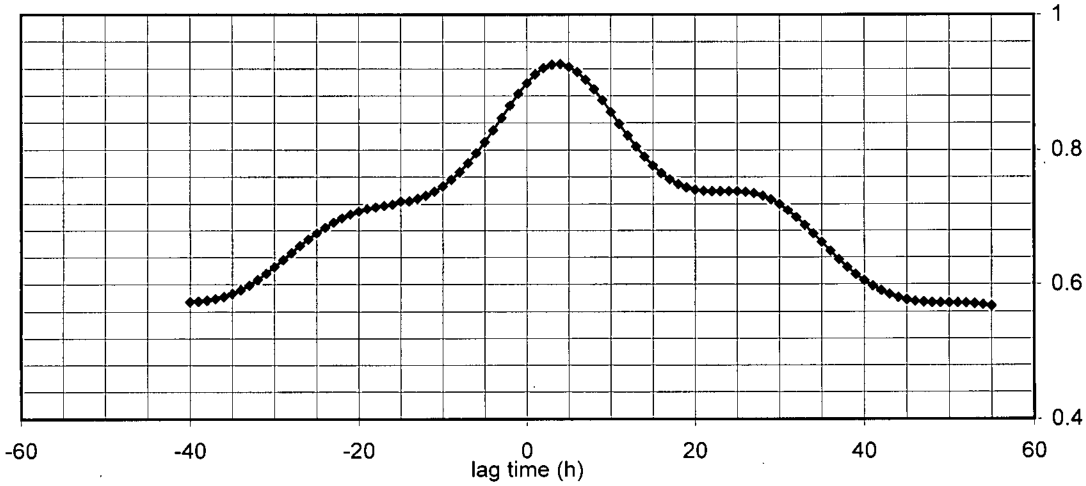

Figure 3.10 Cross-correlation between outflow from the mineral horizon and stream discharge during the monitored portion of the melt season of 1999.

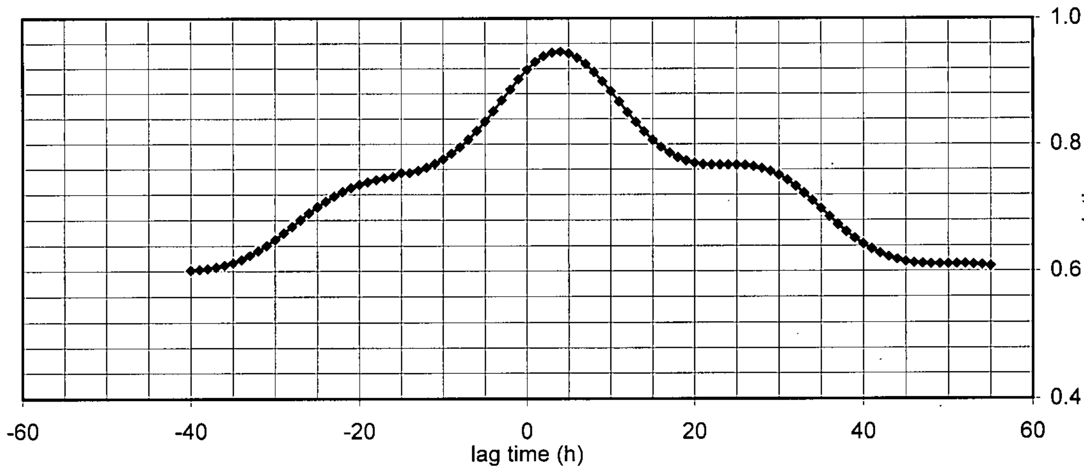

Figure 3.11 Observed subsurface outflows from the organic horizon and individual sections of the mineral horizon during the melt season from June 16 to July 21, 1999.

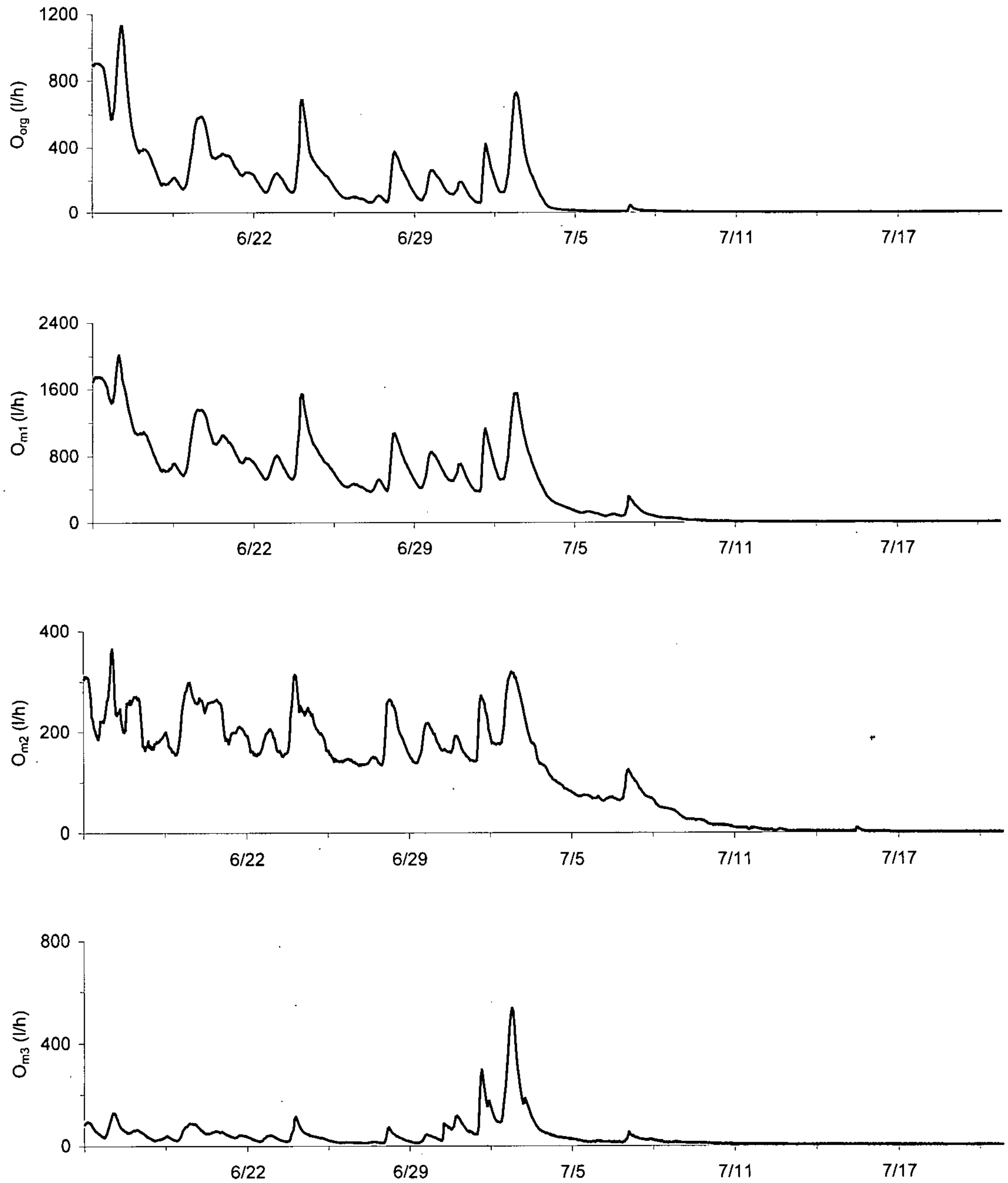

3.2.3.2 Computation of total volumes during the melt season

The total pit outflow during the spring snowmelt season from June 16 to July 21, 1999, was 624.7 m^3. Outflows from components of the pit and their relative contribution to pit outflow are summarized in Table 3.8. The outflow from the organic horizon contributed significantly to pit outflow during the peak of the melt season. Outflow from mineral section 1 contributed 59% of the pit outflow due to coarse, permeable soil with high gravel and rock content. These findings indicate that different hydrologic flowpaths occur within the pit for different soil characteristics.

3.2.3.3 Timing of peak flows from the organic horizon and the mineral sub-sections

Daily peak flow regimes from the organic and mineral horizons are summarized for 16 consecutive days during the melt season in Table 3.9. Peak outflow from the organic horizon responded later than peak outflow from the mineral horizon during 5 of the 16 days. On June 20, peak outflow from the organic horizon occurred 4 hr later than from the mineral horizon; 2 mm of rain fell between these two peak discharges. Peak flow from the organic horizon appeared to rely on peak outflow from the mineral horizon. Depending on soil characteristics, peak flows from individual mineral soil sections occurred within half an hour or less. Mineral section 1 had the fastest time to peak and section 2 had the slowest.

Table 3.8 Total outflow volumes from various components of the pit and their relative contributions to pit outflow

Pit outflow components	Total outflow (m^3)	Contribution to pit outflow (%)
Orgainc horizon	125.4	20
Mineral section 1	369.7	59
Mineral section 2	97.4	16
Mineral section 3	32.2	5

Table 3.9 Comparison of the timing of daily peaks within pit of 16 daily events during snowmelt season in 1999.

	The timing of daily peaks					
	pit	organic horizon	mineral horizon	mineral section 1	mineral section 2	mineral section 3
6/16	18:00	18:00	18:00	18:00	16:00	18:00
6/17	16:00	18:00	16:00	15:00	17:00	17:00
6/18	14:00	14:00	14:00	14:00	17:00	17:00
6/19	18:00	19:00	18:00	18:00	18:00	19:00
6/20	16:00	20:00	16:00	17:00	16:00	16:00
6/21	16:00	16:00	16:00	15:00	17:00	15:00
6/23	18:00	18:00	18:00	18:00	18:00	18:00
6/24	17:00	18:00	17:00	17:00	17:00	17:00
6/26	18:00	18:00	18:00	18:00	18:00	16:00
6/27	17:00	17:00	17:00	17:00	17:00	17:00
6/28	8:00	8:00	8:00	8:00	8:00	7:00
6/29	19:00	19:00	19:00	19:00	20:00	18:00
6/30	22:00	22:00	22:00	22:00	22:00	22:00
7/01	21:00	21:00	21:00	21:00	21:00	21:00
7/02	1:00	2:00	1:00	1:00	1:00	1:00
7/03	12:00	12:00	12:00	12:00	13:00	13:00
Average	15:41	16:15	15:41	15:37	16:00	15:45

3.2.3.4 Dependence of organic horizon outflow on mineral horizon outflow

Relations between outflow from the organic horizon and outflow from the mineral horizon components clearly showed that in order to generate organic horizon outflow, threshold values of outflow from the mineral horizon were required, especially for mineral sections 1 and 2 (Fig 3.12). Outflow from mineral section 3 exhibited a different pattern; during the main melt period (June 16 to June 29) outflow rates were < 150 l/h (indicated by the highlighted points on Fig 3.12). For this low outflow period, lateral flow within the organic horizon was much higher than from the respective mineral horizon. Snow and rain fell on the soil surface and infiltrated into the soil. A portion of the soil water appeared to move above the less permeable mineral horizon in section 3 instead of the entire volume of water infiltrating vertically to bedrock or till. During the last portion of the main melt period (June 30 to July 3), outflow rates from the mineral section 3 increased significantly (Fig. 3.12). During this later period, outflow from the organic horizon followed similar patterns as other graphs with gentler slopes and broader ranges of outflow. To generate outflow from the organic horizon during the last portion of the main melt period (June 30 to July 3), a threshold of outflow from the mineral section 3 was required. Threshold outflow requirements for the overall mineral horizon and individual sections are summarized in Table 3.10.

Figure 3.12 Relations between flow from the organic horizon and flow from individual mineral sections during snowmelt season in 1999.

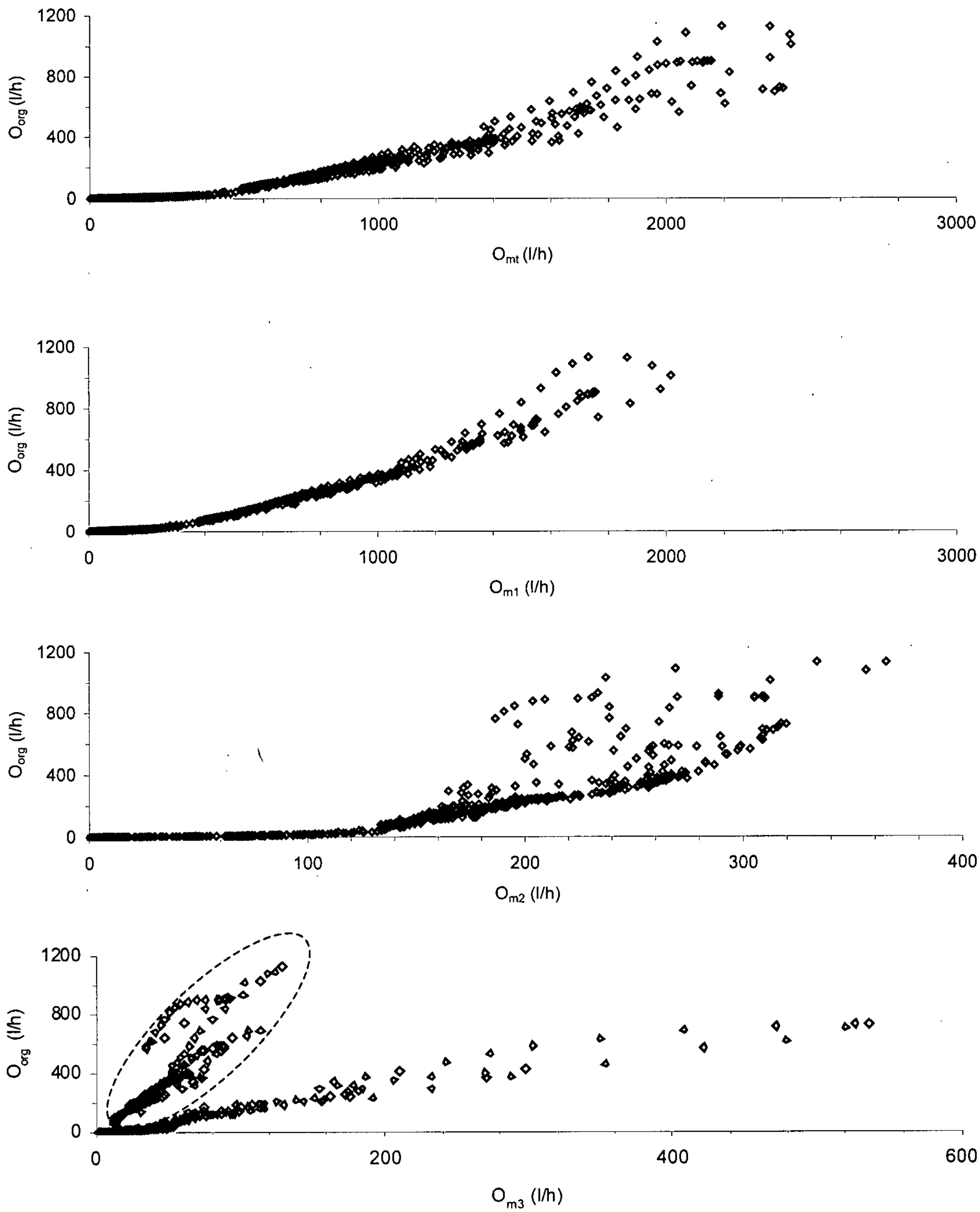

Table 3.10 Threshold values of outflow from mineral horizon and individual mineral sections require to generate organic horizon outflow during snowmelt season in 1999.

The threshold values of outflow (l/h)			
mineral horizon	mineral section 1	mineral section 2	mineral section 3
478.4	300	132	46.4

3.2.3.5 Distribution of outflow among plot sections

The fraction of outflow from the organic horizon and individual mineral sections (compared to total mineral horizon outflow) are plotted in Figure 3.13. Mineral horizon outflow was arbitrarily categorized as: low (< 400 l/hr); medium (400-2000 l/h); and high (>2000 l/hr). For low flow conditions, the fractional flow from the organic horizon was consistently around 0.05. However, during medium and high mineral horizon outflows, this fractional value increased rapidly to approximately 0.35. Fractional outflow from mineral section 1 increased during low flows from 0.24 to 0.57; however, once the value of 0.57 was reached, the ratio was more or less consistent for all higher flows. The fractional outflow from mineral section 2 decreased from 0.44 at lower flows to 0.14 during medium mineral horizon outflows and 0.1 during high flows. For the lowest mineral horizon outflows, mineral section 3 contributed significantly. For outflows greater than 100 l/h from the mineral horizon, section 3 contributed only about 0.1 of total outflow regardless of volume. These results clearly show that the fraction of outflow from the organic horizon and individual mineral sections varied with changes in mineral horizon outflow.

To examine whether the flow ratios were consistent throughout the snowmelt season, fractional outflows from the individual pit segments and the organic horizon were plotted against time (Figure 3.14). Ratios of organic horizon outflow to mineral horizon outflow exhibited daily fluctuations but these fluctuations decreased with time. At the end of melt season, the ratios reached a rather consistent value of 0.05. The ratios of

Figure 3.13 The fraction of flow from the organic horizon and individual mineral sections (compared to total mineral horizon outflow)

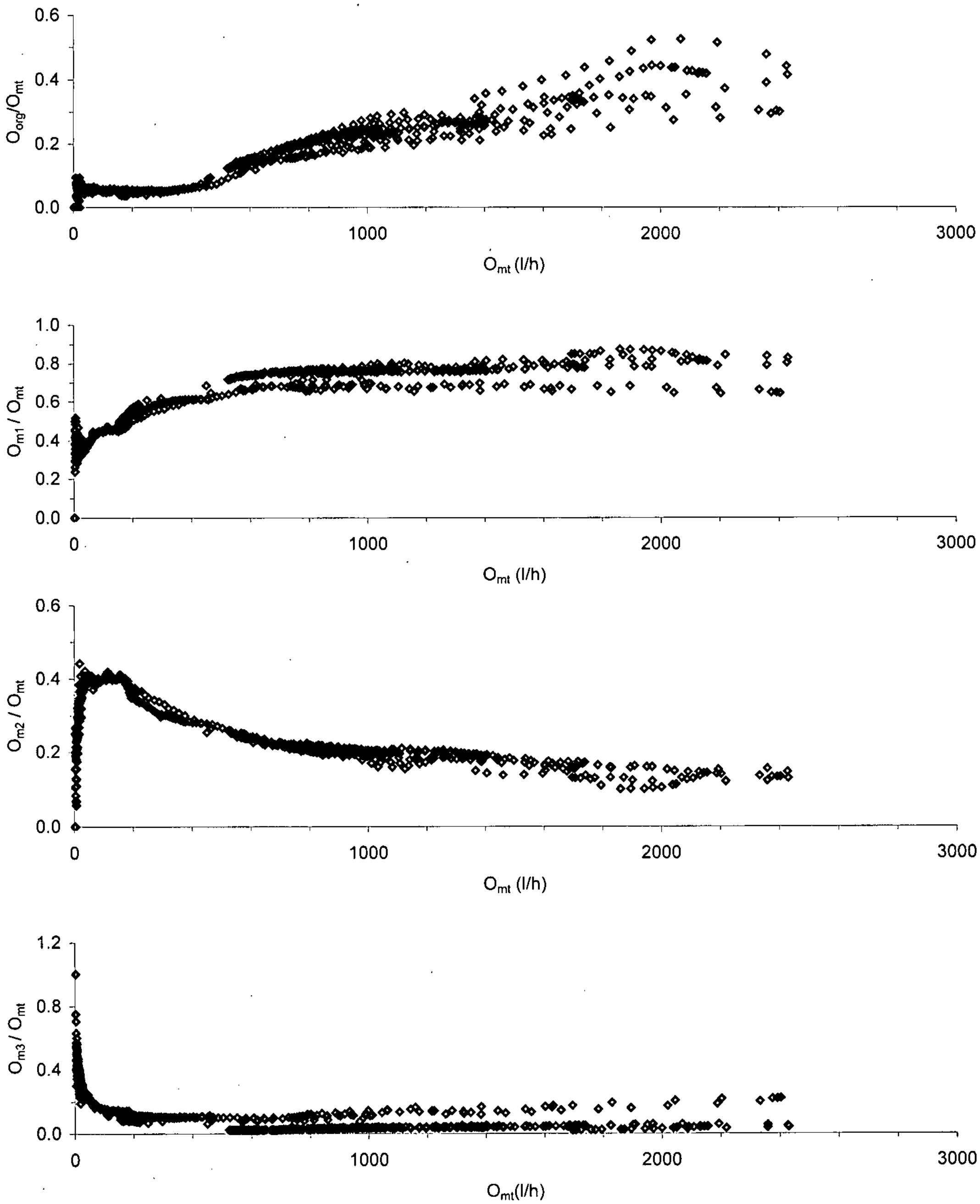

Figure3.14 The fractional outflow from the organic horizon and individual mineral sections throughout the snowmelt season.

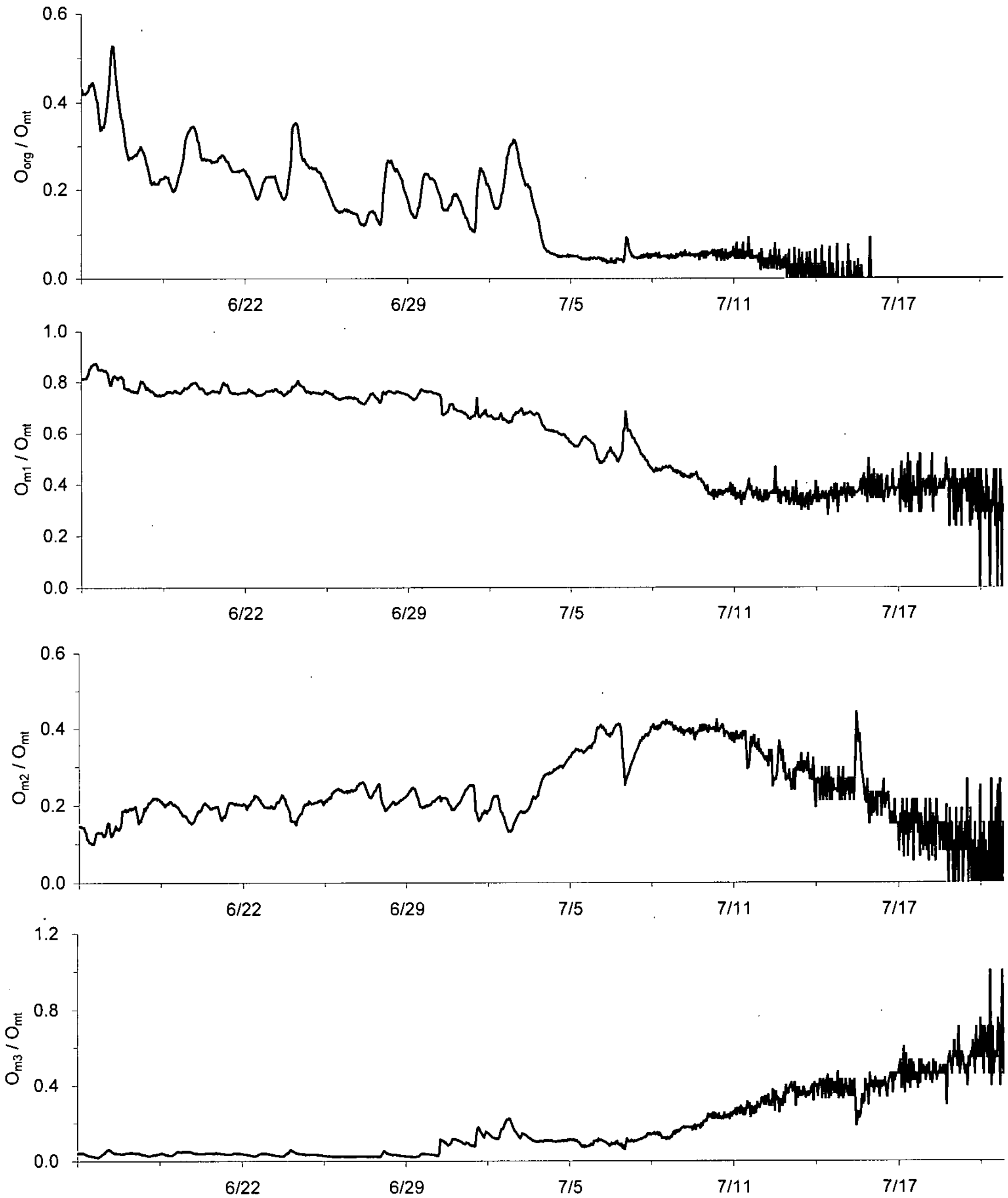

mineral section 1 outflow versus mineral horizon outflow declined gradually from about 0.8 (early in the period) to about 0.5 later in the melt season. By the end of the melt season these ratios declined to a rather consistent value of 0.35. Outflow from mineral section 2 exhibited irregular patterns of contribution to mineral horizon outflow with time ranging from 0.1 to 0.4. Ratios of outflow from the mineral section 3 were consistently low (<0.1) during most of the melt period; in the later part of the melt season this ratio first increased slowly followed by a rapid increase up to 1.0 at the end of the melt season. These results confirm that ratios of organic horizon outflow versus mineral horizon outflow and individual mineral section outflow versus pit outflow varied throughout the melt season.

3.2.4 Relation between pit outflow and water table elevation

In order to determine whether there is a relation between water table elevation and hillslope discharge, both pit outflow and mineral horizon outflow were plotted against water table elevation throughout the melt season (Figures 3.15 and 3.16). Outliers on these graphs occurred from the beginning of the observed melt periods to the end of rising limb of June 17 event (indicated by highlighted points on the graphs). During these anomalous periods, high flow rates were measured from both the pit and mineral horizon (>2000 l/h and >1600 l/h, respectively). Mineral horizon outflow (not including organic horizon outflow) was plotted against the water table elevation since only true subsurface flow was of interest (as discussed earlier, outflow from the organic horizon might be generated as a saturation overland flow via return flow from the mineral soil into the organic horizon and deflection of rainfall and snowmelt infiltrating to the saturated area

Figure 3.15 Relations between outflow from the pit and water table elevation during the monitored portion of the melt season of 1999.

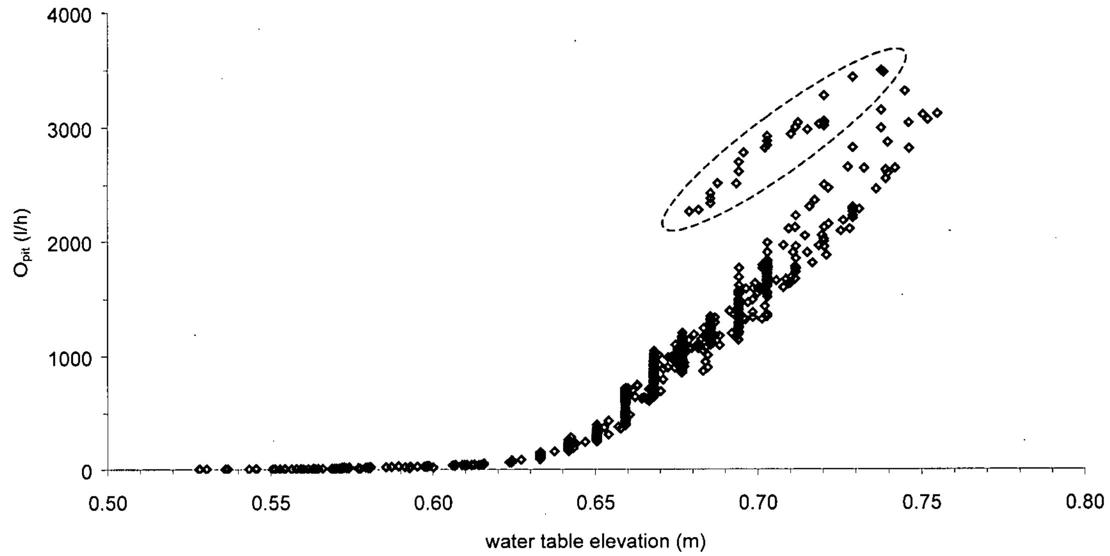

Figure 3.16 Relations between outflow from the mineral horizon and water table elevation during the monitored portion of the melt season of 1999.

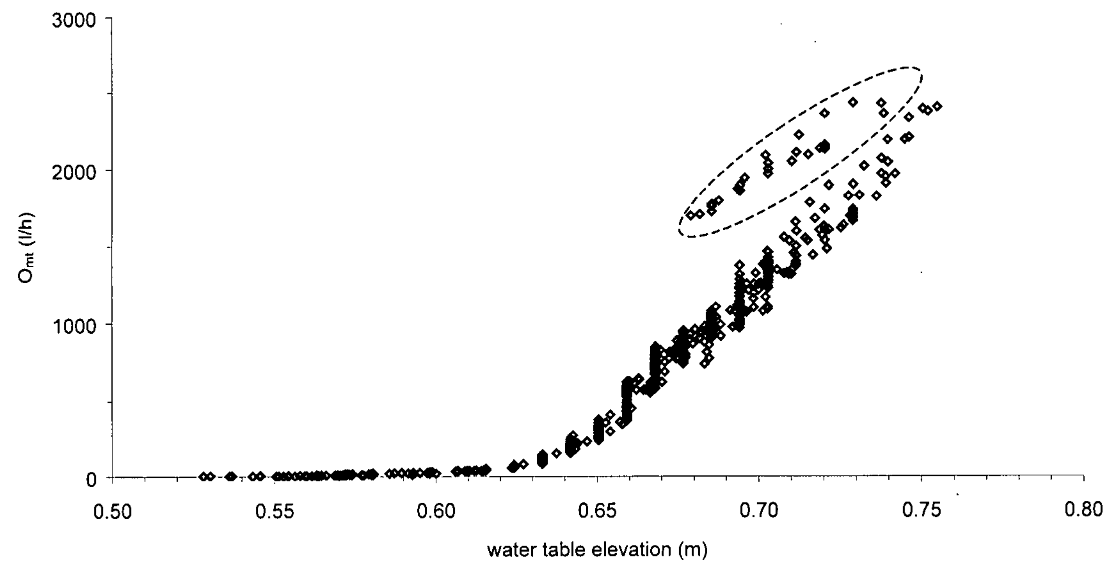

of the organic horizon). Both pit outflow and mineral horizon outflow were highly correlated with water table elevations recorded upslope of the pit.

The minimum water table elevation in both graphs was 0.53 m; thus 70% of the soil depth was below the water table (Figure 3.15 and 3.16). As water tables rose to 0.62 m, very little increase in pit outflow and mineral horizon outflow was evident. However, as water tables rose above 0.62 m both pit outflow and mineral horizon outflow increased markedly. After this response, graphs showed a distinct hysteresis pattern between rising and falling outflow limbs. A possible reason for this hysteresis is the existence of different flow pathways between rising and falling outflow limbs. Pit outflow was plotted against water table elevation for 3 days to illustrate this hysteresis effect (Figure 3.17). In the June 17 event, clockwise hysteresis was evident; the rising limb was higher than the falling limb of pit outflow for the same water table elevation. At the beginning of the melt period, predictions of outflow based on observed water table elevation approximately 11 m above the pit are uncertain. As such, this (June 17) event may indicate a "conditioning period". For the June 24 and July 2 events, counter-clockwise hysteresis patterns were observed. This hysteresis is not as marked (i.e., the distance between rising and falling limbs is smaller than for the June 17 event). Falling limbs of pit outflows were higher than rising limbs for the same water table elevation. Many days during the snowmelt period did not exhibit this hysteresis pattern of flow. However, where clear differences between rising and falling limbs were observed, all patterns were counter clockwise, except day 1.

Figure 3.17 Relations between outflow from the pit and water table elevation for individual events during the monitored portion of the melt season of 1999.

June 17 event

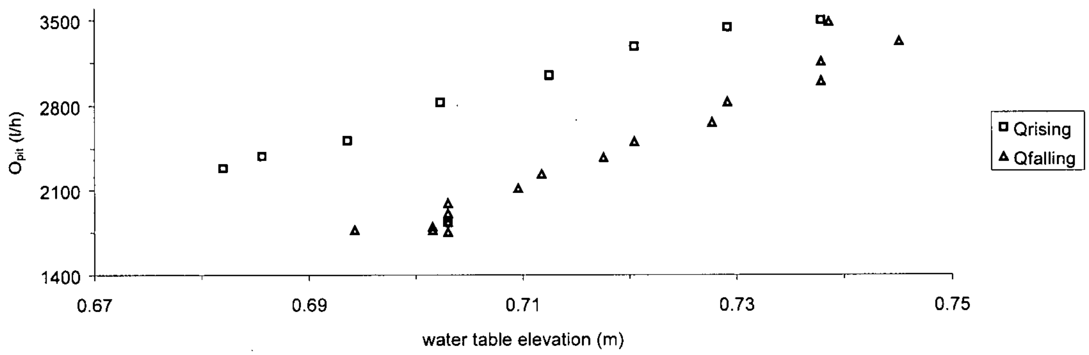

June 24 event

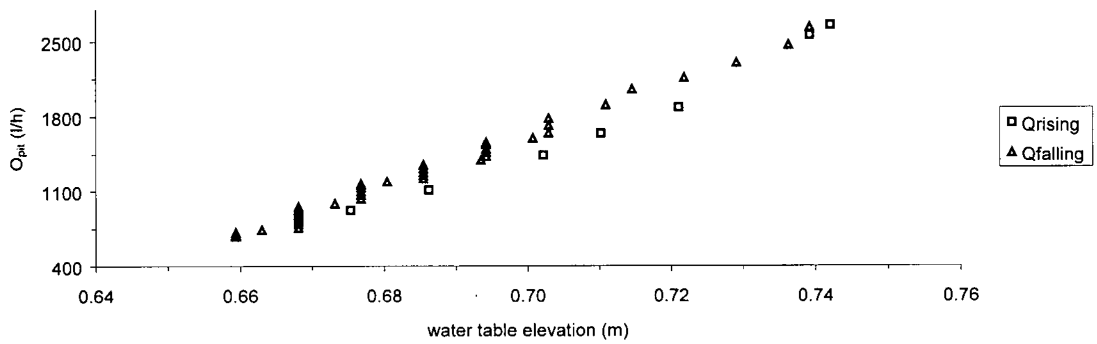

July 2 event

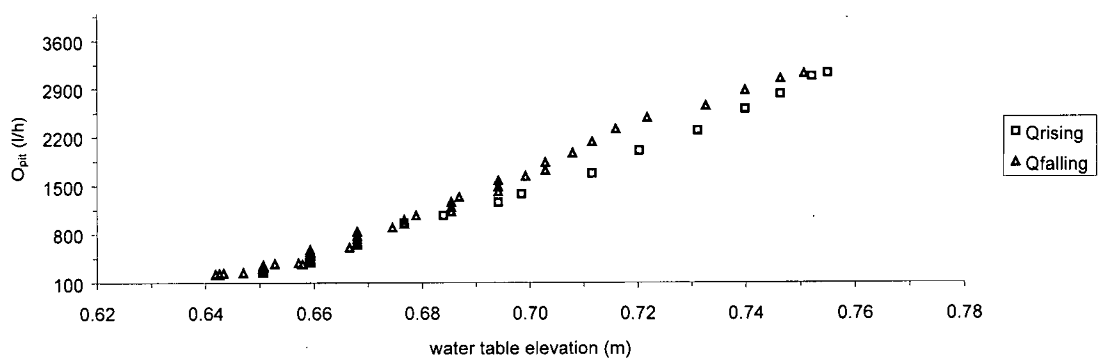

3.3 RAINFALL EVENTS DURING SUMMER-AUTUMN, 1998-1999

3.3.1 Characteristics of rain events

To determine the importance of subsurface flow as a streamflow generation mechanism, the hydrologic responses in the hillslope segment and in the entire upper Gray Creek catchment were compared during the rainy season of 1998. Hydrologic responses can most clearly be demonstrated by presenting data for individual storm events. One event was defined as the period of streamflow response to rainfall from one hydrograph rise to the next rise, after separating baseflow by conventional procedures. One event may include multiple peaks resulting from sporadic rainfall (Hibbert and Cunningham, 1965). The baseflow separation line was determined from the initial rise of the hydrograph at a slope of 2 $m^3 h^{-2} km^{-2}$ (Hewlett and Hibbert, 1967). Five rainfall events were evaluated during autumn 1998. During the sequential events 3 and 4, hydrologic responses in the hillslope segment had evidently responded earlier than the streamflow and prior to the major storm inputs; thus, the Hewlett and Hibbert (1967) hydrograph separation technique was not appropriate. Therefore, event 3 was defined as the period of outflow from mineral section 2 prior to the rising limb of event 4. Because of equipment problems, particularly malfunctioning of magnetic reed switches on the tipping bucket systems, only the outflow data from section 2 are considered completely reliable and are presented. Total volumes and peak flow rates from mineral section 2 along with streamflow and average, minimum, and maximum water table elevations for individual events in fall 1998 are summarized in Table 3.11. The water table did not rise above the ground surface to generate saturated overland outflow during any events. It is interesting that peak outflows from section 2 generated about 0.5 m^3/h during events 2, 3, 4, and 5 regardless of total outflow volume and stream discharge.

Event 1 (October 16)

On October 16 a 17-hour storm delivered 35 mm of rain with a moderate peak intensity of 7 mm/h. The 7-day antecedent precipitation was 50 mm. The recession started on the morning of October 17^{th} and continued through October 25 (Figure 3.18). This storm produced 57.4 m^3 of outflow from section 2 and $53.0 \cdot 10^3$ m^3 of streamflow. Hydrological responses to rainfall were similar in both the hillslope segment and entire catchment. However, hydrological responses in the hillslope segment were more sensitive to rainfall inputs, especially during low rainfall inputs. The outflow hydrograph from section 2 had a very steep rising limb and a steep falling limb (Figure 3.18). The water table elevation increased rapidly and peaked at 0.67 m. After the maximum water table was reached, it slowly declined in a pattern similar to the shape of the outflow hydrograph from section 2. The relative responses of section 2 outflow, water table elevation, and stream discharge were similar.

Event 2 (October 27)

Storm 2 occurred on October 27, 1998 with minor amounts of rain falling on the next 2 days. During the first day 16 mm of rain fell; peak intensity was 5 mm/h. Soil moisture conditions were somewhat dry; 11 mm of rainfall had fallen during the 7 days prior to storm 2. Hydrologic responses of the hillslope segment and entire catchment were similar during rising limbs of hydrographs (Figure 3.19). Following the hydrograph peaks,

Table 3.11 Hydrologic responses from mineral section 2, stream discharge and water table elevation during 5 storm events, 1998.

		mineral section 2		stream discharge		water table elevation		
Event	rainfall duration	total outflow(m^3)	peak(m^3/h)	total discharge(m^3)	peak discharge(m^3/h)	average(m)	minimum(m)	maximum(m)
1	10/16 17:00 ~ 10/18 8:00	57.4	2.414	53016	1806	0.49	0.42	0.67
2	10/27 12:00 ~ 10/29 22:00	10.1	0.590	6887	113	0.48	0.46	0.58
3	11/12 8:00 ~ 11/18 14:00	45.6	0.549	228016	6549	0.61	0.54	0.74
4	11/19 19:00 ~ 11/23 16:00	18.1	0.525	68655	2704	0.58	0.54	0.67
5	11/23 17:00 ~ 11/25 23:00	24.4	0.509	98404	1758	0.55	0.49	0.66

Figure 3.18 Event 1; Hydrologic responses to rainfall of October 16-18, 1998

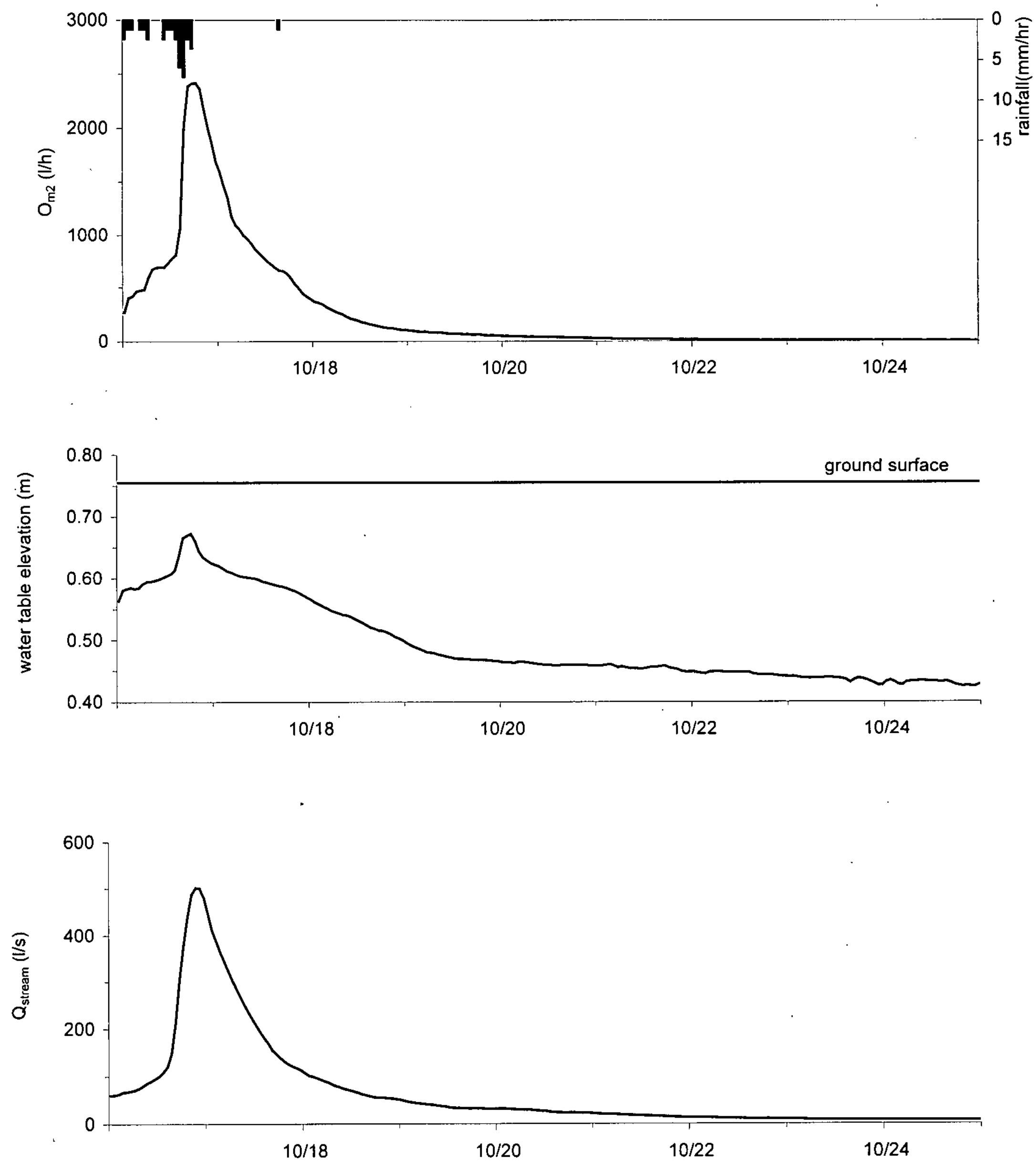

Figure3.19 Event 2; Hydrologic responses to rainfall of October 27-29, 1998

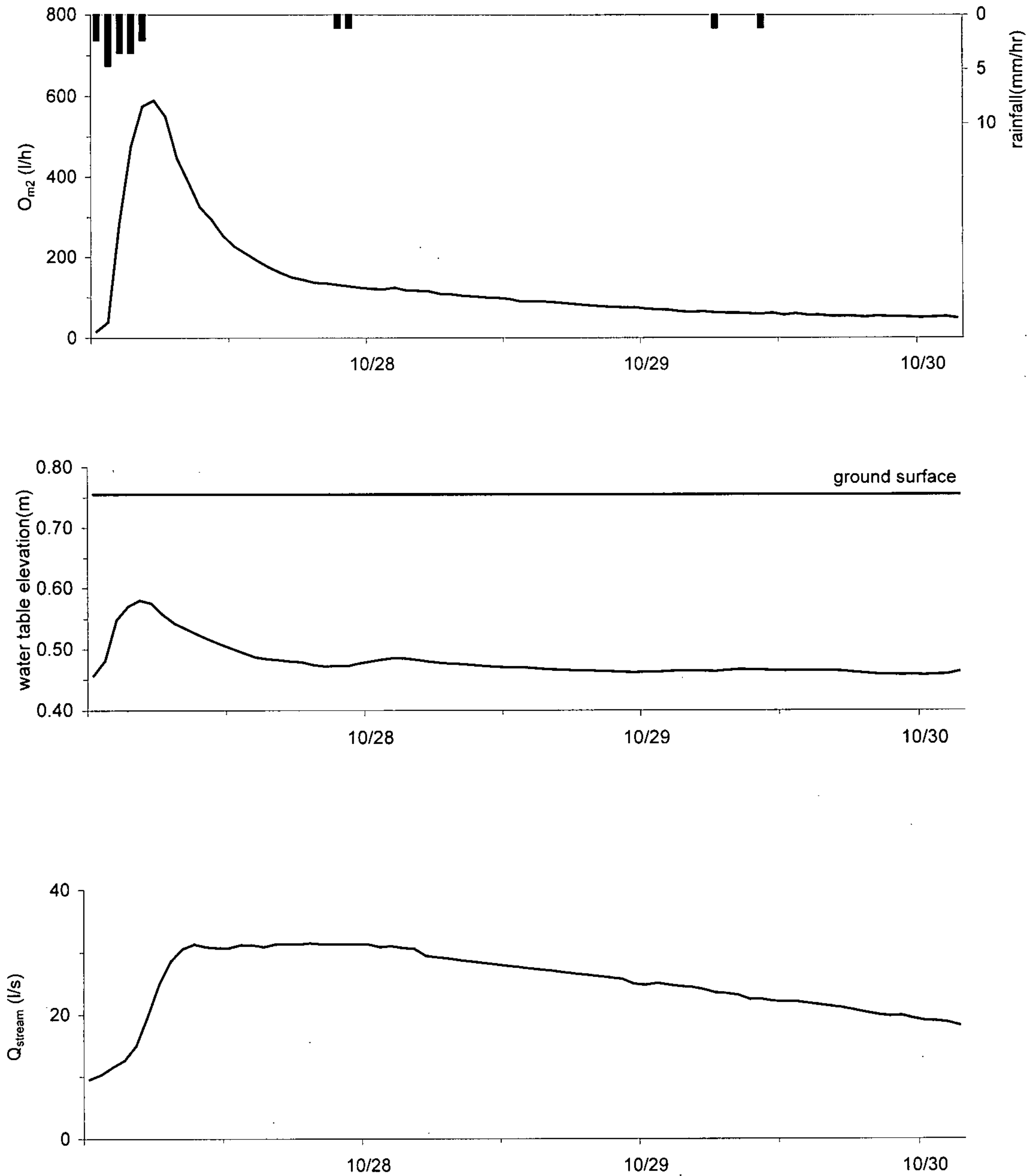

section 2 outflow and water table elevation rapidly decreased, although responding to minor subsequent rainfall inputs. However, streamflow declined very slowly after the peak discharge on October 27.

Event 3 (November 12)

Storm 3 was comprised of 38 mm of rain on November 12 followed by 88 mm of additional rainfall during the next 3 days. As a result, two hydrologic response peaks occurred within 3 days (Figure 3.20). Using the Hewlett and Hibbert (1967) hydrograph separation method, event 3 was treated as a single-peak event. This storm was the largest of the season with 126 mm of total rainfall and a peak intensity of 6 mm/hr. The 7-day antecedent precipitation was 34 mm, which was less than 25% of the rainfall during event 3. Initial stream discharge was 10.5 l/s and increased up to 1820 l/s after 100 mm of rainfall input. Water table elevation rose to within 1.5 cm of the soil surface. The outflow hydrograph from mineral section 2 had a broad peak during this event. On November 15, stream discharge increased rapidly compared to hydrological response from the hillslope segment.

Event 4 (November 19)

Storm 4 occurred from November 19 to 23, 1998. Total precipitation was 75 mm and peak intensity was 6 mm/hr. Soil moisture conditions were wet, with 119 mm of precipitation during the 7-day period prior to storm 4 (Figure 3.21). Hydrologic response of stream discharge was considerably lagged compared to the response of the hillslope segment.

Figure 3.20 Event 3; Hydrologic responses to rainfall of November 12-18, 1998

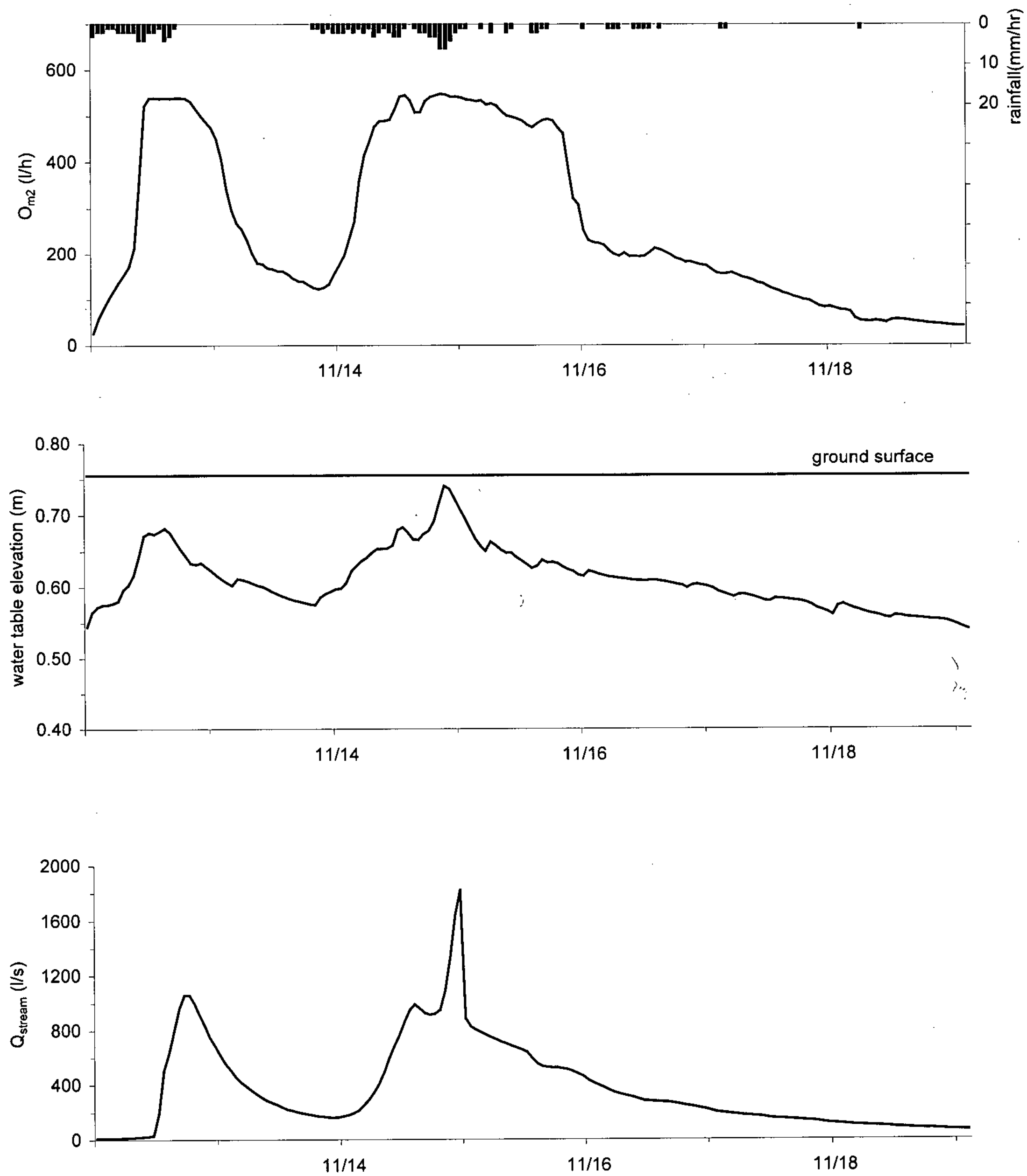

Figure 3.21 Event 4 ;Hydrologic responses to rainfall of November 19-23, 1998

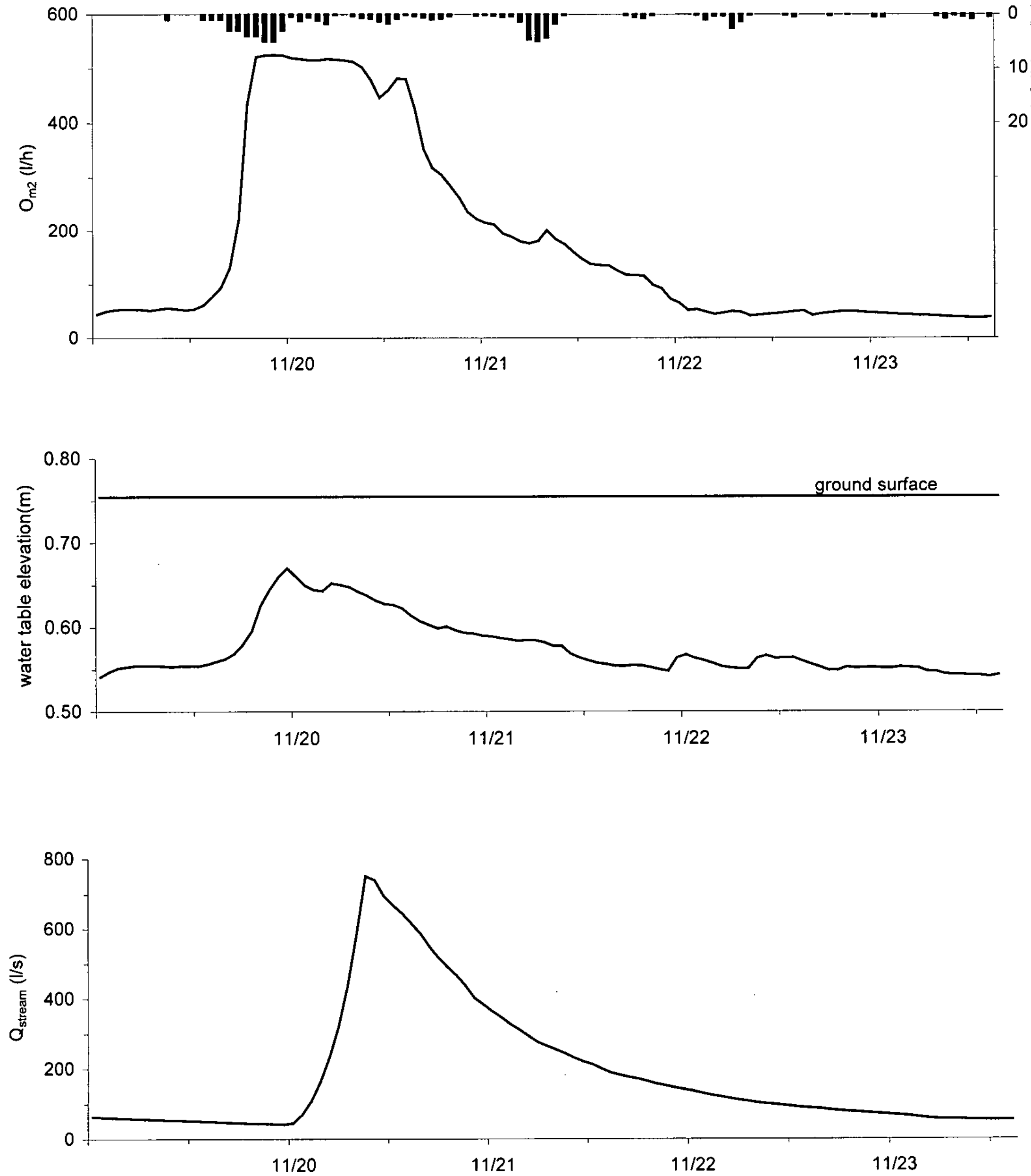

Event 5 (November 23)

Prior to storm 5, soil moisture conditions were wet; antecedent 7-day precipitation was 97 mm. Total rainfall was 62 mm with a peak intensity of 6 mm/hr. During storm 5, the hydrograph responses both in the hillslope segment and in the entire upper Gray Creek catchment exhibited double peaks within a 2-day period (Figure 3.22). On November 25, outflow from section 2 produced a broad discharge peak. Groundwater table elevation observed at a well about 11 m above the soil pit responded sporadically to precipitation.

Figure 3.22 Event 5; Hydrologic responses to rainfall of November 23-25, 1998

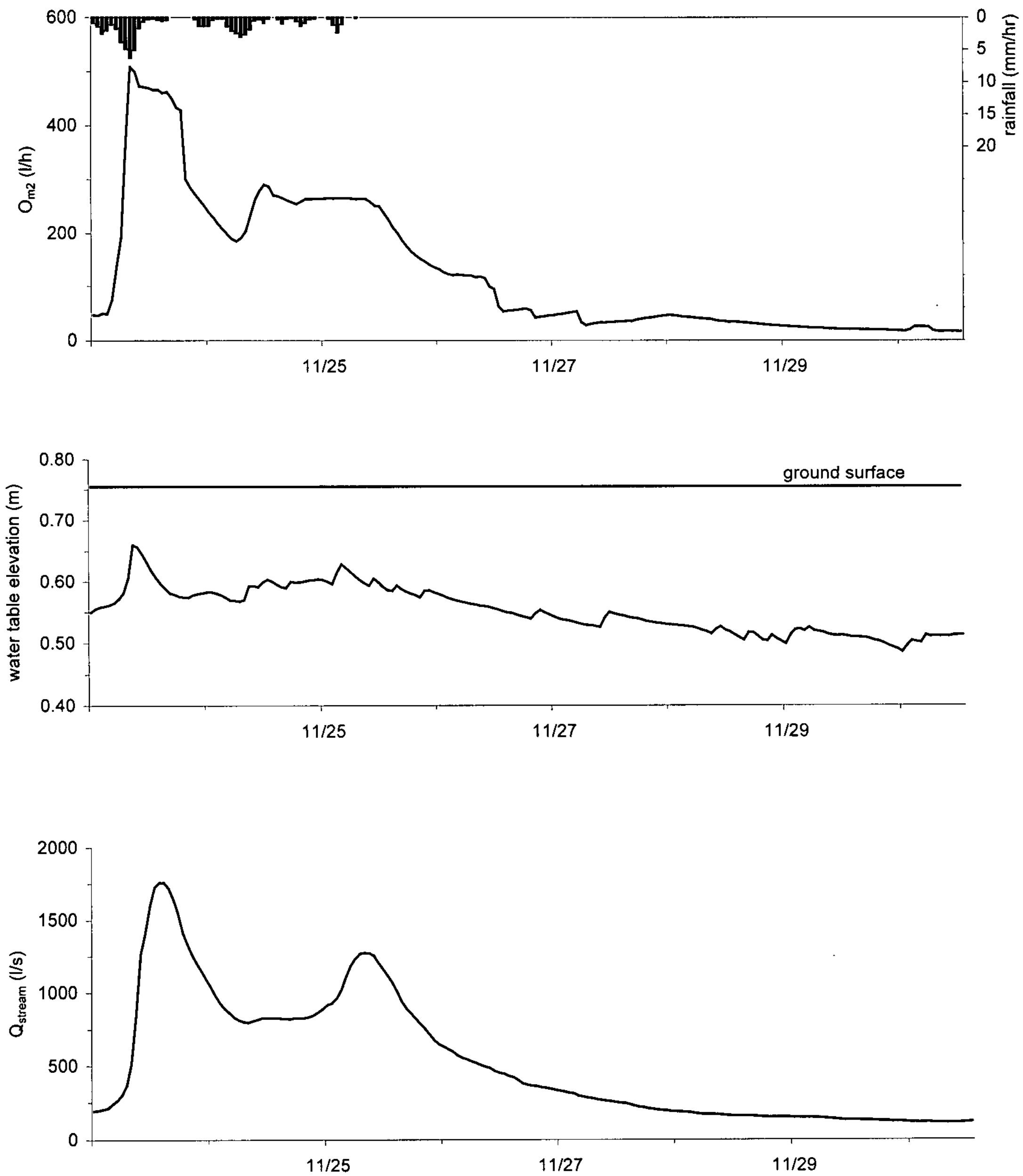

3.3.2 Variability within pit

To estimate the effects of increasing antecedent moisture on hydrologic response within a hillslope segment, general runoff processes in the transition from dry to wet moisture conditions were plotted based on 3 storms in the rainy season of 1999 (Figures 3.23, 3.24, and 3.25). These storms were selected because they had complete, reliable outflow measurements from all sections of the pit. Rainfall characteristics and related hydrological responses in the hillslope segment to these 3 storms in 1999 are summarized in Table 3.12.

September 4-6, 1999 storm

The September 4-6 storm consisted of 26 mm of total rainfall with a peak intensity of 3 mm/hr. The storm produced 0.39 m^3 of pit outflow, mainly from mineral sections 1 and 2. Soil moisture conditions were relatively dry; 7-day antecedent precipitation was only 13 mm. In the beginning of the rain event, outflow from the organic horizon occurred earlier than from the mineral horizons. This indicated rapid outflow from the shallower soil layer (organic horizon) than from the deeper layers (mineral horizon) during initial rainfall under dry soil moisture conditions. However, once the mineral horizons began to produce discharge, their temporal response patterns to rainfall inputs were similar to the organic horizon (Figure 3.23). Outflow from the organic horizon was a bit more irregular compared to mineral horizon outflow, probably related to flow through preferential flow pathways (e.g. root channels, zone of highly permeable organic material) and perhaps hydrophobic conditions at the interface between the organic horizon and mineral horizons. Outflows from mineral section 1 and 2 were about an order of magnitude

Figure 3.23 Hillslope hydrologic responses to rainfall of September 4-6, 1999 more or less dry antecedent conditions

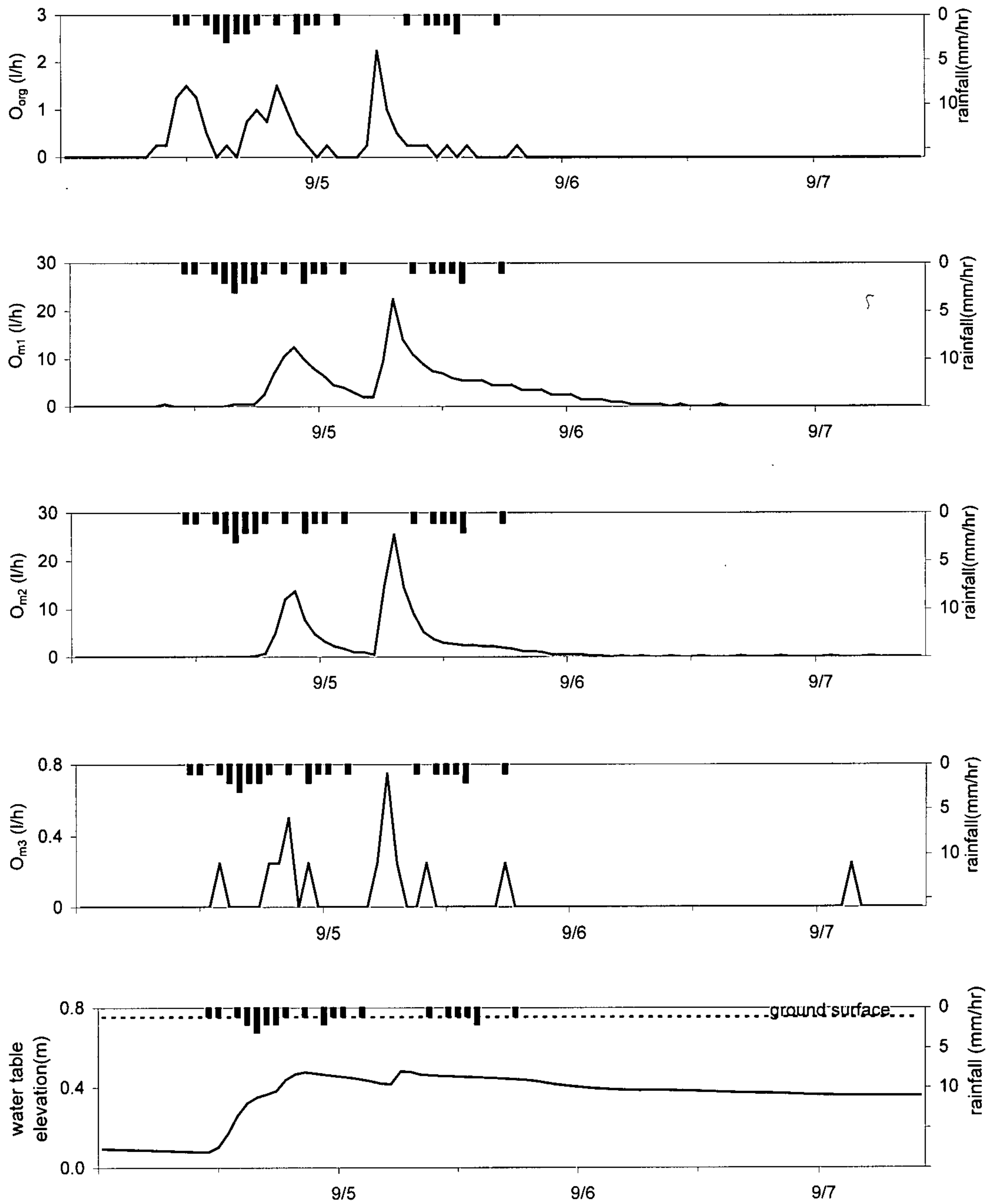

Figure 3.24 Hillslope hydrologic responses to rainfall of September 23-25, 1999 dry antecedent conditions

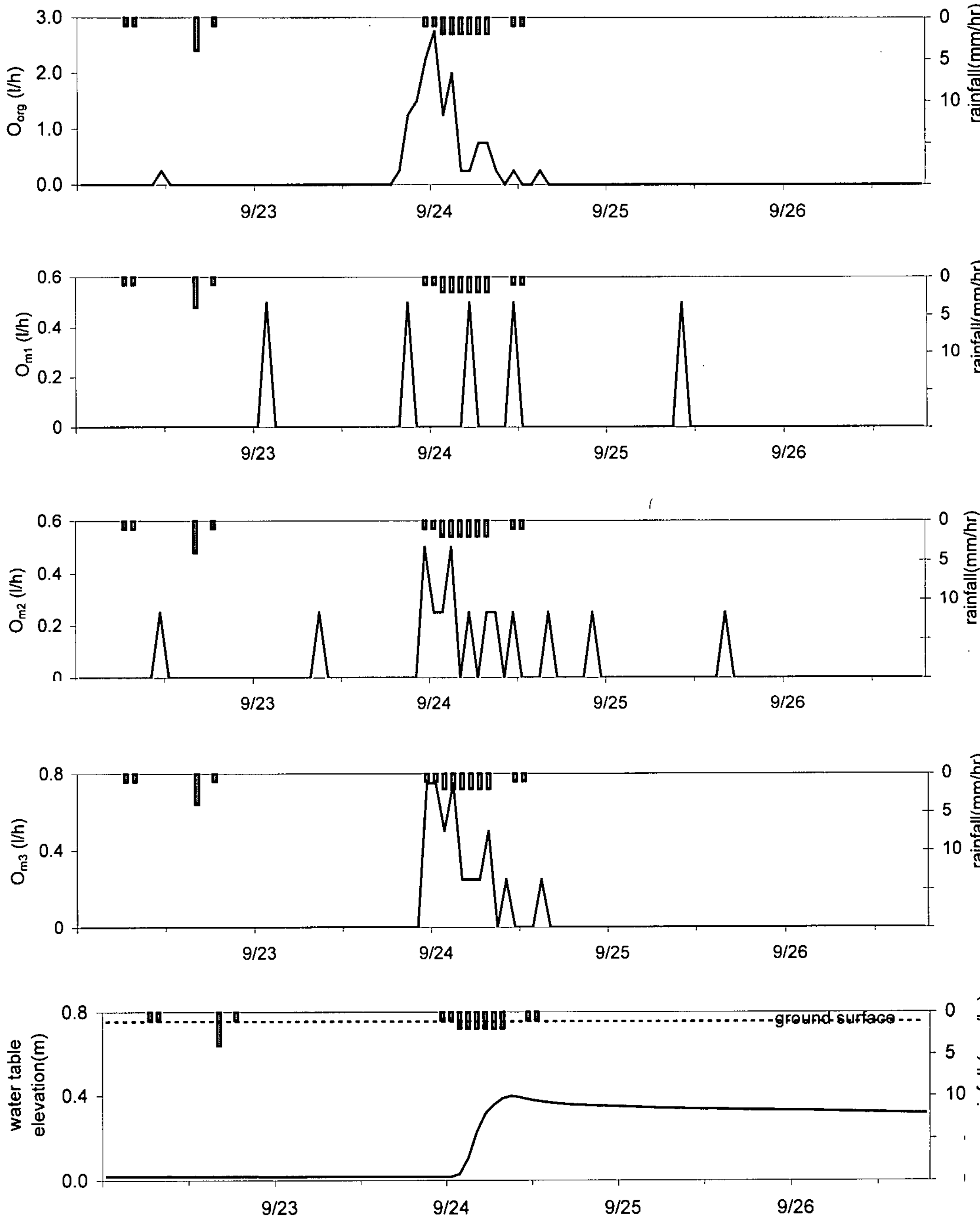

Figure 3.25 Hillslope hydrologic responses to rainfall of November 15-16 1999
wet antecedent conditions

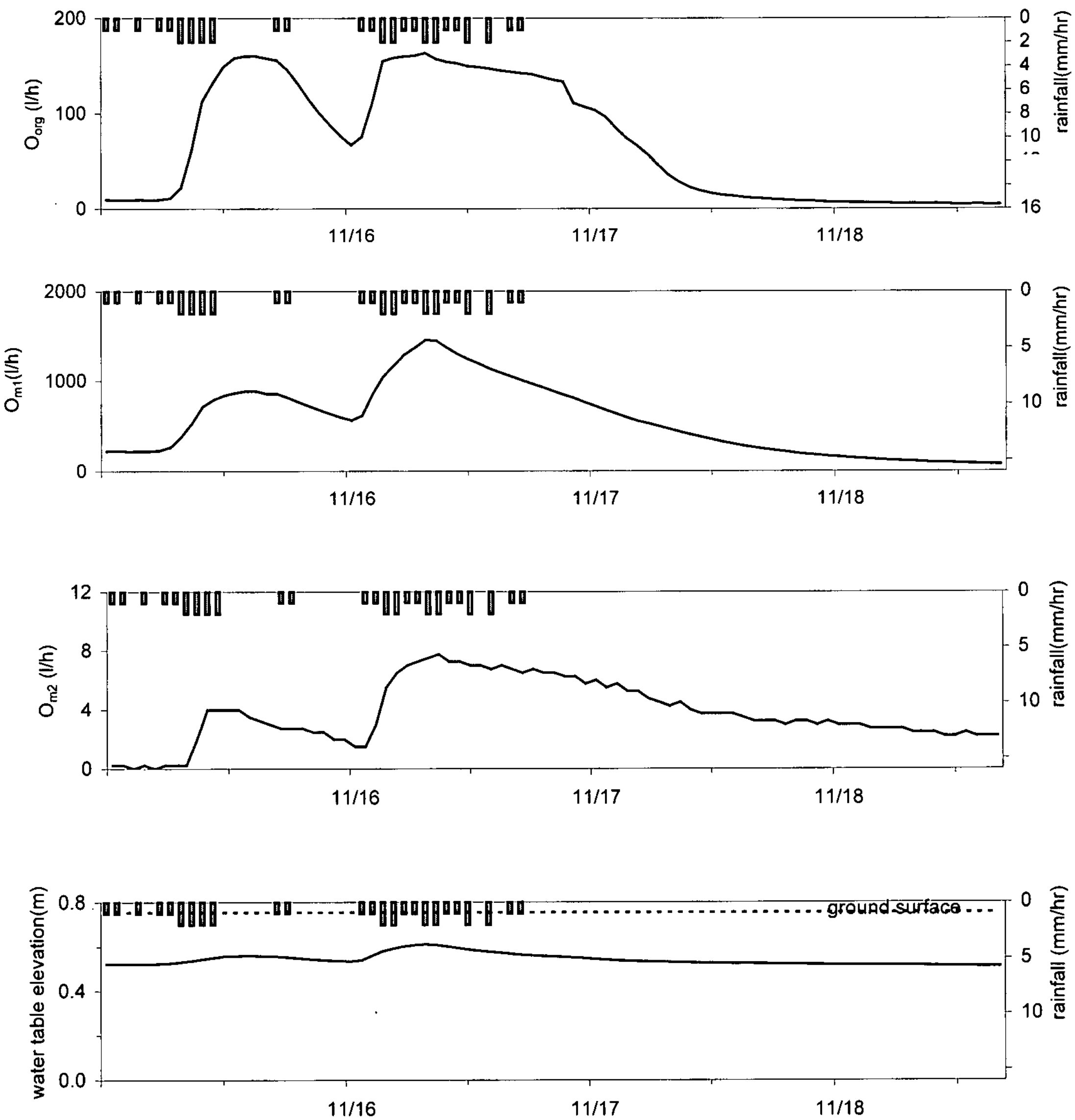

Table 3.12 Rainfall characteristics and hydrological responses at the hillslope segment to storms in 1999.

	Date of event									
	September 4-6 storm				September 23-25 storm				November 15-16 strom	
	timing of start		timing of end		timing of start		timing of end		timing of start	timing of end
Volume	09/04 21:00		09/06 5:00		09/23 05:00		9/25 02:00		11/15 08:00	11/16 23:00
rainfall variables										
total rainfall (mm)	26				23				35	
peak rainfall (mm/hr)	3				4				2	
API_7 (mm)	13				0				159	
outflow volume	total outflow(l)	contribution to total pit outflow(%)	peak outflow (l/h)	contribution to peak pit outflow(%)	total outflow(l)	contribution to total pit outflow(%)	peak outflow (l/h)	contribution to peak pit outflow(%)	total outflow(l)	peak outflow (l/h)
organic horizon	17	4	2.3	5	14	57	2.8	73	6004	163.5
mineral section 1	219	56	22.5	46	3	10	0.5	13	48394	1456.0
mineral section 2	154	39	25.5	52	4	15	0.5	13		
mineral section 3	4	1	0.8	2	5	18	0.8	20	323	7.8
pit	392		49.3		25		3.8			
ground water observation										
peak water table elevation (m)	0.48				0.40				0.61	
average water table elevation (m)	0.35				0.20				0.54	

API_7 Antecedent precipitation 7 days index higher than outflow from the organic horizon. The water table elevation responded quickly to rainfall, rising from 0.09 to 0.48 m, but then declined slowly. This response indicated that saturation overland flow did not develop during this early autumn storm nor did the watertable everreach the organic horizon.. Outflow from the organic horizon occurred as a lateral subsurface flow facilitated by the lower hydraulic conductivity of the underlying mineral soil and possibly hydrophobic conditions and the organic/mineral horizon boundary.

During this storm, outflows from sections 1 and 2 lagged rainfall inputs (Figure 3.23). A portion of this lag can be explained by the lag time of the pit monitoring system during dry soil moisture conditions; outflow from each section was routed from the concrete trough via connected pipes and tubing, finally arrived at the tipping bucket. During dry conditions there may be a long initial transit time to reach the tipping bucket, thus the actual first tip response may be delayed. Mosley (1979) mentioned that for very low discharge rates at the beginning of a storm, the time period taken to fill such tipping buckets might be quite long and lead to a significant overestimate of the time to the onset of runoff.

September 23-25, 1999 storm

The size of the September 23-25 storm was similar to that of September 4-6 storm; 23 mm of rainfall fell with a peak intensity of 4 mm/hr. However, the storm produced only 25 L of pit outflow. Soil moisture conditions were extremely dry; no rain had fallen during the 7 days prior to the storm. During the early portion of the storm, after 7 mm of rainfall, groundwater levels did not respond and remained at 0.02 m (Figure 3.24). Water table elevation peaked at 0.4 m on September 24 and slowly declined afterwards. Hydrological response from the organic horizon was earlier than from mineral section 1 and similar to the response from mineral section 2; however, in both cases discharge from the organic horizon was nearly an order of magnitude greater. As during the September 4-6 storm, outflow from the organic horizon was generated as lateral subsurface flow because a water table did not develop close to the organic horizon and hydrophobic conditions likely existed at the organic horizon and mineral soil interface.

November 15-16,1999 storm

Another moderate-intensity storm occurred from November 15 to 16, 1999; 41 mm of total rain fell with peak intensity of 4 mm/hr. For this late season storm, 7-day antecedent precipitation was high (159 mm). Discharge from mineral horizon 2 is not shown in Fig. 3.25 due to equipment malfunction. Outflows from the organic horizon, mineral sections 1 and 3 and ground water table elevations responded similarly to precipitation (Figure 3.25). Rising and falling limbs of hydrographs were smoother compared to storm responses during drier antecedent moisture periods. The water table was initially high (0.52 m) and rose to a peak of 0.61 m, and then slowly declined. Two days after the peak, water table elevation had declined to pre-storm levels.

Contributions from the organic horizon and individual mineral soil sections to total pit outflow are shown for 2 storm periods (September 4-6, September 23-25) (Table 3.12). As soil moisture decreased from September 4 to September 23 stormflow from the organic horizon increased from 4% to 57% of total pit outflow, although outflows from the organic horizon for both storms were of similar magnitude.

The fractions of outflow from the organic horizon and individual mineral sections were plotted against pit outflow for the two September storms (Figure 3.26 and 3.27). During the September 4-6 storm, neither the organic horizon nor any of the mineral sections contributed in a consistent manner to increasing pit outflow (Figure 3.26). For higher pit outflows, the contribution from the organic horizon was small during such dry antecedent conditions compared to the relatively high outflows during the snowmelt season. The relative contribution of outflow from the mineral section 1 tended to decline with increasing pit outflow during the September 4-6 storm; this response was similar to the response in the snowmelt season. The contribution of mineral section 2 to pit outflow increased with increasing pit outflow rates during the September 4-6 storm, as opposed to results during the snowmelt season, where the trend was a decrease with increasing outflow rates from mineral horizons (Figure 3.13). Contributions of mineral section 3 to pit outflow decreased with increasing pit outflow rates. This result is similar to the snowmelt season.

During the September 23-24 storm, individual pit components also did not respond consistently to increasing pit outflow (Figure 3.27). Contributions of the organic horizon to pit outflow were significant but highly variable. Contributions of mineral sections 1, 2 and 3 to pit outflow were also variable but tended to decrease with increasing pit outflow rates (Figure 3.27).

Figure 3.26 Plots of outflows from the organic horizon and individual mineral sections against pit outflow for the September 4-6 storm period in 1999.

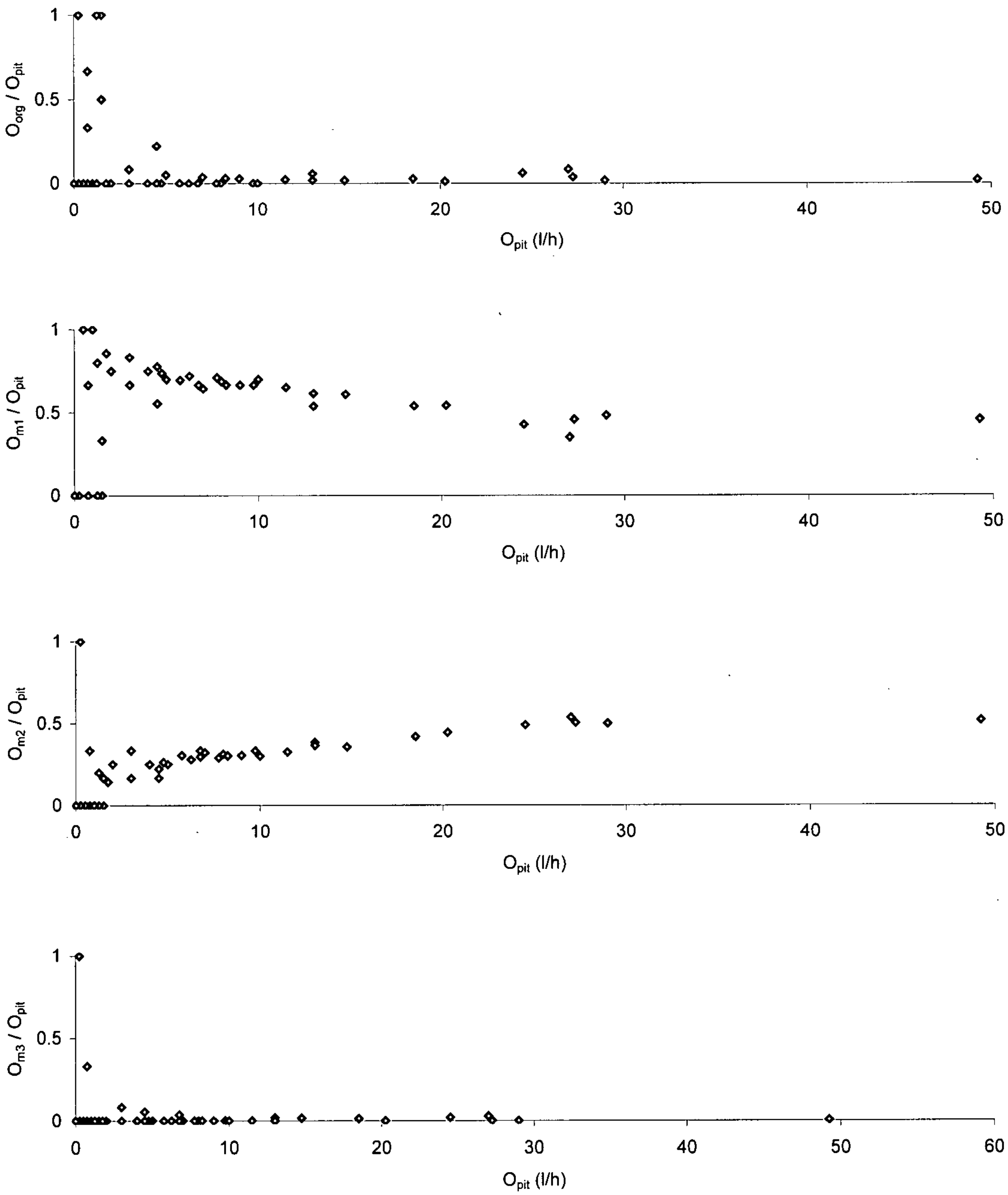

Figure 3.27 Plots of outflows from the organic horizon and individual mineral sections against pit outflow for the September 23-25 storm period in 1999.

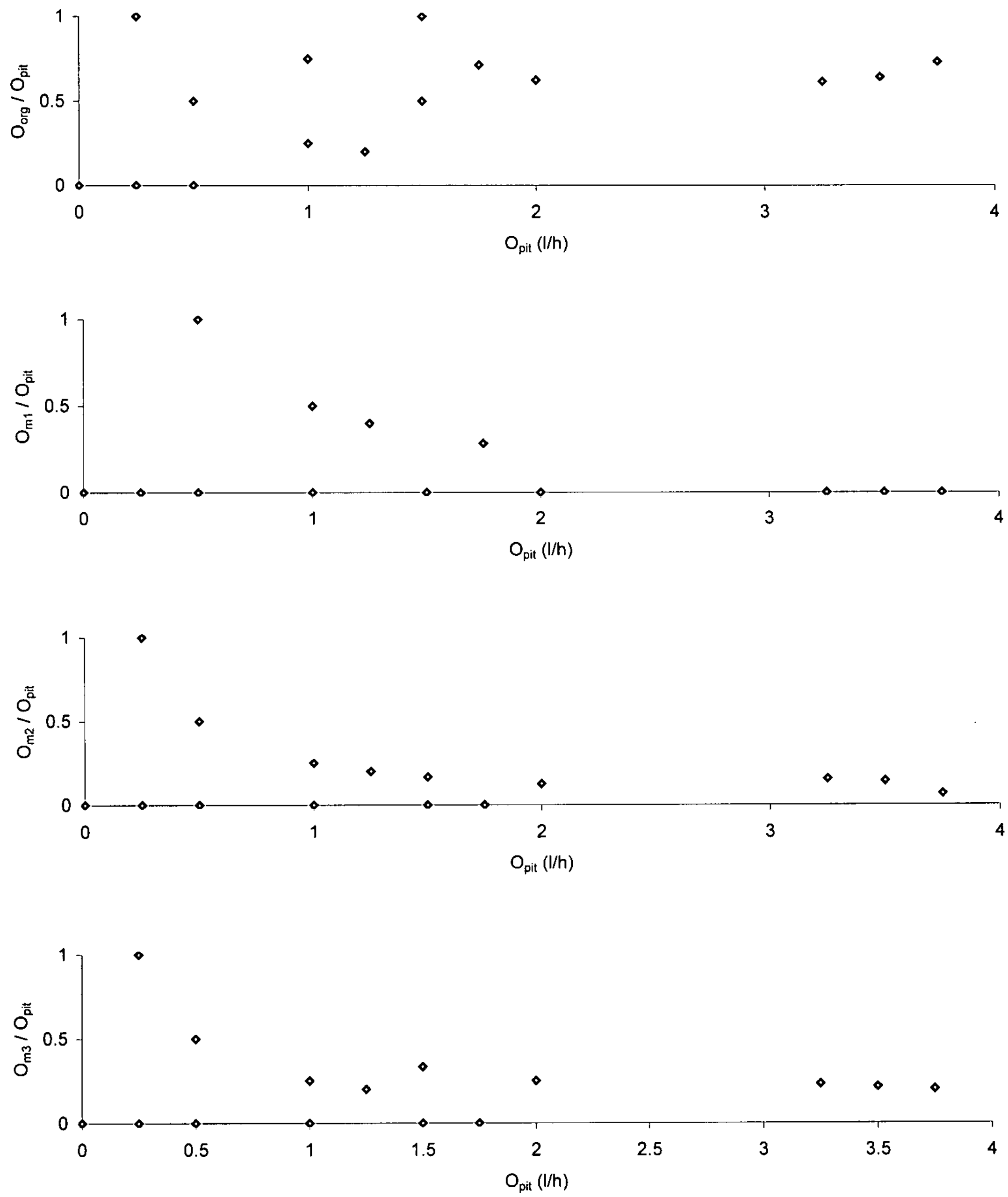

3.3.3 Timing of outflow

The response of subsurface flow to rainfall was very rapid once antecedent moisture deficits were satisfied – i.e., the wetter portion of the fall storm season. This subsurface flow obviously contributed to stormflow generation during rainfall periods in 1998 (Figures 3.18 to 3.22). The timing of peaks of outflow from mineral section 2, water table elevation and streamflow for the five storms during the rainy season in 1998 is shown in Table 3.13. There was no systematic pattern related to the timing of peak flows from the hillslope segment and the entire catchment. Simultaneous plots of outflows from mineral section 2 and streamflow as well as water table elevation for two wet season storms were plotted together with respective rainfall hyetographs (Figures 3.28 and 3.29). Both the outflow for mineral section 2 and the water table in the hillslope segment responded faster to rainfall inputs than streamflow. Lag times for peak outflow from section 2 and for peak stream discharge were computed in order to estimate whether or not subsurface flow in the hillslope segment was rapid enough to contribute to stream discharge. Lag time is defined as the time from the mass centroid of the rainfall hyetograph to the mass centroid of the peak of hydrograph. The median lag time for outflow from mineral section 2 was 2 h and ranged from 0 to 4 h. However, the median lag time for stream discharge was 8 h and ranged from 3 to 18 h. The difference in lag times between outflow from mineral section 2 and stream discharge was 7 h and ranged from 3 to 14 h. This difference may simply be due to the much larger contributing area of the catchment and the resulting routing time for water to reach the outlet.

Table 3.13 Comparison of timing of peaks and lag times for outflow from mineral section 2 water table elevation,and streamflow during the autumn rainy season, 1998

Timing of peaks and lag time						
date	mineral section 2		water table elevation		streamflow	
	peak time	lag time	peak time	lag time	peak time	lag time
10/17	11:00	3	11:00	3	14:00	6
10/27	17:00	4	16:00	3	10/28 7:00	18
11/15	4:00	0	5:00	1	7:00	3
11/20	7:00	1	8:00	2	17:00	9
11/24	1:00	0	2:00	2	7:00	6

where lag time is time difference between peak flow from the mineral section 2, water table elevation, and stream and peak of rainfall

Figure 3.28 Simultaneous plots of outflow from mineral section 2 and stream discharge as well as water table elevation for the October 16 storm together with respective rainfall hyetograph.

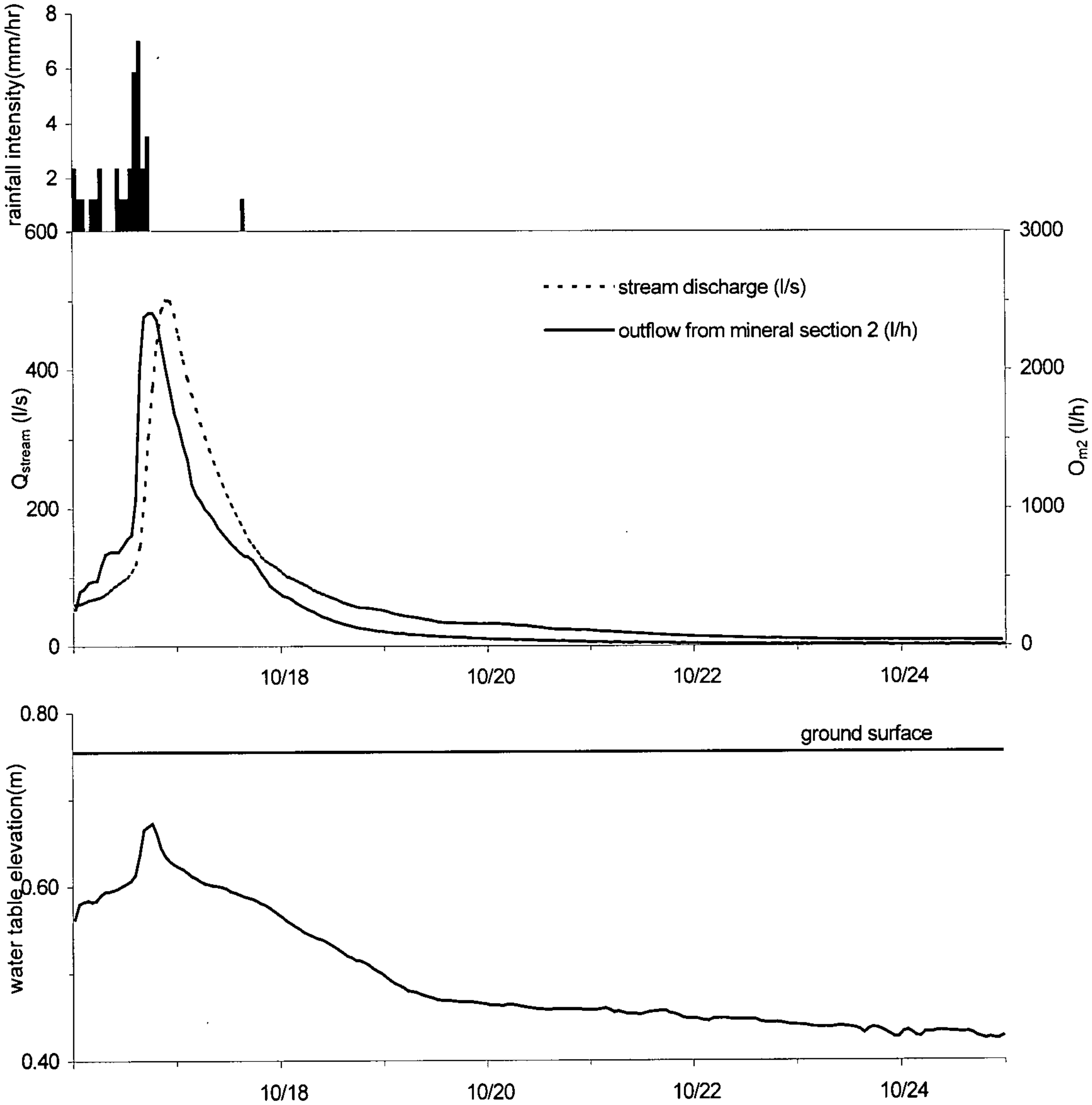

Figure 3.29 Simultaneous plots of outflow from mineral section 2 and stream discharge as well a water table elevation for November 12-18 storm together with respective rainfall hyetograph.

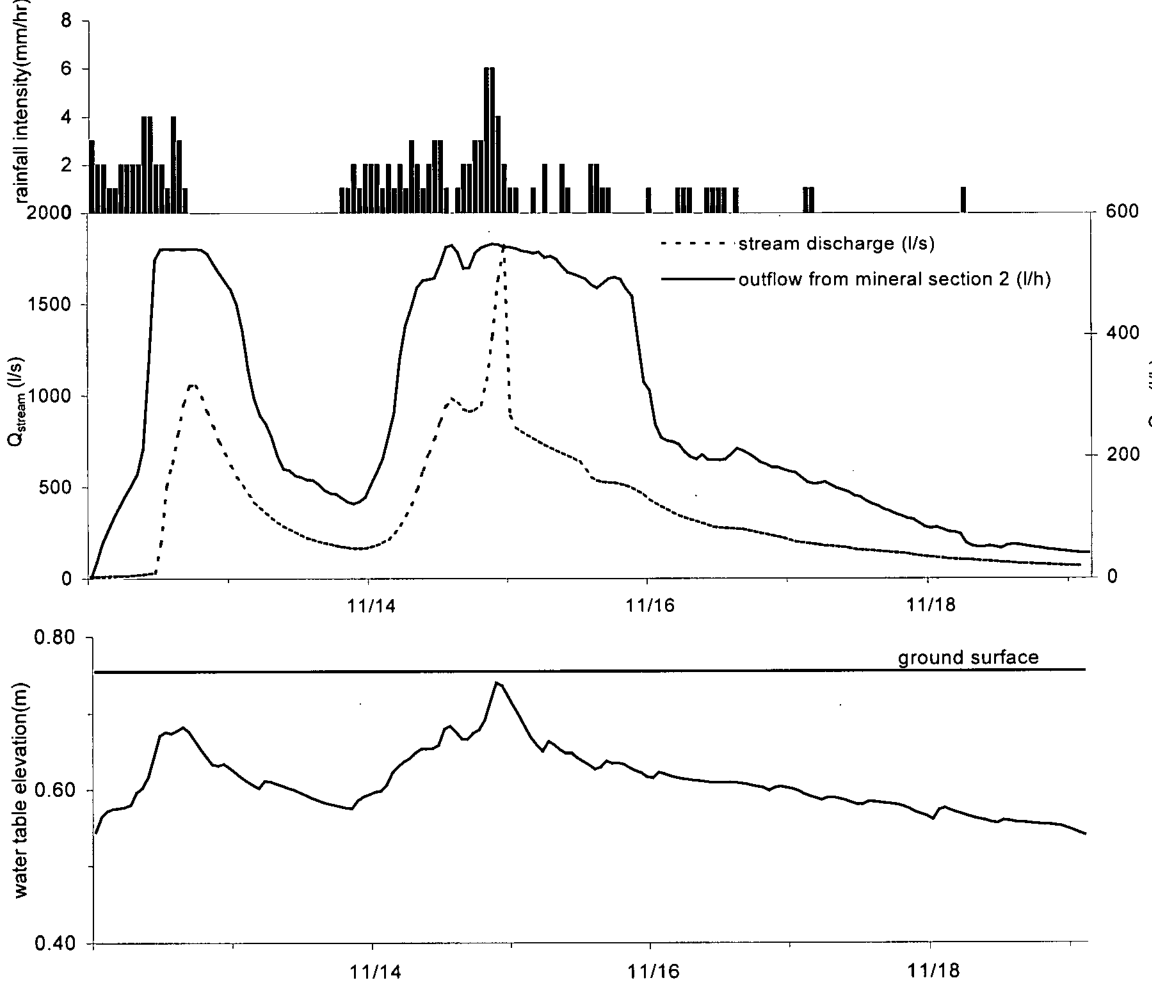

Three events were selected for cross-correlation analysis to determine an aggregated lag time between outflow from mineral section 2 and stream discharge (Figure 3.30). During event 1 (October 16-18, 1998), cross-correlation between outflow from mineral section 2 and stream discharge showed that a maximum correlation (0.99) was obtained at a lag time of 3 hr. For event 2 (October 27- 29, 1998), the maximum correlation (0.70) occurred at a lag of 18 hr. This long lag time occurred due to the flat and long-term hydrograph maximum (Figure 3.19). because of the lower correlation coefficient and the flat peak, precise estimate of lag time is questionable. During event 3 (November 12-18, 1998), the maximum correlation (0.89) was obtained at a lag of 4 hr.

3.3.4 Relations between pit outflow and antecedent precipitation

Peak rainfall, total precipitation, 7-day antecedent moisture conditions (API_7), and outflow from mineral section 2 are summarized for 7 rainfall events in 1998-99 (Table 3.14). Relations either between 7-day antecedent precipitation and peak rainfall or between total precipitation and peak rainfall were poor: R^2=0.19 (p =0.34) and R^2=0.18 (p=0.34), respectively (Figures 3.31 and 3.32). Outflow from mineral section 2 was highly correlated to peak rainfall (R^2=0.83, p=0.005) (Figure 3.33). However, outflow from mineral section 2 was only weakly correlated to total precipitation (R^2=0.28, p=0.22) (Figure 3.34).

Multiple linear regression analysis (SAS program, 1988a, b) was used to predict total outflow from mineral section 2 as a function of peak rainfall, total precipitation, and API_7

Figure 3.30 Cross-correlation between outflow from mineral section 2 and stream discharge

Event 1 (October 16-25,1998)

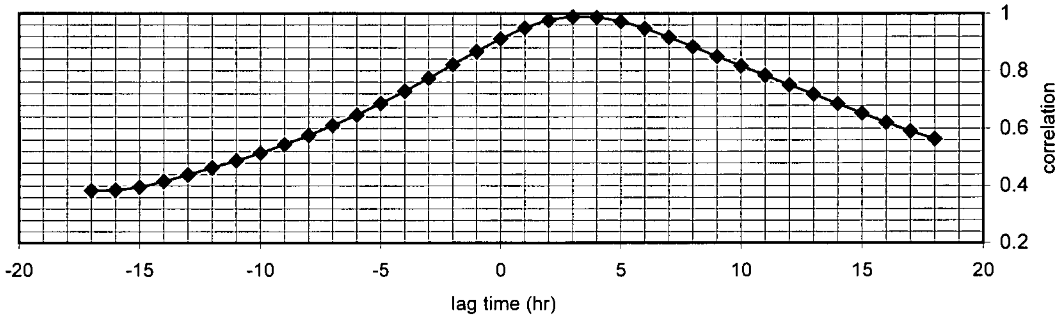

Event 2 (October 27-30, 1998)

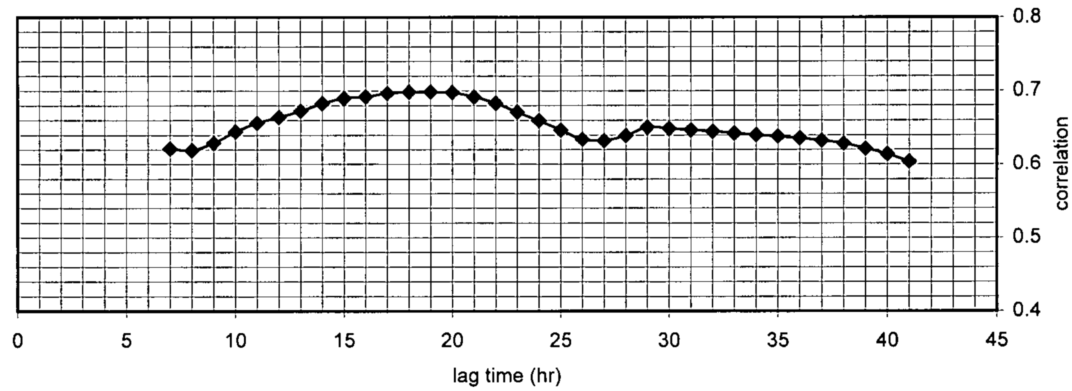

Event 3 (November 12-19,1998)

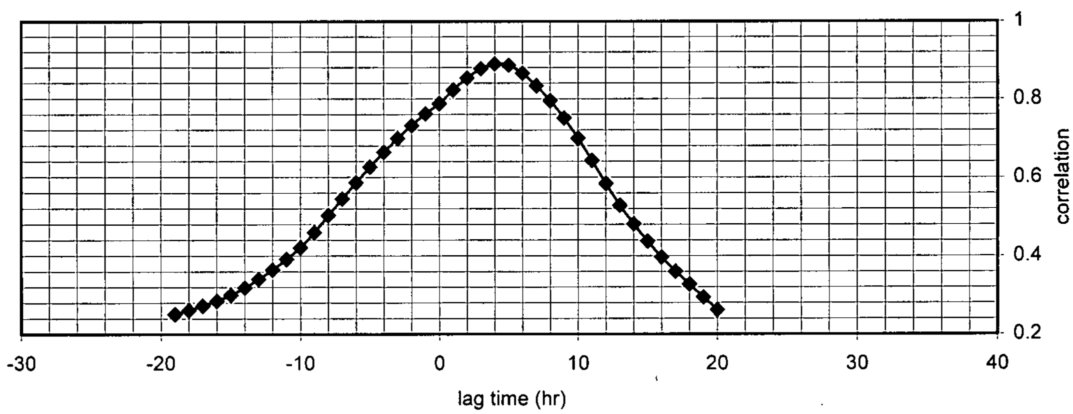

Table 3.14 Rainfall characteristics and outflow from mineral section 2 of 7 events, 1998-99.

No.event	peak rainfall (mm/hr)	total precipitation (mm)	API $_7$ (mm)	Outflow from mineral section 2 (litres)
1	7	36	50	57394
2	5	21	11	10114
3	6	126	34	45628
4	5	75	119	18141
5	6	62	97	24397
6	3	26	13	154
7	4	23	0	4

Figure 3.31 Relations between 7-day antecedent precipitation and peak rainfall for 7 events of 1998-99.

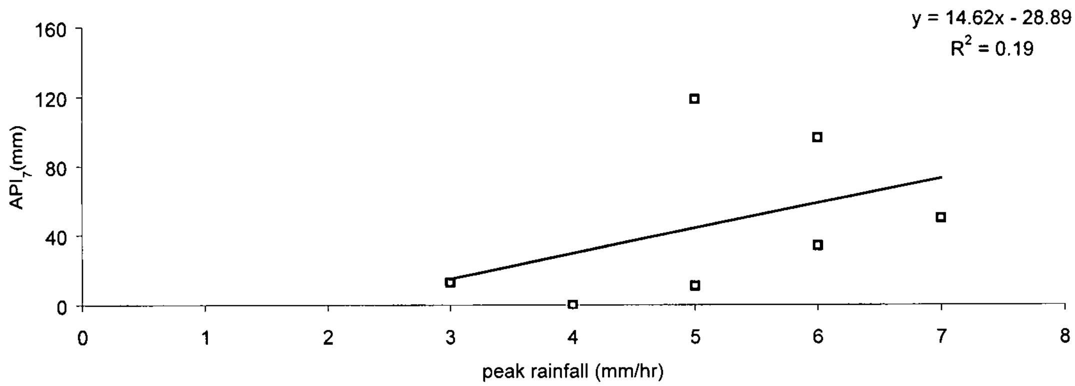

Figure 3.32 Relations between total precipitation and peak rainfall for 7 events of 1998-99.

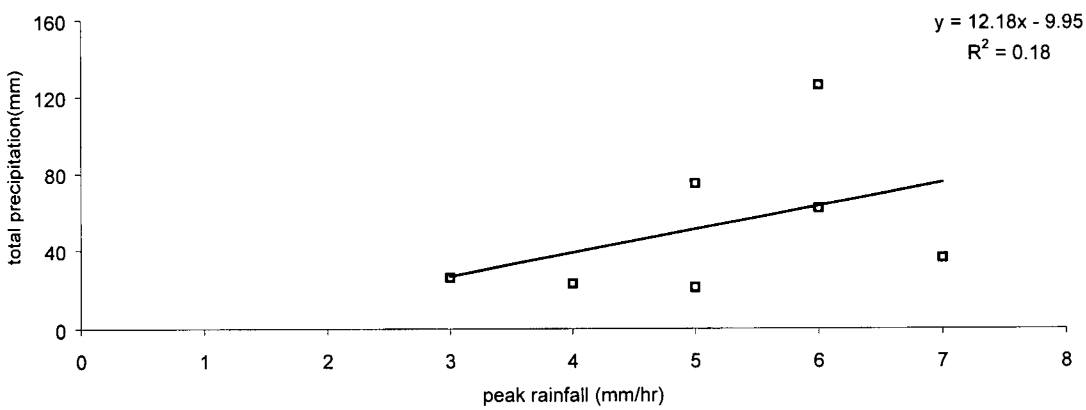

Figure 3.33 Relations between outflow from mineral section 2 and peak rainfall for 7 events of 1998-99.

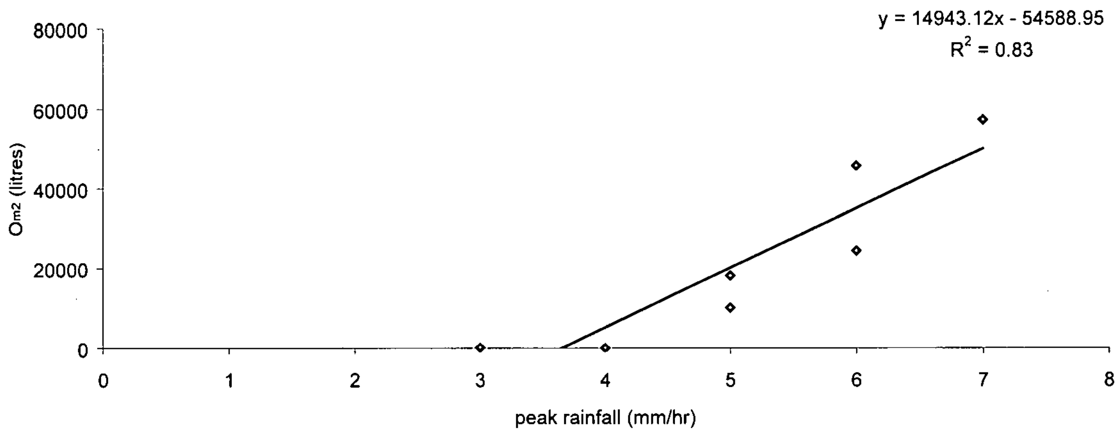

Figure 3.34 Relations between outflow from mineral section 2 and total precipitation for 7 events of 1998-99.

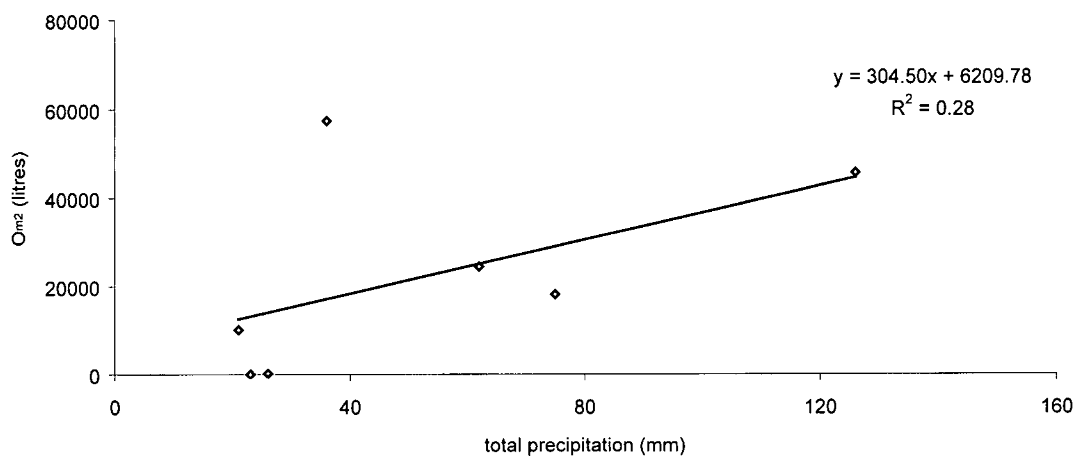

for 7 events in 1998 and 1999 (Table 3.14). The following model was used in the regression analysis:

$$Y = b_0 + b_1 X_1 + b_2 X_2 + b_3 X_3 \qquad (3\text{-}10)$$

where Y is total outflow from mineral section 2 (l); X_1 is peak rainfall (mm/hr); X_2 is total precipitation (mm); X_3 is API_7 (mm); and b_0, b_1, b_2, and b_3 are regression coefficients. Because of the small sample size, this analysis is considered exploratory. In order to derive significant inferences more observations would be required. The "best-fit" relation based on these seven storms using a stepwise procedure

$$Y=-54588.47+14943.09X_1 \text{ (P-value=0. 005, Adjusted } R^2\text{=0.79)} \qquad (3\text{-}11)$$

Peak rainfall explains 79% of the variation in total outflow volume from mineral section 2. Inclusion of total precipitation and/or antecedent precipitation did not improve the fit and were not significant.

3.3.5 Relations between pit outflow and water table elevation

Both total pit outflow rates and mineral horizon outflow rates were plotted against water table elevation during the September 4-6 storm period in 1999 (Figure 3.35), which had slightly moist antecedent conditions. Relations between pit outflow and water table elevation and between mineral horizon outflow and water table elevation are not linear. Initial water table elevations in both plots were 0.09 m (12% of soil depth saturated). As

Figure 3.35 Relations between pit outflow and water table elevation and between outflow from mineral horizon and water table elevation during the September 4-6 storm period in 1999.

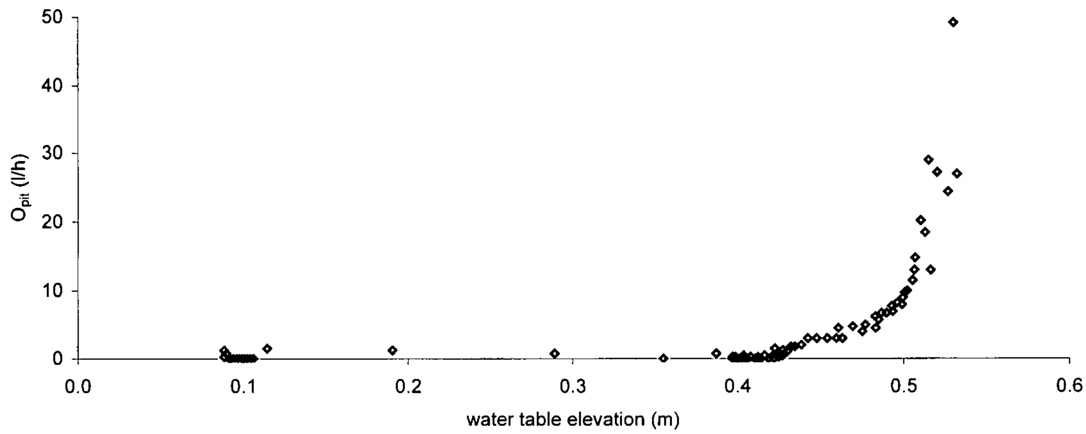

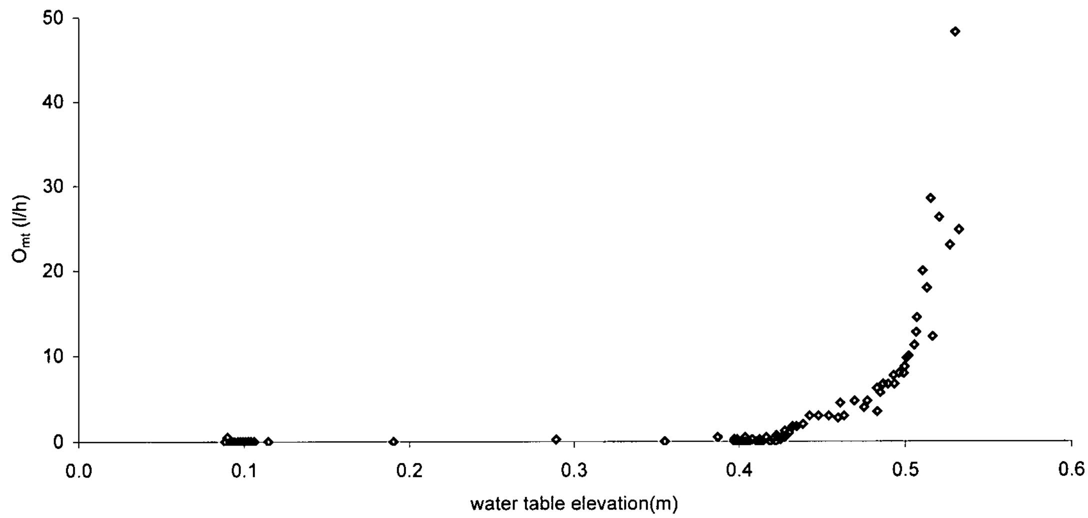

the water table rose to 0.43 m, neither pit outflow nor section outflow increased measurably. However, once the water table elevation exceeded 0.43 m, both pit and mineral horizon outflows increased markedly up to a water table elevation of 0.53 m. At that elevation the water table was still far below the surface (0.23 m below the ground surface); thus, saturated overland flow did not occur.

Both pit outflow rates and mineral horizon outflow rates were plotted against water table elevation during the September 23-25 storm in 1999 (Figure 3.36). Prior to this storm, soil moisture was dry; 7-day antecedent precipitation was zero. No relations were found between pit outflow and water table elevation or between mineral horizon outflow and water table elevation (Figure 3.36). Subsurface flow - groundwater relations were characterized by scattered data and low discharge values during the drier period.

3.4 ESTIMATION OF HYDRAULIC CONDUCTIVITY

Saturated hydraulic conductivity values were determined by two different methods in the field. In early November (during the rainy season) of 1999, slug tests were conducted in piezometers located 11, 26, and 51 m upslope of the soil pit. Based on the results of the slug test, a shape factor (C) was calculated (Youngs, 1968), which determined the values of C/r (r is radius and C/r is dimensionless). Radius of the cavity, r, is 0.0127 m. The shape factors for the upslope distances of 11, 26, and 51 m were 0.201, 0.198, and 0.206, respectively. The time interval for recording the water level recovery was 30 seconds. The length of cavity, H_c, is 0.0762 m. Because the boundary of the impermeable layer was not known, piezometers were drilled as deep as possible until a

Figure 3.36 Relations between pit outflow and water table elevation and between outflow from mineral horizon and water table elevation during the September 23-25 storm period in 1999.

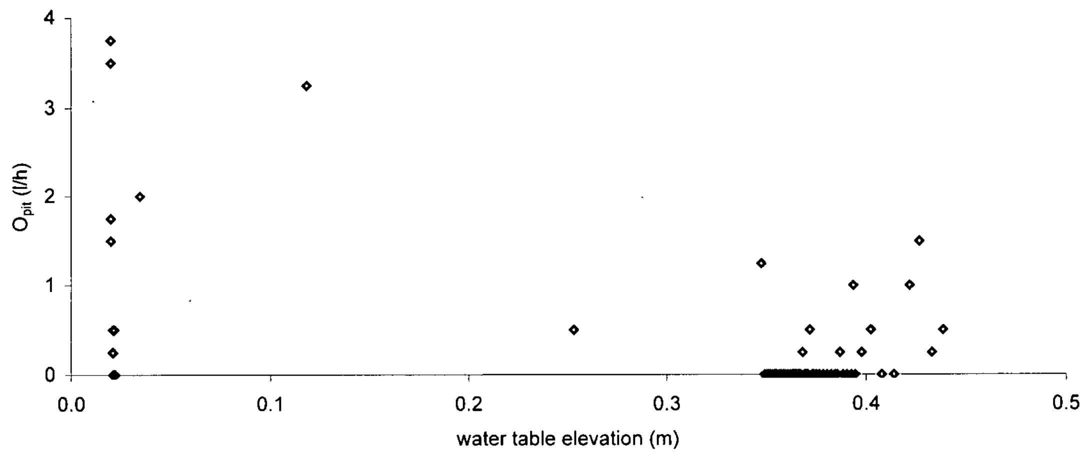

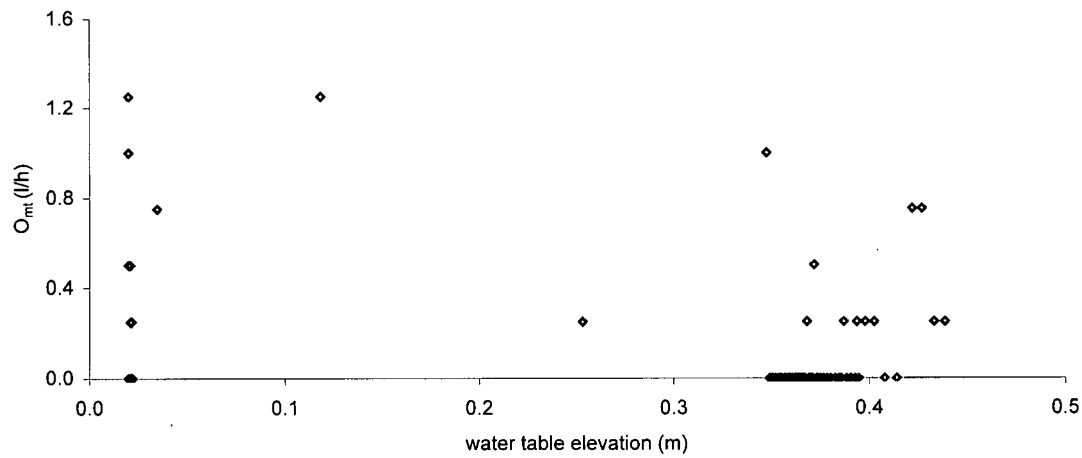

restrictive layer was reached that prevented further drilling. The bottom of the cavity was assumed to be the impermeable layer. Saturated hydraulic conductivities 11, 26, and 51 m upslope of the pit were $8.83 \cdot 10^{-6}$ m/s, $7.52 \cdot 10^{-5}$ m/s, $7.91 \cdot 10^{-5}$ m/s, respectively. The geometric mean of the saturated hydraulic conductivity in the hillslope was $3.75 \cdot 10^{-5}$ m/s.

The second method for estimating K was based on Darcy's law. Darcy's law is best applied in field sites where soils are homogeneous. During the snowmelt season, soils were nearly saturated and highly responsive to melt and precipitation inputs. Therefore, saturated hydraulic conductivity (K_{sat}) was calculated by Darcy's law:

$$K_{sat}=-(Q/A)\cdot dh/dl \qquad (3\text{-}12)$$

where Q is hourly discharge (L/h); A is the flux discharge area (m^2); and dh/dl is the hydraulic gradient in the direction of flow (dimensionless).

Total hourly discharge (Q), $2.43 \cdot 10^3$ L/h, was determined by summing hourly outflow from all mineral sections of the pit, not including the organic horizon outflow for the June 17 snowmelt events in 1999. Flow from the organic horizon was excluded since it was possibly generated as saturation overland flow. Flux discharge area (A) was 1.87 m^2, determined by summing the areas of the mineral and till layers. The hydraulic gradient (dh/dl) was assumed to be equal to the topographic gradient (0.41).

Therefore, the saturated hydraulic conductivity estimated by Darcy's law was $8.8 \cdot 10^{-4}$ m/s. This represents a more integrated value of hydrological influence over the hillside. Saturated hydraulic conductivity calculated by Darcy's law was higher than saturated hydraulic conductivity values derived from slug tests measured in small soil volumes.

3.5 SUMMARY OF KEY FINDINGS

3.5.1 Comparison of pit outflow and stream discharge

Pit outflow at the hillslope segment and streamflow for the entire watershed responded similarly to precipitation during the snowmelt season of 1999. However, both rising limbs and recession limbs of the pit outflow hydrograph were steeper than those of the stream hydrograph due to the presence of rapid flowpaths in the hillslope segment.

Timing

The outflow from mineral section 2 responded faster to rainfall inputs than streamflow. For 16 daily events during the snowmelt season, lag times ranged from 1 to 7 hours between peak flows from the pit and the stream discharge and also between outflow from the mineral horizon and the stream discharge. In addition, an aggregated lag time between pit outflow and stream discharges was estimated to be 4 hr by cross-correlation analysis.

Volume

Ratios of outflows from the pit and the mineral horizon to streamflow were higher for daily peak values than for total volumes of flow. The ratios for 16 daily peak pit outflow and mineral horizon outflows were 0.0024 and 0.0019 of peak stream discharge, respectively. Accumulated pit outflow and mineral horizon outflow contributed 0.0018 and 0.0015 of total stream discharge during the melt period from June 16 to July 21, 1999.

The ratio of pit outflow to stream discharge was much higher than the ratio of pit length to the length of stream bank seepage faces in the watershed or the ratio of the effective contributing area of the pit to the entire watershed area. The effective contributing area to pit drainage calculated from the ratio of total snowmelt runoff from the pit versus total snowmelt stream discharge was much higher than estimates by the topographic survey or water balance calculation.

3.5.2 Variability of subsurface flow

Relations between pit outflow and antecedent precipitation

Peak rainfall alone explained 79% of the variation in total outflow volume from mineral section 2. Total precipitation and 7-day antecedent precipitation were not found to be significant in explaining total outflow.

Generation of outflow from organic horizon

Peak outflow from the organic horizon responded later than peak outflow from the mineral horizon during 5 of the 16 monitored days during the snowmelt season. Outflow from the organic horizon was generated as a lateral subsurface flow for dry soil moisture conditions during autumn storms because a water table did not develop close to the organic horizon and a hydrophobic conditions likely existed at the organic horizon and mineral soil interface.

During the snowmelt season, when wet soil moisture conditions were sustained, snowmelt discharge from the organic horizon comprised approximately 20% of total pit outflow. However, for the driest antecedent moisture conditions on September 23-25, storm outflow from the organic horizon contributed 57% of total pit outflow. As soil moisture decreased from September 4 to September 23, the stormflow from the organic horizon increased from 4% to 57% of total pit outflow.

Variability of outflow from the organic and mineral pit sections

The fraction of outflow from the organic horizon and individual mineral sections varied with changes in mineral horizon outflow and with time throughout the snowmelt season and with changes in pit outflow during autumn storms.

During the snowmelt season, outflow from the organic horizon only occurred when outflow from the mineral horizons exceeded a threshold value, especially mineral sections 1 and 2. However, for the drier conditions during the summer and autumn rain events, outflow from the organic horizon occurred even at very low values of outflow from the mineral sections.

Relations between water table elevation and hillslope discharge were non-linear throughout the melt season and during autumn storms. Furthermore, counter-clockwise hysteresis occurred during all snowmelt events (except the June 17 event) during the melt season. The June 17 event exhibited clockwise hysteresis, possibly reflecting a "conditioning" period.

3.5.3 Effective hydraulic conductivity

Saturated hydraulic conductivity back-calculated from Darcy's law was $8.8 \cdot 10^{-4}$ m/s. This value is more than an order of magnitude higher than the saturated hydraulic conductivity values derived from slug tests, which had a geometric mean of $3.75 \cdot 10^{-5}$ m/s.

CHAPTER 4

DISCUSSION

4.1 SUBSURFACE FLOW AS A CONTRIBUTOR TO STORMFLOW

4.1.1 Timing, peak flows and volumes

Subsurface flow responded rapidly enough to rainfall and snowmelt to contribute to stormflow at the catchment scale. During both the snowmelt and the rain events, pit outflow at the hillslope segment always peaked earlier than stream discharge at the watershed outlet. Lag times between hillslope outflow and stream discharge were due to runoff generated at variable contributing areas reaching the outlet of watershed at later times throughout the year. On a contributing-area basis, subsurface flow significantly augmented peak stormflow at the catchment scale. These results are consistent with the observations of Peters et al. (1995) and Turton et al. (1992). During spring and fall rainstorms in the forested slopes of the Canadian Shield, essentially all stormflow occurred within the thin soil on basin side slopes (Peters et al., 1995). Likewise, Turton et al. (1992) reported that the response of subsurface flow to rainfall in a forested catchment in Okalahoma was rapid enough to contribute to quickflow and peak flow generation. Subsurface flow accounted for 5 to 48% of quickflow.

Pit outflow tended to exhibit a "flashier" response than streamflow during rainfall and snowmelt events. This behaviour may reflect greater storage capacity at the catchment scale, particularly in the form of the small ponds located in the central and upper portions of the catchment.

4.2 VARIABILITY OF SUBSURFACE FLOW

4.2.1 Controls on response to rain events-mineral soil layers

Peak rainfall intensity alone explained 79% of the variation in total outflow volume from mineral section 2. The inclusion of total precipitation and 7-day antecedent rainfall in a multiple linear regression did not significantly improve the fit. However, only 7 storm events were available, limiting the ability to detect significant effects. In contrast, Turton (1992) found that total precipitation and API_7 together determined 70% of the variation in subsurface flow volume, and that peak rainfall was not a significant factor for determining the quantity of subsurface flow. Istok and Boersma (1986) reported that during very low-intensity rainstorms, antecedent rainfall was more important for determining the amount of runoff rather than rainfall magnitude and rainfall intensity. Wallach and Zaslavsky (1991) calculated rainfall infiltration into a layered profile of an infinite uniform slope. They found that the total rainfall rather than the rainfall intensity was the primary control of the lateral flow.

The storms of September 4-6 and September 23-25 had similar total rainfall and peak intensity (Table 3.9), but hydrological responses in pit outflows were very different. Total pit outflow from the September 4-6 storm was about 16 times larger than from the September 23-25 storm. This could be explained by antecedent soil moisture conditions. The September 23-25 storm event, which occurred on relatively dry soils (no rain during the 7 days prior to the event) produced only 25 L of pit outflow. The September 4-6 storm fell on slightly moist soils (13 mm of 7-day antecedent precipitation prior to event) and produced 392 L of soil pit outflow. Thus, in autumn, antecedent soil moisture conditions played a major role in producing subsurface flow. Sidle et al. (2000) also found similar patterns of subsurface flow contributions to stream discharge during storms with dry to very wet antecedent moisture conditions throughout a typhoon season in Japan.

4.2.2 Generation of outflow from the organic horizon

During the snowmelt season, soil moisture was often close to saturation with water table levels approaching the soil surface. When downslope flow arrived at the subsurface flow interception troughs at the bottom of hillslope segment, the water table rose above the top of the mineral horizon. During the snowmelt period, peak outflow from the organic horizon responded later than peak outflow from the mineral horizon during 5 of the 16 consecutive monitored days during the snowmelt season. This suggests that outflow from the organic horizon was derived from saturated throughflow and overland flow, as a result of the rising water table. Dunne and Leopold (1978) reported that saturation overland flow and subsurface flow are the two most important mechanisms in streamflow generation processes on undisturbed forest watersheds in humid temperate regions.

During the summer and autumn rain events, drier soil moisture conditions dominated, as indicated by lower water table levels. Although a water table did not develop close to the organic horizon, outflow from the organic horizon occurred, even at very low values of outflow from the mineral sections. Wilcox et al. (1997) studied a semiarid ponderosa pine hillslope in New Mexico and found that a perched saturated zone developed within about 1 m of the soil surface, forcing lateral subsurface flow. Based on oxygen isotope variations, McDonnell et al. (1991) inferred that large proportions of storm runoff occurred as flow through the organic horizon, perched on the mineral soil layer, with negligible flow from the mineral horizon. However, they did not directly observe lateral flow from the organic horizon. Mosley (1979) studied the stormflow-generating mechanisms in the Tawhai State Forest, near Reefton, New Zealand. He observed that a large proportion of the runoff occurred above the surface of the A horizon even though the saturated hydraulic conductivity (0.007 cm/sec) of the mineral horizon suggested that all of the water should have infiltrated. Brown et al. (1999) found that for unsaturated soil moisture conditions, water content recession curves for shallow soils had steeper slopes than for the deeper soils, and inferred more rapid drainage from the shallower soils than from the deeper soils during dry summer periods (7-days with no precipitation). They suggested that lateral flow in the upper soil layer, caused by the hydrophobicity of the organic matter, was an important cause of rapid drainage. My results confirm that outflow from the organic horizon can occur as a lateral subsurface flow under dry soil moisture conditions during autumn storms. During very dry conditions, hydrophobic characteristics of organic soil layer may promote lateral flow at the organic horizon and mineral soil boundary.

4.2.3 Relative contributions of flow from the mineral sections

For very wet conditions, the fraction of outflow from the individual mineral sections varied with changes in total mineral horizon outflow and with time throughout the snowmelt season. This result was similar under dry soil moisture conditions. The fraction of outflow from the organic horizon and individual mineral sections varied with changes in pit outflow during autumn storm events. These findings were consistent with those of Woods and Rowe (1996). They observed that spatial variability of subsurface flow changed with time. Only two of 30 troughs had high percentage contributions to total subsurface flow at very low total flows and flow was most distributed at high total flows. Hutchinson and Moore (2000), using 9 concrete troughs (each trough 0.97 to 1.57 m wide), similarly found a systematic shift in the relative contributions to total outflow as flow increased.

Relations between hillslope discharge, both total pit outflow and mineral horizon outflow, and water table in the hillslope segment were non linear throughout the melt season and during the autumn storms. In addition, hillslope discharge and water table relations exhibited hysteresis, which contradicts the assumption of quasi-steady state subsurface flow. The hysteresis indicates that different flow pathways occur between rising and falling outflow limbs throughout the snowmelt season. Hutchinson and Moore (2000) also found nonlinear relations between hillslope discharge and the water table elevation in a 10 m wide plot. However, they did not observe hysteresis between pit outflow and water table elevation.

4.2.4 Scaling from hillslope segments to the catchment

Simple estimates of the contribution of throughflow to stormflow have used the ratio of the length of monitored hillslope output to the total length of streambank seepage faces on the catchment (e.g., Weyman, 1970; McDonnell, 1990; Turton et al., 1992). Sidle et al. (1995) calculated stormflow from all watershed components on a unit contributing area basis to compare runoff per unit contributing area of all watershed components, including a second-order basin, two first-order basins, a zero-order basin, and a hillslope segment. During drier antecedent conditions, stormflow is generated largely by saturated overland flow contributions from the riparian zone (Sidle et al., 1995, 2000). However, as wetness increased, subsurface flow from a hillslope segment contributed 2.0-3.4 times the runoff on a unit contributing area basis as the entire forest basin. The results of this study showed that simple scaling ratios based on contributing areas or slope widths do not appear to provide a reliable means of scaling up from the hillslope to the catchment scale. These findings concur with those of other studies (e.g., Woods and Rowe, 1996; Freer et al., 1997; Hutchinson and Moore, 2000). Woods and Rowe (1996) pointed out that if the stream discharge is concentrated in a small portion of the streambank (e.g., topographic convergence), such an approach is not suitable and spatial variability of subsurface flow must be considered for estimating throughflow contribution to stormflow generation. Woods and Rowe's (1996) study clearly showed that subsurface flow was not consistent with surface topography; thus, the assumption in most hydrological models that subsurface flow is spatially uniform is violated. In a field study at Panola catchment, Freer et al. (1997) showed that the spatial flow paths on the hillslope could be predicted by subsurface topography. Hutchinson and Moore (2000) monitored the spatial and temporal variability of throughflow in a shallow forest hillslope near Vancouver, BC, and found that variability of subsurface flow was controlled by the topography of the confining till at the lowest flows; however, at higher flows, surface topography controlled piezometric levels. Therefore, when subsurface flow dominates, relations between subsurface flow and topography-driven patterns of soil moisture deficit and saturated soil moisture storage should be considered (Anderson and Burt, 1978; Woods and Rowe, 1996; Hutchinson and Moore, 2000).

Effective contributing areas estimated from surface topography may be subject to errors. A topographic survey about 51 m upslope from the soil pit was used as one method to estimate active contributing area. In the hillslope segment above the soil pit, the slope gradient is initially fairly steep. About 51 m upslope from the pit there is a break in gradient after which the gradient steepens again to the ridgeline. However, total contributing area to the pit drainage, the upslope area from the pit to the top of the watershed boundary, could be larger. Tree density obscured measurements during the topographic survey, thus some error may have been introduced. Another limitation for estimating accurate contributing area based on surface topography was the assumption that flow directions were related to hydraulic gradients derived from surface topography (i.e., the dynamics of subsurface flow pathways were not considered).

Effective contributing areas to pit drainage estimated by water-balance calculations were greater than those estimated by surface topography. Assumptions of negligible evaporation losses and no change in soil moisture storage may have slightly underestimated effective contributing areas via water-balance calculations.

4.2.5 Implications for validity of simple slope hydrology models

Models such as TOPMODEL, DHSVM, and TOPOG assume that lateral flow within soils occurs only below the water table. Furthermore, the assumption of quasi-steady state subsurface flow combined with the topographically driven flow assumption, implies that subsurface flow through a given contour segment at any time is proportional to the upslope contributing area as determined from surface topography. An inference from this assumption is that the fractional allocation of subsurface discharge should not vary with time or discharge. The results of this study contradict these modelling assumptions. Given that prediction of water chemistry requires an accurate knowledge of flow paths, violations of these modelling assumptions indicates that models based on them cannot provide accurate simulations of water chemistry (e.g., Burns et al., 1998).

4.3 EFFECTIVE HYDRAULIC CONDUCTIVITY

Saturated hydraulic conductivity back-calculated from Darcy's law was $8.8 \cdot 10^{-4}$ m/s, more than an order of magnitude higher than the saturated hydraulic conductivity values derived from slug tests, which had a geometric mean of $3.75 \cdot 10^{-5}$ m/s. Saturated hydraulic conductivities based on other subsurface stormflow studies are summarized in Table 4.1. Saturated hydraulic conductivity values estimated from this study by both methods were rather large compared with 'typical' forested hillslope values (Cosby et al., 1984), but within the range of other studies (Table 4.1). The larger estimated saturated

Table 4.1 Saturated hydraulic conductivities based on other subsurface stormflow studies in the forested area.

reference	place	slope angle, S°	K_{sat}(m/s)	method
Whipkey (1965)	Ohio	23	7.9E-05	Darcy's law outflow field stduy
Weyman (1970, 1973)	Mendip, U.K.	15	8.4E-05	Darcy's law outflow field study
			2.1E-05	
			7.0E-06	
Anderson and Burt (1978)	Somerset, England	25	1.0E-05	Darcy's law outflow field stduy
			1.0E-03	
Mosley (1979)	New Zealand	39	1.4E-03	
			7.0E-05	
Luxmoore (1981)			2.0E-05	laboratory determinations of retention properties on soil cores method
			6.7E-06	
Turton et al. (1992)	Oklahoma	8	2.6E-03	Darcy's law outflow field stduy
			1.9E-03	
Bazemore et al. (1994)	Virginia, USA	30	1.0E-04	Darcy's law outflow field study
Taha et al. (1997)	Maurets, France	8	3.0E-05	Measured in the field with Guelph permeameter and multi-disc infiltrometers
Kendall et al. (1999)	Vermont	7.4	1.0E-06	measured in the wells using Horvlev method
			7.1E-06	
			1.5E-05	
Hutchinson and Moore (2000)	Vancouver, Canada	17	1.0E-04	Darcy's law outflow field stduy
			7.0E-04	

conductivities indicate that macropores resulting from root channels, pipes, seepage zones and biological activity were important in generating subsurface stormflow. Taha et al. (1997) observed that the high saturated conductivity of the upper layer is due to the presence of macropores, especially root channels in a forest soil. Hutchinson and Moore (2000) reported the importance of roots as preferred pathways.

CHAPTER 5

CONCLUSION

5.1 SUMMARY OF MAIN FINDINGS

5.1.1 The importance of subsurface flow as a stormflow generating process

The timing of peak outflows from the pit at the hillslope segment was compared to the timing of peak stream discharge at the watershed outlet during both the snowmelt and rainy seasons. Subsurface flow at the hillslope segment responded rapidly enough to inputs of rain and snowmelt to contribute to stormflow at the catchment scale. Outflow from the pit at the hillslope segment delivered 0.24% of peak stream discharge and accumulated outflow from the pit at the hillslope segment delivered 0.18% of total stream discharge during the snowmelt season. Thus subsurface flow appeared to contribute significantly to peak runoff at the catchment scale.

Estimates of catchment-wide subsurface flow based on a simple ratio of pit length to length of streambank seepage faces in the watershed and a simple ratio of effective contributing area of the pit to the entire watershed estimated by surface topography were compared to the ratio of total snowmelt runoff from the pit versus total snowmelt stream discharge. Both simple scaling ratios based on contributing areas derived from surface topography and slope widths were not reliable for scaling up from the hillslope to the catchment.

Estimates of effective contributing area to pit drainage in a small hillslope segment were calculated using the ratio of total snowmelt runoff from the pit versus total snowmelt stream discharge, topographic surveys, and water-balance methods. Contributing area estimates based on runoff ratio were much higher than estimates derived from the topographic survey and water-balance methods. Also, contributing area estimates based on water balance methods were greater than those based on topographic surveys. The lower estimates based on the topographic survey may partly be due to some measurement errors. Flow directions are linked with hydraulic gradients derived from surface topography without considering dynamic subsurface flow pathways and effective contributing areas are only considered 51 m upslope from the pit.

5.1.2 The variability of subsurface flow

Peak rainfall intensity alone explained 79% of the variation in total subsurface flow volume from mineral section 2; total precipitation and 7-day antecedent precipitation were not significant factors in determining the quantity of subsurface flow for 7 rainfall events in 1998-99. However, in the summer and autumn rain events, antecedent soil moisture conditions had a major influence on producing subsurface flow.

During the snowmelt season, outflow from the organic horizon was derived from saturated throughflow and overland flow as a result of a rising water table. However, during the autumn storms, outflow from the organic horizon was generated as a lateral subsurface flow under dry soil moisture conditions during autumn storms.

Hydrophobicity of organic soil characteristics may facilitate lateral flow at the organic horizon and mineral soil boundary.

5.1.3 The validity of modelling assumptions

Models such as TOPMODEL and TOPOG assume that lateral flow only occurs below the water table. Additionally conceptual models that invoke macropore flow make similar assumptions (McDonnell, 1990; Tani, 1997). The results of this study showed that lateral flow was generated above the water table during dry soil conditions. Although soil was not fully saturated, outflow from the organic horizon occurred, likely due to hydrophobic conditions at the interface between the organic horizon and mineral soil. Other field investigations have show that saturated flow can occur in macropores within an otherwise unsaturated soil matrix (Tsuboyama et al., 1994; Noguchi et al. 1999).

Another assumption of subsurface flow models is quasi-steady state lateral flow. This assumption, combined with the assumption of topographically driven flow, indicate that subsurface flow through a given contour segment at any time is proportional to the upslope contributing area derived from surface topography. For wet soil moisture conditions, the fraction of outflow from the individual mineral sections varied with time and with changes in mineral horizon outflow throughout the melt season. For dry soil moisture conditions, the fraction of outflow from the organic horizon and individual mineral sections varied with changes in pit outflow during autumn storms. Furthermore, relations between hillslope discharge and water table elevation exhibited hysteresis and non-linear response throughout the melt season and during autumn storms. Therefore, the results of my study contradict these common model assumptions.

5.1.4 Effective hydraulic conductivity

Saturated hydraulic conductivity back-calculated from Darcy's law was more than an order of magnitude higher than the saturated hydraulic conductivity values derived from slug tests at piezometers. The results of both methods were within range of results of other studies in forested areas. The higher back-calculated hydraulic conductivities were more reliable and likely due to existence of root channels as preferred pathways in the forested hillslope. Point measurements of slug tests cannot be used to represent hydraulic conductivity in large forested hillslope.

5.2 SUGGESTIONS FOR FUTURE RESEARCH

Studies using hydrometric techniques indicate the importance of subsurface flow as a contributor to stormflow. Combined hydrometric and chemical/isotopic studies have been conducted in some previous studies, both at the hillslope and catchment scales (e.g., Bottomley et al., 1984; Wels et al., 1991a, b; McDonnell, 1990; Hinton et al., 1994; Peters et al., 1995). McDonnell (1990) found that estimates of the relative portions of soil water that contribute to streamflow based on results from chemical and stable isotope studies were contradictory to results from hydrometric studies of flow pathways in a steep, humid catchment. However, only Burns et al. (1998) appear to have combined a study of the lateral variability of pit outflow across a slope with chemical or isotopic studies. Further studies should be conducted that combine the two approaches (hydrometric studies and chemical/isotopic studies) at other sites for a clear understanding of the lateral variability of subsurface outflow.

This study indicated that lateral flow occurred above the water table. This lateral flow was not in a quasi-steady state and these lateral flow pathways were not controlled by surface topography. These findings contradict simplified modelling assumptions used in shallow forest soils. Such findings are similar to results of Woods and Rowe (1996), Freer et al. (1997) and Hutchinson and Moore (2000). Further research should be conducted on the controls on flow paths in shallow forest soils to provide a basis for more realistic parameterization of subsurface flow dynamics used in models.

During the summer and autumn rain events, lateral flow in the organic horizon occurred during dry soil moisture conditions. Hydrophobic conditions at the base of the organic horizon may contribute to this lateral flow. Further research related to this phenomenon is needed so that a better understanding of the role of hydrophobicity on subsurface flowpaths in forest soils can be developed.

Estimated saturated hydraulic conductivities in this study were in the higher range (more or less larger) of other studies in forested areas where macropores existed. Such macropore systems are important in controlling the hydraulic properties of forest soils (Tsuboyama et al., 1994; Hutchinson and Moore, 2000; Sidle et al., 2001). Further research is needed to clarify preferential flow in such interconnected macropore systems in forest hillslopes for both saturated and unsaturated conditions.

REFERENCES

Abdul AS, Gillham RW. 1984. Laboratory studies of the effects of the capillary fringe on streamflow generation. *Water Resources Research* **20**: 791-698.

Amoozegar A, Warrick AW. 1986. Hydraulic conductivity of saturated soils: field methods: In A. Klute (editor), *Methods of Soil Analysis, Part1. Physical and Mineralogical Methods*. Second Edition. American Society of Agronomy, Madison, 735-770.

Anderson MG, Burt TP. 1978. The role of topography in controlling throughflow generation. *Earth Surface Processes and Landforms* **3**: 331-344.

Anderson MG, Burt TP. 1990. Subsurface runoff. In: Anderson, M.G. and Burt, T.P. (eds), *Process studies in Hillslope Hydrology.* John Wiley and Sons, Chichester: 365-400.

Atkinson TC. 1978. Techniques for measuring subsurface flow on hillslopes. In: M.J. Kirkby (Editor), *Hillslope Hydrology.* Wiley, New York: 73-120.

Bazemore DE, Eshleman KN, Hollenbeck KJ. 1994. The role of soil water in stormflow generation in a forested headwater catchment: synthesis of natural tracer and hydrometric evidence. *Journal of Hydrology* **162**: 47-75.

Beven K. 1986. Hillslope runoff processes and flood frequency characteristics, in Abrahams, A. D. (Ed.), *Hillslope Processes*, Allen and Unwin, Boston.187-202.

Beven K, Germann P. 1982. Macropores and water flow in soils. *Water Resources Research* **18**: 1311-1325.

Beven KJ, Kirkby MJ. 1979. A physically based variable contributing area model of the basin hydrology. *Hydrological Science Bulletin* **24**: 43-69.

Bottomley DJ, Craig D, Johnston LM. 1984. Neutralization of acid runoff by groundwater discharge to streams in Canadian Precambrian Shield watersheds. *Journal of Hydrology* **75**: 1-26.

Brown VA, McDonnell JJ, Burns DA, Kendall C. 1999. The role of event water, a rapid shallow flow component, and catchment size in summer stormflow. *Journal of Hydrology* **217**: 171-190.

Burns DA, Hooper RP, McDonnell JJ, Freer JE, Kendall C, Beven K. 1998. Base cation concentrations in subsurface flow from a forested hillslope: The role of flushing frequency. *Water Resources Research* **34**: 3535-3544.

Burt TP, Butcher DP. 1985. On the generation of delayed peaks in stream discharge. *Journal of Hydrology* **78**: 361-378.

Buttle JM, Sami K. 1992. Testing the groundwater ridging hypothesis of streamflow generation during snowmelt in a forested catchment. *Journal of Hydrology* **135**: 53-72.

Chapman and Gray Creeks Integrated Watershed Management Plan. 1998. Ministry of Environment, Lands and Parks, Ministry of Forests (Sunshine Coast Forest District).

Chappell NA, Ternan JL, Williams AG, Reynolds B. 1990. Preliminary analysis of water and solute movement beneath a coniferous hillslope in mid-Wales, U.K. *Journal of Hydrology* **116**: 201-215.

Cosby BJ, Hornberger GM, Clapp RB, Ginn TR. 1984. A statistical exploration of the relationships of soil moisture characteristics of the physical properties of soils. *Water Resources Research* **20**: 682-690.

De Vries J, Chow TL. 1978. Hydrologic behaviour of a forested mountain soil in coastal British Columbia. *Water Resources Research* **14**: 935-942.

Dunne T, Black RG. 1970a. An experimental investigation of runoff production in permeable soils. *Water Resources Research* **6**: 478-490.

Dunne T, Black RG. 1970b. Partial area contributions to storm runoff in a small New England watershed. *Water Resources Research* **6**: 1296-1311.

Dunne T, Leopold LB. 1978. Water movement in an experimental planning. W.H. Freeman, San Francisco, California.

Eschner AR, Leonard RE, Leaf AL. 1969. Soil moisture priming, soil temperature and water available for snowmelt runoff. *In: Proc. Annu. Eastern Snow Conf.* Portland, Maine: 19-23.

Espeby B. 1990. Tracing the origin of natural waters in a glacial till slope during snowmelt. *Journal of Hydrology* **118**: 107-127.

Freer J, McDonnell J, Beven KJ, Brammer D, Burns D, Hooper RP, Kendal C. 1997. Topographic controls on subsurface storm flow at the hillslope scale for two hydrologically distinct small catchments. *Hydrological Processes* **11**: 1347-1352.

Golden Software Inc.1994. *SURFER for windows,* Version 5. Golden Software Inc.: Golden, Co.

Hendershot WH, Courchesne F, Schemenauer RS. 1992. Soil acidification along a topographic gradient on Roundtop Mountain, Quebec, Canada. *Water, Air, and Soil Pollution* **61**: 235-242.

Hewlett JD, Hibbert AR. 1967. 'Factors affecting the response of small watersheds to preceipitation in humid areas', in Sopper,Wm. E. and Lull, H. W. (Eds), *International symposium on Forest Hydrology,* Pergamon Press, Oxford: 257-290.

Hibbert AR, Cunningham GB. 1965. Streamflow data processing opportunities and application. *International symposium on of forest hydrology, Aug 29-sept 10, 1965, Forest hydrology, proceedings of a national science foundation advanced science seminar*: 725-736.

Hinton MJ, Schiff SL, English MC. 1994. Examining the contributions of glacial till water to storm runoff using two- and three-component hydrograph separations. *Water Resources Research* **30**: 983-993.

Hovorslev MJ. 1951. Time lag and soil permeability in groundwater observation. US. Army Corps Engineering. *Waterways Exp. Sta. Bull.* 36, Vicksburg, MA.

Hudson R. 2000. Snowpack recovery in regenerating coastal British Columbia clear-cuts. *Canadian Journal of Forest Research* **30**: 548-556.

Hutchinson DG, Moore RD. 2000. Throughflow variability on a forested hillslope underlain by compacted glacial till. *Hydrological Processes* **14**: 1751-1766.

Istok JD, Boersma L. 1986. Effect of antecedent rainfall on runoff during low intensity rainfall. *Journal of Hydrology* **88**: 329-342.

Jardine PM, Wilson GV, Luxmoore RJ, McCarthy JF. 1989. Transport of inorganic and natural organic tracers through an isolated pedon in a forest watershed. *Soil Science Society of America Journal* **53**: 317-323.

Jenkins A, Ferrier RC, Harriman R, Ogunkoya YO. 1994. A case study in catchment hydrochemistry: Conflicting interpretation from hydrological and chemical observations. *Hydrological Processes* **8**: 335-349.

Jurdant M, Bernier B. 1965. Carte écologique de la forêt Montmorency, Université Laval. In: M. Côté, (Editor), 1968. Plan d×aménagement de la forêt Montmorency de l'Université Laval, P.U.L., Qué: 157pp.

Kane DL, Stein J. 1983. Field evidence of groundwater recharge in interial Alaska. *Proceedings Permafrost: 4th International Conference*, National Academy Press, Washington, D.C: 572-577.

Kane DL, Stein J. 1984. Plot measurements of snowmelt runoff for varying soil conditions. *Geophysica* **20**: 123-135.

Kendall KA, Shanley JB, McDonnell JJ. 1999. A hydrometric and geochemical approach to test the transmissivity feedback hypothesis during snowmelt. *Journal of Hydrology* **219**: 188-205.

Kirkby MJ. 1978. Implications for sediment transport, in Kirkby, M.J. (Ed.*), Hillslope hydrology*. John Wiley, Chichester: 325-363.

Kitahara H. 1993. Characteristics of pipe flow in forested slopes. Exchange processes at the land surface for a range of space and time scales: *Proceedings of an International Symposium held at Yokohama*, Japan, 13-16 July 1993. IAHS Press, Wallingford, UK: 235-242.

Lamb R, Beven K, Myrabø S. 1997. Discharge and water table predictions using a generalized TOPMODEL formulation. *Hydrological Processes* **11**: 1145-1167.

Luxmoore RJ, Ferrand LA.1993. Towards pore-scale analysis of preferential flow and chemical transport. *Water flow and solute transport in soils: developments and applications.* Springer-Verlag GmbH & Co. KG, Berlin, Germany: 45-60.

Luxmoore RJ. 1981. Micro-, meso-, and macroporosity of soil. *Soil Science Society of America Journal* **45**: 671-672.

Marks D, Domingo J, Susong D, Link T, Garen D. 1999. A spatially distributed energy balance snowmelt model for application in mountain basions. *Hydrological processes* **13**: 1935-1959.

McDonnell JJ. 1990. A rational for old water discharge through macropores in a steep, humid catchment. *Water Resources Research* **26**: 2821-2832.

McDonnell JJ, 1997.Comment on "The changing spatial variability of subsurface flow across a hillside" by Woods R and Rowe L. *Journal of Hydrology (New Zealand)* **36**: 97-100.

McDonnell JJ, Buttle JM. 1998. Comment on "A deterministic-empirical model of the effect of the capillary-fringe on near-stream area runoff. 1. Description of the model" by Jayatilaka CJ and Gillham RW. *Journal of Hydrology* **207**: 280-285.

McDonnell JJ, Owens JF, Stewart MK. 1991. A case study of shallow flow paths in a steep zero-order basin. *Water Resources Research* **27**: 679-685.

Mosley MP. 1979. Streamflow generation in a forested watershed, New Zealand. *Water Resources Research* **15**: 795-806.

Mosley MP. 1982. Subsurface flow velocities through selected forest soils, South Island, New Zealand. *Journal of Hydrology* **55**: 65-92.

Mulholland PJ, Wilson GV, Jardine PM. 1990. Hydrogeochemical response of a forested watershed to storms: effects of preferential flow along shallow and deep pathways. *Water Resources Research* **26**: 3021-3036.

Noguchi S, Tsuboyama Y, Sidle RC, Hosoda I. 1997. Spatially distributed morphological characteristics of macropores in forest soils of Hitachi Ohta experimental watershed, Japan, *Journal of Forest Research* **2**: 207-215.

Noguchi S, Tsuboyama Y, Sidle RC, Hosoda I. 1999. Morphological characteristics of macropores and the distribution of preferential flow pathways in a forested slope segment. *Soil Science Society of America Journal* **63**: 1413-1423.

Noguchi S, Tsuboyama Y, Sidle RC, Hosoda I. 2001. Subsurface runoff characteristics from a forest hillslope soil profile including macropores, Hitachi Ohta, Japan. *Hydrological Processes* **15**: 2131-2149.

O'Loughlin EM. 1986. Prediction of surface saturation zones in natural catchments and their relations to soil and topography. *Water Resources Research* **22**: 794-804.

Pearce AJ. 1990. Streamflow generation processes: An Austral view. *Water Resources Research* **26**: 3037-3047.

Peters DL, Buttle JM, Taylor CH, LaZerte BD. 1995. Runoff production in a forested, shallow soil, Canadian Shield basin. *Water Resources Research* **31**: 1291-1304.

Pilgrim DH, Huff DD. 1978. A field evaluation of surface and subsurface runoff, I, Tracer studies. *Journal of Hydrology* **28**: 299-318.

Price AG, Hendrie LK. 1983. Water motion in a deciduous forest during snowmelt. *Journal of Hydrology* **64**: 339-356.

Quinn PF, Beven KJ, Chevalier P, Planchon O. 1991. The prediction of hillslope flow paths for distributed hydrological modelling using digital terrain models. *Hydrological Processes* **5**: 59-79.

Quinn PF, Beven KJ, Lamb R. 1995. The ln(α/tanβ) index: how to calculate it and how to use it within the TOPMODEL framework. *Hydrological Processes* **9**: 161-182.

Roberge J, Plamondon AP. 1987. Snowmelt runoff pathways in a boreal forest hillslope, the role of pipe throughflow. *Journal of Hydrology* **95**: 39-54.

SAS Institute, Inc. 1988a. *SAS Language Guide for Personal Computers,* release 6.03 ed. Cary, N. C.

SAS Institute, Inc.1988b. *SAS Procedures Guide,* release 6.03 ed. Cary, N. C.

Sevink J, Imeson AC, Verstraten JM. 1989. Humus form development and hillslope runoff, and the effects of fire and management, under Mediterranean forest in NE-Spain. *Catena* **16**: 461-475.

Sidle RC, Noguchi S, Tsuboyama Y, Laursen K. 2001. A conceptual model of preferential flow systems in forested hillslopes: evidence of self-organization. *Hydrological Processes* **15**: 1675-1692.

Sidle RC, Tsuboyama Y, Nogichi S, Hosoda I, Fujieda M, Shimizu T. 1995. Seasonal hydrologic response at various spatial scales in a small forested catchment, Hitachi Ohta, Japan, *Journal of Hydrology* **168**: 227-250.

Sidle RC, Tsuboyama Y, Noguchi S, Hosoda I, Fujieda M, Shimizu T. 2000. Stormflow generation in steep forested headwaters: a linked hydrogeomorphic paradigm. *Hydrological Processes* **14**: 369-385.

Sklash MG, Farvolden RN. 1979. The role of groundwater in storm runoff. *Journal of Hydrology* **43**: 46-65.

Slaughter, C.W. and Kane, D.L., 1979. Hydrologic role of shallow organic soils in cold climates. *In: Proc. Can. Hydrol. Symp.*, Natl. Res. Council Canada, Ottawa, Ont: 380-389.

Stagnitti F, Parlange JY, Steenhuis TS, Parlange, MB, Rose CW. 1992. A mathematical model of hillslope and watershed discharge. *Water Resources Research* **28**: 2111-2122.

Storck P, Bowling L, Wetherbee P, Lettenmaier D. 1998. Application of a GIS-based distributed hydrology model for prediction of forest harvest effects on peak stream flow in the Pacific Northwest. *Hydrological Processes* **12**: 889-904.

Taha A, Gresillon JM, Clothier BE. 1997. Modelling the link between hillslope water movement and stream flow: application to a small Mediterranean forest watershed. *Journal of Hydrology* **203**: 11-20.

Talsma T, Hallan PM. 1980. Hydraulic conductivity measurement of forest catchments. *Australian Journal of Soil Research* **30**: 139-148.

Tanaka T, Yasuhara M, Sakai H, Marui A. 1988. The Hachioji Experimental Basin study-storm runoff processes and the mechanism of its generation. *Journal of Hydrology* **102**: 139-164.

Tani M.1997. Runoff generation processes estimated from hydrological observations on a steep forested hillslope with a thin soil layer. *Journal of Hydrology* **200**: 84-109.

Troendle CA. 1970. Water storage, movement and outflow from a forested slope under natural rainfall in West Virginia. *Transactions of the American Geophysical Union* **51**: 279.

Troendle CA, Reuss JO. 1997. Effect of clear cutting on snow accumulation and water outflow at Fraser, Colorado. *Hydrology and Earth System Sciences* **1**: 325-332.

Tsuboyama Y, Sidle RC, Noguchi S, Hosoda I. 1994. Flow and solute transport through the soil matrix and macropores of a hillslope segment. *Water Resources Research* **30**: 879-890.

Tsukamoto Y. 1961. An experiment on subsurface flow. *Journal of the Japanese Society of Forestry* **43**: 61-68.

Tsukamoto Y, Ohta T. 1988. Runoff processes on a steep forested slope. *Journal of Hydrology* **102**: 165-178.

Turton DJ, Haan CT, Miller EL. 1992. Subsurface flow responses of a small forested catchment in the Ouachita Mountains. *Hydrological Processes* **6**: 111-125.

Vertessy RA, Hatton TJ, O'Shaughnessy PJ, Jayasuriya MDA. 1993. Predicting water yield from a mountain ash forest catchment using a terrain analysis based catchment model. *Journal of Hydrology* **150**: 665-700.

Wallach R, Zaslavsky D. 1991. Lateral flow in a layered profile of an infinite uniform slope. *Water Resources Research* **27**: 1809-1818.

Wels C, Cornett RJ, LaZerte BD. 1991a. Hydrograph separation: A comparison of geochemical and isotopic tracers. *Journal of Hydrology* **122**: 253-274.

Wels C, Taylor CH, Cornett RJ. 1991b. Streamflow generation in a headwater basin on the Precambrian Shield. *Hydrological Processes* **5**: 185-199.

Weyman DR. 1970. Throughflow on hillslopes and its relation to the stream hydrograph. *Bulletin of the International Association of Scientific Hydrology* **15**: 25-33.

Weyman DR. 1973. Measurements of the downslope flow of water in a soil. *Journal of Hydrology* **20**: 267-288.

Whipkey RZ. 1965. Subsurface stormflow on forested slopes. *Bulletin of the International Association of Scientific Hydrology* **10**: 74-85.

Whipkey RZ. 1967. Theory and mechanics of subsurface stormflow, *in Proceedings of the International Symposium on Forest Hydrology*. Pergamon, New York: 255-260.

Whipkey RZ. 1969. Storm runoff from forested catchments by subsurface routes. *In: Floods and Their Computation,* Vol. II. I.A.S.H. Publ., 85.

Wigmosta MS, Vail LW, Lettenmaier DP. 1994. A distributed hydrology-vegetation model for complex terrain. *Water Resources Research* **30**: 1665-1679.

Wilcox BP, Newman BD, Brandes D, Davenport DW. 1997. Runoff from a semiarid ponderosa pine hillslope in New Mexico. *Water Resources Research* **33**: 2301-2314.

Wilson GV, Alfonsi JM, Jardine PM. 1989. Spatial variability of saturated hydraulic conductivity of the subsoil of two forested watersheds. *Soil Science Society of America Journal* **53**: 679-685.

Wilson GV, Jardine PM, Luxmoore RJ, Jones, JR. 1990. Hydrology of a forested hillslope during storm events. *Geoderma* **46**: 119-138.

Wilson GV, Luxmoore RJ. 1988. Infiltration, macroporosity and mesoporosity distributions on two forested watersheds. *Soil Science Society of America Journal* **52**: 329-335.

Wolock DM, McCabe GJ. 1995. Comparison of single and multiple flow direction algorithms for computing topographic parameters in TOPMODEL. *Water Resources Research* **31**: 1315-1324.

Wolock DM, Price CV. 1994. Effects of digital elevation model map scale and data resolution on a topography-based watershed model. *Water Resources Research* **30**: 3041-3052.

Woods R, Rowe L. 1996. The changing spatial variability of subsurface flow across a hillside. *Journal of Hydrology (New Zealand)* **35**: 49-84.

Woods RA, Sivapalan M, Robinson JS. 1997. Modeling the spatial variability of subsurface runoff using a topographic index. *Water Resources Research* **33**: 1061-1073.

Wu W, Sidle RC. 1995. A distributed slope stability model for steep forested basins. *Water Resources Research* **31**: 2097-2110.

Youngs EG. 1968. Shape factors for Kirkham's piezometer method for determining the hydraulic conductivity of soil in situ for soils overlying an impermeable floor or infinitely permeable stratum. *Soil Science***106**: 235-237.